

Koninklijke Sterrenwacht van België
Observatoire royal de Belgique
Royal Observatory of Belgium



Jaarverslag 2016
Rapport Annuel 2016
Annual Report 2016

Cover illustration: astrographic equatorial telescope which has contributed since 1908 to the mapping of the Uccle zone for the "Carte du Ciel" project (Photo: P. Van Cauteren).

De activiteiten beschreven in dit verslag werden ondersteund door

Les activités décrites dans ce rapport ont été soutenues par

The activities described in this report were supported by

De POD Wetenschapsbeleid
Le SPP Politique Scientifique
The Belgian Science Policy



De Nationale Loterij
La Loterie Nationale
The National Lottery



Het Europees Ruimtevaartagentschap
L'Agence Spatiale Européenne
The European Space Agency



De Europese Gemeenschap
La Communauté Européenne
The European Community



Het Fonds voor Wetenschappelijk Onderzoek –
Vlaanderen



Le Fonds de la Recherche Scientifique



Table of contents

Preface	6
Reference Systems and Planetology.....	7
Global Navigation Satellite System (GNSS).....	8
Time – Time Transfer	14
Earth Rotation, Geodesy and Geophysics of Terrestrial Planets.....	16
Seismology and Gravimetry.....	21
Seismic activity.....	22
Negative magnitude???	23
A New Paradigm for Large Earthquakes in Stable Continental Plate Interiors	24
Stratification at the Earth's largest hyperacidic lake and its consequences	25
Visualizing Cross-Sectional Data in a Real-World Context	26
Transpiring forest influences gravity	27
Our expertise in <i>Nature Physics</i>	28
Astronomy and Astrophysics	30
The project Gaia.....	31
The BINA project.....	34
Luminous Blue Variables: animaging perspective on their binarity and near environment & Long-term spectroscopic monitoring of the Yellow Hypergiant Rho Cas.	35
Solar Physics and Space Weather	37
Highlights in solar radio astronomy at ROB.....	38
Numerical and Observational Study of Stealth CMEs	40
CCSOM – Constraining CMEs and Shocks by Observations and Modelling throughout the inner heliosphere	42
Topical issue of Solar Physics "Sunspot Number Recalibration"	44
MHD modeling of torsional waves in the solar corona	46
The detection of ultra-relativistic electrons by the LYRA on-board PROBA2.....	48
Information service.....	50
Information to public, media and authorities	51
Website	52
Social networks @ ROB.....	52
Night of the Shooting Stars	52
Exhibitions.....	53
The Planetarium.....	54
Oniroscopy and New York at the Planetarium	55
New show: "Solar superstorm / Les colères du Soleil"	55
The star projector Zeiss amongst the 100 masterpieces of Brussels	56

Special activities.....	56
Annex 1: Publications	57
Publications with peer review	58
Publications without peer review.....	68
Other publications	72
Annex 2: Human Resources	73
Personnel / Personnel.....	74
Staff statistics.....	79

Preface

This report describes the highlights of scientific activities and public services at the Royal Observatory of Belgium in 2016.

A list of publications and the list of personnel is included at the end.

Due to lack of means and personnel the report is only in English.

If you need more or other information on the Royal Observatory of the Belgium and/or its activities please contact rob_info@oma.be or visit our website <http://www.astro.oma.be>.

Ronald Van der Linden
Director General

Reference Systems and Planetology

This Operational Directorate Reference Systems and Planetology contributes to the elaboration of reference systems and timescales, integrates Belgium in the international reference frames, and studies the interior, rotation, dynamics, and crustal deformation of the Earth and other terrestrial planets and moons of our solar system

The principal activities are grouped into two general themes:

- 1. Space geodesy and timescales with GNSS (Global Navigation Satellite System), and*
- 2. Rotation and interior structure of the Earth and other terrestrial planets and satellites.*

Global Navigation Satellite System (GNSS)

European Center for the monitoring of scientific GNSS data and meta-data

EUREF Permanent GNSS Network (EPN)

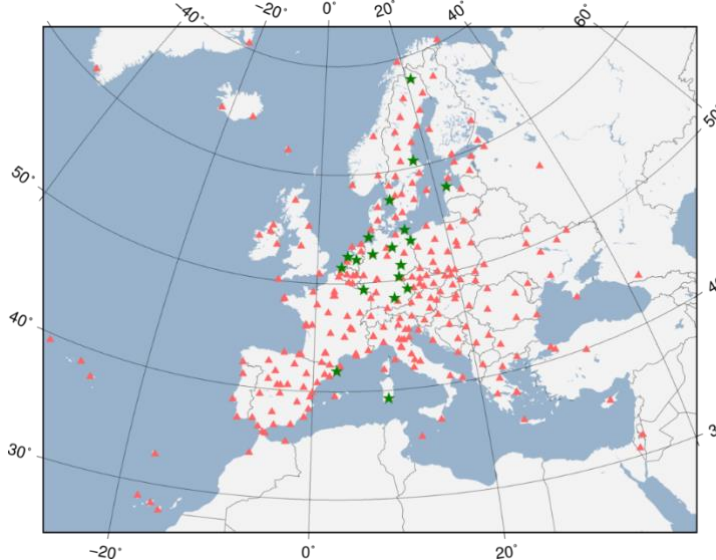
The EUREF¹ Permanent GNSS Network (EPN) maintains and provides access to the European Terrestrial Reference System (ETRS89). ETRS89 is the standard precise GNSS coordinate system throughout Europe. Supported by [EuroGeographics²](#) and endorsed by the [INSPIRE³](#) Directive 2007/2/EC, the ETRS89 forms the backbone for geolocation data on the European territory, both on a national as on an international level. ROB is responsible for the EPN Central Bureau (CB) that performs the daily management of the EPN. In 2016, ROB integrated 19 new stations in the EPN network: 1 in Italy, 3 in Sweden, 1 in Latvia, 3 in the Netherlands, 1 in Spain, and 10 in Germany. The total number of EPN stations is now 294, distributed over 40 countries.

Next to the core EPN network, ROB also collects and validates the standardized station description information of the EPN densification network. As a result, ROB is today providing access to a unique collection of GNSS meta-data for about 1400 European GNSS stations.

A brand new web site for the EUREF Permanent Network (EPN, <http://www.epncb.oma.be/> or <http://www.epncb.eu/>), including the results of our new multi-GNSS monitoring procedures, went on line in Nov. 2016. The web site includes now:

- Improved GNSS data quality checks (multi-GNSS) on both RINEX⁴ 2 and RINEX 3,
- Improved station position time series,
- Improved GNSS data availability and data latency checks on both RINEX 2 and RINEX 3,
- Full implementation of long RINEX 3 station names,
- Extended monitoring of real-time data streams, now also including RTCM3.2⁵ and all 3 regional EPN broadcasters,
- Extended station list with more station metrics,
- More intuitive menu structure to navigate through the web site.

In 2016, the number of users of our EPN web site increased with 20% compared to the previous year. In total, in 2016, the web site had more than 7 million page views.



EPN GNSS tracking stations, status Dec. 2016. Green stars (*) indicate new stations included in 2016.

¹ EUREF is the sub-commission for the European Reference Frame of the International Association of Geodesy (IAG).

² EuroGeographics represents the European national mapping, cadastral and land registry authorities.

³ Infrastructure for spatial information in Europe, a European Union spatial data infrastructure for the purposes of EU environmental policies.

⁴ RINEX – Receiver Independent EXchange Format.

⁵ The Radio Technical Commission for Maritime Services (RTCM) has defined new standard for streaming differential correction data or other kinds of Global Navigation Satellite System (GNSS) data to stationary or mobile users over the Internet.

Welcome !

EUREF Permanent GNSS Network

The EUREF Permanent GNSS Network consists of

- a network of continuously operating GNSS (Global Navigation Satellite Systems, such as GPS, GLONASS, Galileo, Beidou, ...) reference stations,
- data centres providing access to the station data,
- analysis centres that routinely analyze the GNSS data,
- product centres or coordinators that generate the EPN products,
- and a Central Bureau that is responsible for the daily monitoring and management of the EPN.

The network is operated under the umbrella of the IAG (International Association of Geodesy) Regional Reference Frame sub-commission for Europe, [EUREF](#).

All contributions to the EPN are provided on a voluntary basis, with more than 100 European agencies/universities involved. The EPN operates under well-defined international standards and [guidelines](#) which are subscribed by its contributors. These guidelines guarantee the long-term quality of the EPN products.



The primary purpose of the EPN is to provide access to the [European Terrestrial Reference System 89](#) (ETRS89) which is the standard precise GNSS coordinate system throughout

Home page of the new EPN CB web site : <http://www.epnbc.eu/> or <http://www.epnbc.oma.be/>

European Plate Observing System – EPOS

ROB participates to the construction of the European Plate Observing System (EPOS) which is the large European research infrastructure aiming at understanding the Solid Earth through the integration of multi-disciplinary observations (amongst which GNSS). We are, for example, contributing to the development of the framework that will be used for GNSS data discovery and dissemination.

In 2016, the GNSS community defined the future EPOS-GNSS services that will run once EPOS will be operational (2019). For ROB, the agreed-upon EPOS services are a natural follow up of the 20 years of commitment as EPN Central Bureau: ROB will be responsible for the EPOS-GNSS network coordination, the center where all EPOS-GNSS station meta-data are submitted and validated, and the monitoring of the GNSS data quality. ROB is now gradually working towards merging its EPN Central Bureau activities with its future responsibilities in EPOS.

ROB also prepared the draft Consortium Agreement (CA) for the future operational EPOS-GNSS service. The CA is presently under review at the legal departments of the 11 partners. ROB has estimated the total cost of the full EPOS-GNSS service to 1.27M€. The partners that will contribute to this service are committed to cover 75% of this cost from national funding.

At the end of 2016, Belgium became a full member of the EPOS Board of Governmental Representatives (BGR). With this, Belgium has now officially expressed its interest to take on a future member status within EPOS ERIC⁶.

Quick Station Links

[Information](#) [Coordinates](#) [Time Series](#)

Data Quality

(select a station)

Next Meetings

2017-03-14 / 2017-03-16 :
[Munich Satellite Navigation Summit](#) (Munich, Germany)

2017-04-03 / 2017-04-07 :
[GEODETA 2017](#) (Rosario - Santa Fe, Argentina)

2017-04-23 / 2017-04-28 :
[European Geosciences Union General Assembly 2017](#) (Vienna, Austria)

[More ...](#)

Job Opportunities

2017-02-03 :
[Open PhD Candidate on GNSS Satellite Orbit Modelling](#) at AIUB (deadline: 2017-03-31)

2017-01-31 :
[PhD student at Noveltis and Toulouse Business School in Toulouse](#) (deadline: 2017-05-30)

⁶ European Research Infrastructure Consortium

Antarctica

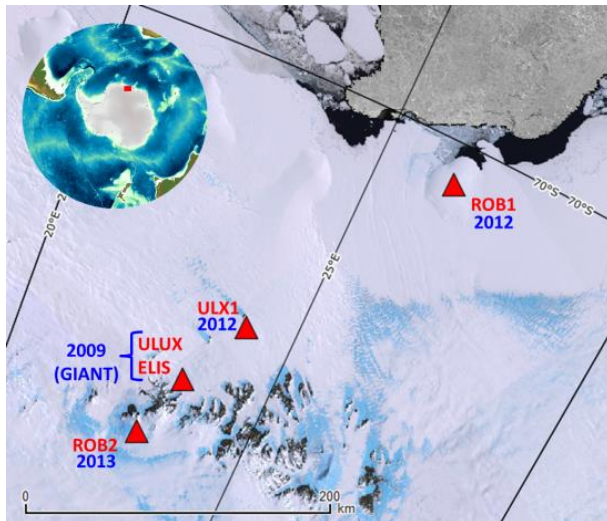
Measuring ground deformations using GNSS

The IceCon⁷ project, which studies the isostatic rebound and snow accumulation in East Antarctica, went into its last year of funding. ROB analyzed the new GNSS data gathered during the BELARE⁸ 2015-2016 mission at, and around the Princess Elisabeth Research Station (PERS) in Antarctica, to update the mean velocities of the Antarctic GNSS stations (see Figure on the right). The results show that the station ROB1, installed on the ice on Derwael ice rise, increases its west-velocity over time. In addition, its subsidence rate decreases each year. The mean subsidence rate is about 1.35 m/year and can be explained by ice and snow compaction, surface thinning and vertical motion of the ice (submergence velocity). It is clear that the length of the observation period as well as (bi) annual signals degrade the accuracy of the estimated velocity. The velocities of the stations ULUX/ELIS, both installed at the PERS, agree within 1 mm/year in all three components. In addition, their up-velocity continues to agree with gravity measurements.

ROB also analyzed the kinematic GNSS data from the BELARE 2015-2016 season to study the ice-shelf channels in East Antarctica. For this purpose, we developed a processing strategy, based on GAMIT-GLOBK software v10.6, able to analyze the GNSS data acquired on the field without any internet connection. The goal was to estimate accurately the positions of geophysical instruments (e.g., the ice-penetrating radar) and to infer the morphology of several ice-shelf channels. This work permitted to show that esker ridges are formed at the surface by sediments deposited by subglacial water conduits.

Ionosphere

In order to investigate the effect of space weather events in the Antarctic region, ROB computed the vertical Total Electronic Content (vTEC) above Antarctica for the period 2009-2016 using GPS and GLONASS data from 96 permanent GNSS stations. The network comprises stations from the International GNSS Service (IGS) as well as the five stations we installed since 2009 around the Princess Elisabeth station in the frame of the GIANT-LISSA (Geodesy for Ice in ANTarctica – Lithospheric and Intraplate Structure and Seismicity in Antarctica) and IceCon (Constraining Ice Mass Change in Antarctica) projects. The computed vTEC was then employed to constrain an empirical model to predict the vTEC every 15-min from the F10.7P solar index⁹ using a least-squares adjustment. Among all the tests, the optimal model to predict the TEC every 15 min presented mean differences with observed values of 0.0 ± 4.5 TECu (2.9 ± 4.5 TECu for the absolute differences). We identified 13 zones where sufficient TEC data are available to constrain the ionospheric climatological models. Then we analyzed three characteristic zones with relevant ionospheric



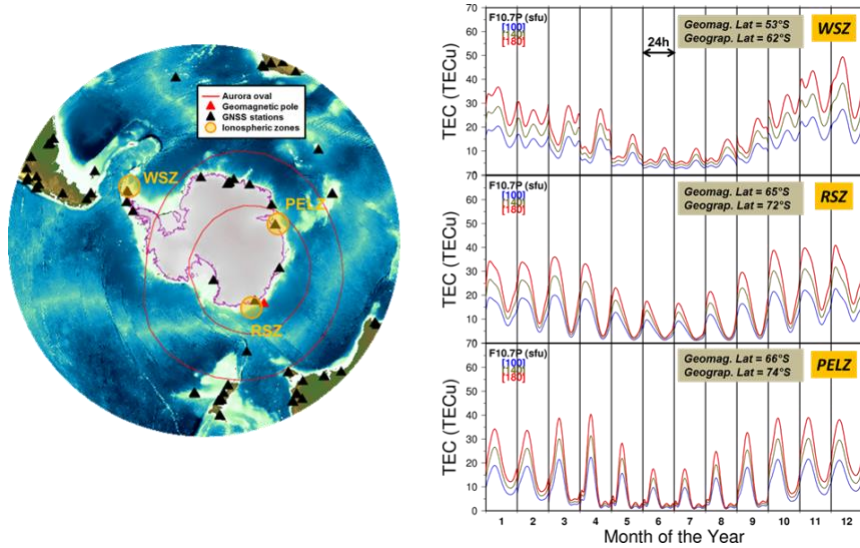
GNSS stations installed in the framework of the IceCon (Constraining Ice Mass Change in Antarctica) and GIANT (Geodesy In ANTarctica) projects (including their installation date).

⁷ IceCon = Land Constraining ice mass changes in coastal Dronning Maud Land, Antarctica, BELSPO SD/CA/06A, collaboration with ULB.

⁸ BELARE = Belgian Antarctic Expeditions

⁹The flux emitted by the Sun changes daily with the sunspot number, and thus also follows the solar cycle. This is observed from the radiation in the 10.7 cm wavelength over the entire solar disk. This value is called F10.7, and F10.7P is computed from averages of continuous routine measurements.

behaviors (see Figure below): the Weddell Sea Zone (WSZ), the Ross Sea Zone (RSZ) and the Princess Elisabeth Land Zone (PELZ). The three zones followed the solar activity and seasonal variations. For the diurnal behaviors, WSZ and RSZ are dependent on the Local Time (LT) mainly with seasonal dependencies. Concerning PELZ, the combination of UTC, LT and Magnetic LT (using geomagnetic coordinates under the dipole approximation) could explain the maximum vTEC values observed. This work will continue in the future in the frame of the GRAPE (GNSS Research and Application for Polar Environment) Expert Group of SCAR (Scientific Committee on Antarctic Research).



Climatological behavior of vTEC above Antarctica. Left: GNSS network used in this study. The black triangles are the GNSS stations processed for the period 2009–2016. In orange are represented the 3 zones presenting the different climatological patterns. Right: Monthly climatological behavior of the TEC over Antarctica over PELZ, RSZ and WSZ for different levels of solar activity: high (red), transition (green) and low (blue) solar activity level.

Improving the knowledge of the Earth's atmosphere

As GNSS signals travel through the Earth's atmosphere, they contain information on the state of the ionosphere and the troposphere. To extract this information from GNSS signals, networks of continuously observing GNSS stations, with well-known station positions, are used. For that purpose, ROB members maintain a network of continuously observing GNSS stations and contribute actively to the elaboration and extension of the European GNSS network, known as the EUREF Permanent Network (EPN). Besides providing positions and velocities of the stations, the GNSS data are used to compute information on the state of the Earth's ionosphere and troposphere.

Troposphere

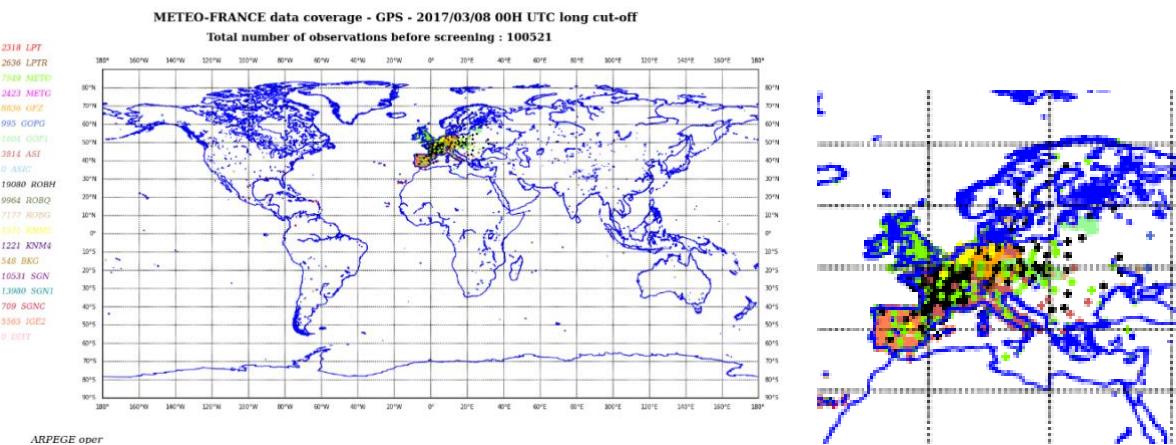
ROB uses GNSS stations for monitoring short-term variations in the tropospheric water vapor (linked to meteorological applications and short-term forecasting) and for assessing long-term behavior of the tropospheric water vapor (linked to re-analysis and climate applications).

Within E-GVAP¹⁰, ROB upgraded its services to use operationally the latest Bernese GNSS software 5.2 and the latest state-of-the-art modelling techniques. In addition to its legacy service based on more and more European GNSS stations and serving hourly data assimilation in European NWP (Numerical Weather Prediction) models, ROB offers now two additionally products:

- Tropospheric products based on an hourly analysis of a world-wide GNSS network. This product is used for data assimilation in global NWP models;

¹⁰ E-GVAP= EIG (Economic Interest Grouping) EUMETNET (network of European National Meteorological Services) GNSS Water Vapour Program.

- Tropospheric products based on a 15-min updated analysis of a GNSS network centered over the BENELUX and UK. This product is used within rapid-update cycle data assimilation for numerical now-casting applications.



The monitoring of the data assimilation system at Météo France shows that the solutions from the new generation of the three tropospheric monitoring systems (European hourly ‘ROBH’, sub-hourly ‘ROBQ’ and global ‘ROBG’) built at ROB are used for data assimilation. It also shows the relatively high number of estimates provided by ROB w.r.t. to other analysis centers and w.r.t. the total number of ‘observations’ (Status: 8 March 2017). Right: zoom on the figure on the left.

Within the CORDEX.be¹¹ project, ROB analyzed historical GNSS observations (period 2000-2010) and established a GNSS-based climate-quality dataset. This dataset is accessible to all partners to validate their high-resolution climate model runs. Aside from CORDEX.be, ROB also collaborated with RMI to validate their climate model ALARO-0 when coupled with the SURFEX land surface scheme using GNSS-based Integrated Water Vapor (IWV) time series elaborated from the IGS tropospheric product. First results over (only) 6 years showed a good agreement between GNSS-based and model IWV values (i.e. within ± 1 mm of IWV).

In the framework of the COST Action ES1206 GNSS4SWEC¹², ROB was nominated co-editor of a special issue jointly organized between Atmospheric Measurement Techniques (AMT), Atmospheric Chemistry and Physics (ACP), and Annales Geophysicae (ANGE). ROB also co-led a work package on “Homogenization of tropospheric time series”, welcomed a STSM – Short-Term Scientific Mission (tropospheric synthetic datasets for homogenization benchmarking), and co-organized with RMI a workshop on this subject (under the umbrella of the STCE).

Finally, ROB scientists were nominated vice-chair of two IAG working groups, one on “Real-time GNSS tropospheric products” (IAG WG 4.3.7) and the other on “GNSS tropospheric products for Climate” (IAG WG 4.3.8). These two working groups intend to continue the work started within the COST Action ES1206 GNSS4SWEC (finishing in spring 2017), while broadening these activities in a larger international context.

Ionospheric monitoring and Solar Radio Bursts

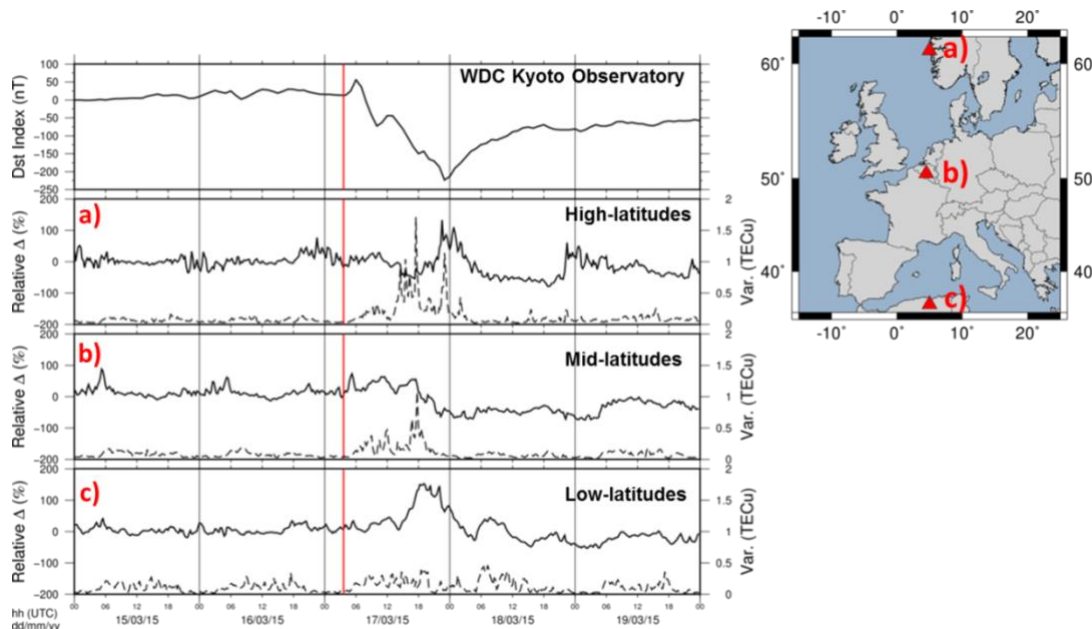
ROB is involved in the Real Time Ionosphere Monitoring - Working Group (RTIM-WG) of the International Association of Geodesy (IAG). The goals of this group are to (1) summarize the current status of Real-Time (RT) Ionosphere Monitoring; (2) compare existing Real-Time Ionosphere Monitoring approaches from different perspectives for a specific period (in 2016 the Saint-Patrick

¹¹ CORDEX.be: BRAIN-BE project “COmbining Regional Downscaling EXPertise in Belgium: CORDEX and Beyond” (CORDEX.be) aiming to gather the major actors (ROB, RMI, BISA, RBINS, VITO, UCL, KUL, ULg) involved in climate research in Belgium and to foster the establishment of climate services in Belgium.

¹² COST Action ES1206 GNSS4SWEC: “Advanced Global Navigation Satellite Systems tropospheric products for monitoring severe weather events and climate”.

Storm of the 17 March 2015 was investigated); (3) develop a procedure to automatically compare on a daily basis a subset of real-time ionospheric products in a common compatible format (i.e. IONEX format); (4) validate the products with external data sources, such as dual-frequency altimeters; and (5) open the discussion towards new concept(s) on RT Ionosphere Monitoring.

In 2016, ROB ionospheric warning system has communicated four ionospheric events to the public via the web site www.gnss.be and the STCE newsletter. In addition, the software that routinely delivers these products was optimized and tested with Galileo data.



Saint Patrick storm 2015. DST¹³ index and ROB-TEC products for the period March 15 to March 19, 2015. The red line is the storm onset of the intense geomagnetic storm on March 17. Top: the DST index as delivered by the WDC Kyoto Observatory. Bottom: the three time-series extracted from ROB-TEC maps at three different geographic locations shown on the map (top-right). The bold line represents the relative differences between the ROB-TEC values and the median from the 15 previous days. The dashed line is the variability of the vTEC estimated in nearly real time.

ROB continued to investigate the impact of Solar Radio Bursts (SRB) on the GNSS signal reception. It maintains now in near-real time a 4-level warning system that assesses the impact of SRB events on GNSS and informs users about their potential harm on GNSS applications. The private company Fugro started to use our SRB alert system, but no SRB event affecting GNSS occurred in 2016. In addition, the method was tested in other regions (South America and Africa) than Europe for the SRB of the 4th November 2015. Results showed that in South America, the impact of the SRB was high, whereas in Africa the impact was comparable to the one in Europe.

> Level	> GNSS ΔC/N0 Fade	> Effect
> Quiet	> < -1dB-Hz	> None
> Moderate	> > -1 dB-Hz	> SRB detected but should not impact GNSS applications
> Strong	> > -3 dB-Hz	> Potential impact on GNSS applications
> Severe	> > -10 dB-Hz	> Potential failure of the GNSS receivers

Index level for SRBs that can affect GNSS signal reception

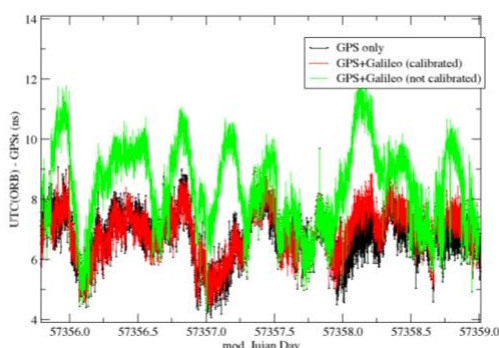
¹³ The Disturbance Storm Time (DST) index gives information about the strength of the [ring current](#) around Earth caused by solar protons and electrons.

Time – Time Transfer

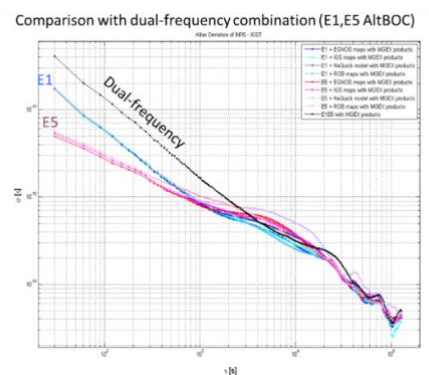
Precise time transfer for timescales

ROB Service 1 works on time-transfer, i.e. remote clock comparisons, an essential part of the realization of timescales like the Universal Time Coordinated (UTC), based on an ensemble of atomic clocks distributed in the world and which must be continuously compared relative to each other. ROB has developed tools available to the scientific community and based on GNSS (Global Navigation Satellite System). The principle consists in connecting the atomic clocks that we want to monitor to GNSS receivers. By analyzing the GNSS observations, it is possible to determine the synchronization error between the clock connected to the GNSS receiver and the satellite clocks. These satellite clocks serve as a reference and allow then to compare the ground clocks to each other. This method is constantly improved over the years. While only GPS was used in the past, in 2016, ROB developed and distributed to the time laboratories a new R2CGGTTS (RINEX to Common GNSS Generic Time Transfer Standard) software (version 7.1) allowing the analysis of RINEX 3 files, containing data from satellites from three constellations: GPS, GLONASS and Galileo (US, Russian and European GNSS systems).

In parallel, ROB Service 1 studied the possibilities of the Galileo signals for time transfer, and especially the broadband Galileo E5 AltBOC (Alternative Binary Offset Carrier modulation) code, characterized by a very low noise and multipath. It was shown that the E5 AltBOC code improves the frequency steering for averaging times shorter than 15 Minutes, but for synchronization on UTC disseminated by Galileo, E1 should be preferred to E5 AltBOC because of the uncertainties on the ionospheric corrections of which the impact is larger than the noise difference between E1 and E5 AltBOC.



Time differences between UTC (ORB) and GPS Time as computed from GPS only or GPS+Galileo for a receiver calibrated or not calibrated.

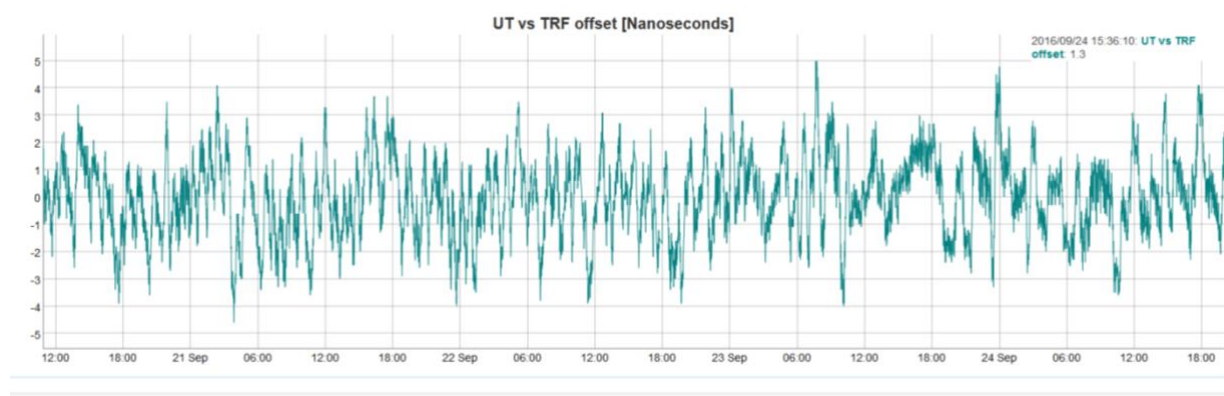


Stability (given by the Allan deviation) of the frequency of UTC (ORB)-GST as computed using either E1, E5 AltBOC or a dual-frequency combination.

It was also demonstrated that, when using the combination of GPS and Galileo satellites for synchronization or frequency steering, due to the different hardware delays of GPS and Galileo signals, the use of the Galileo-to-GPS-Time-Offset (GGTO) broadcast in the navigation message degrades the solution, except when a dual-frequency combination is used and when the receiver has been calibrated for GPS and Galileo. In all other cases, the GGTO should rather be determined at the same time as the position and clock solution in the data analysis).

Time services to end-users

ROB Participated to the ambitious project DEMETRA, “DEMonstrator of EGNSS (European GNSS) services based on Time Reference Architecture”, a project developed in the frame of the H2020 European research and innovation program to demonstrate the feasibility for providing EGNSS early Time services to end-users (<https://www.demetratime.eu>). In that frame, ROB developed a remote synchronization system based on real-time GNSS streaming and common view. Using this service, the user has its low cost oscillator synchronized in real time within five nanoseconds of the remote reference. The figure below provides the performance of the system, showing the difference between the user clock located at a distance of 700 km of the reference clock.



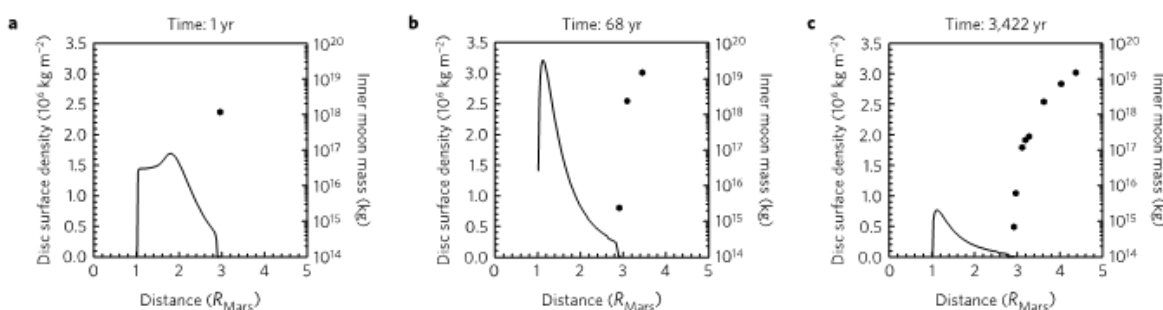
Time differences between the user terminal at ORB and the reference in Turin as measured from GPS time transfer.

ROB Service 1 was also responsible for the monitoring of the time signals disseminated by EGNOS (European Global Navigation Satellite Systems) and by Galileo, and provided advises on the calibration corrections to be introduced in the signals in order to increase the accuracy of timing solutions based on Galileo and EGNOS.

Earth Rotation, Geodesy and Geophysics of Terrestrial Planets

The origin of the Martian moons: Theory of accretion

Phobos and Deimos, the two small satellites of Mars, are thought either to be asteroids captured by the planet or to have formed in a disc of debris surrounding Mars following a giant impact. Both scenarios, however, have been unable to account for the current Mars system. We used numerical simulations to suggest that Phobos and Deimos accreted from the outer portion of a debris disc formed after a giant impact on Mars of a smaller body of one fourth to one third the size of Mars that might have occurred 4 Gyr ago. In our simulations, the material in the debris disk is concentrated at close distance to Mars (below the Roche limit at 3 Mars' radii) and the larger moons form from material in the denser inner disc and migrate outwards due to gravitational interactions with the disc. They capture the smaller debris of the outer disk in mean motion resonances, facilitating close encounters between them, and so accretion into larger bodies. The inner moons below the synchronous orbit (at 6 Mars radii) fall back to Mars after about 5 million years due to the tidal pull of the planet, after which the two outer satellites evolve into Phobos- and Deimos-like orbits. The proposed scenario can explain why Mars has two small satellites instead of one large moon. Our model predicts that Phobos and Deimos are composed of a mixture of material from Mars and the impactor. A paper describing this study was published in *Nature Geoscience*.

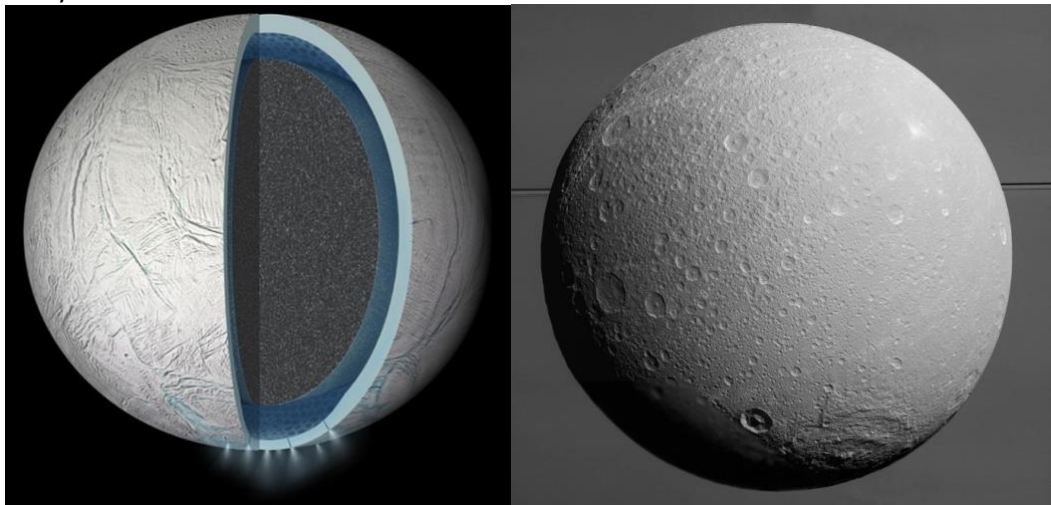


Formation of moons from the inner disc below the Roche limit. a–c, Time evolution of the surface density of the inner disc (solid line) and the masses of the moon (solid black circles) as a function of the distance from Mars. a, After only one year, disc material crosses the Roche limit (at about 3 Mars radii) and conglomerates into moons. b, In less than one century a few moons are produced and migrate outwards due to the gravitational interactions with the disc. c, The most massive moon reaches the maximal distance of about 4.4 Mars radii after approximately 3,400 years.

Oceans of the mid-sized icy moons Enceladus and Dione

In 2015, small variations in the rotation rate of the mid-sized icy moon Enceladus have been observed by an American team. These librations are due to the gravitational torque of Saturn on the non-spherically symmetric mass distribution of the satellite. ROB Service 1 demonstrated that the observed libration amplitude of Enceladus indicates that the moon has a global subsurface ocean and that the ice shell is on average between 14 km and 26 km thick. Previous gravity-topography data predicted a thicker ice shell for Enceladus, in contradiction of the thin shell implied by recent libration data. These studies, however, used a model to relate gravity to topography by assuming isostasy that loses its validity at the largest scale for which there are data about Enceladus. We developed a new approach to spherical isostasy based on self-consistent gravito-elastic equations and by imposing minimization of the crustal deviatoric stress. By applying this model to Enceladus, it could be shown that a correct gravity-topography analysis predicts the same thin crust for Enceladus as estimated from librations. The crust is much thinner (about 7 km) at the south pole where geysers

erupt. Applying the same approach to Saturn's moon Dione resulted in the first prediction of a present-day ocean within this satellite.



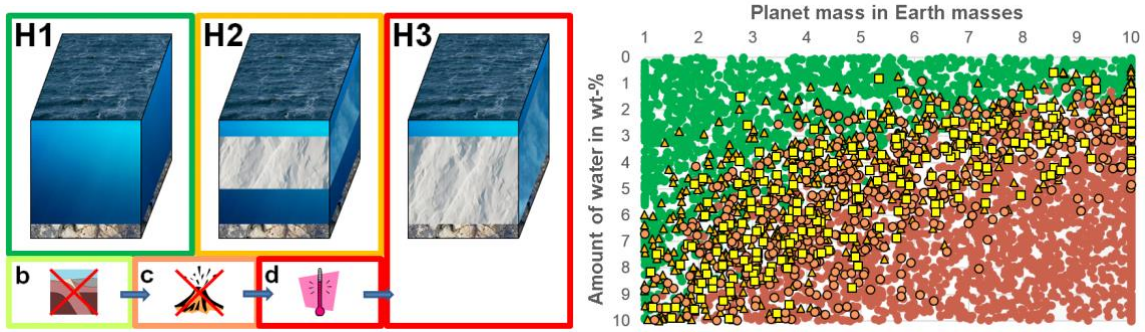
Left: interior model of Enceladus resulting from applying a new spherical isostasy approach to gravity-topography data, and compatible with libration data. The rocky core is surrounded by a deep ocean and a thin ice shell. The ice shell is 23 km-thick on average, but only 7 km-thick at the south pole where geysers erupt. **Right:** Mosaic view of Dione, now suspected to harbor a global subsurface ocean under a 100 km-thick ice shell (image credit: NASA/JPL-Caltech and Space Science and space science institute).

A newly developed model to calculate tidal dissipation in subsurface oceans was applied to Enceladus. The results show that Enceladus's crust strongly damps tides within the underground ocean, and that oceanic dissipation can only be large if the ocean is very shallow, in which case it could protect it from freezing.

Habitability of water-rich exoplanets

Water is necessary for the origin and survival of life as we know it. In the search for life-friendly worlds, water-rich planets therefore are obvious candidates and have attracted increasing attention in recent years. The surface H₂O layer on such planets (containing a liquid water ocean and possibly high-pressure ice below a specific depth) could potentially be hundreds of kilometers deep depending on the water content and the evolution of the proto-atmosphere.

We studied possible constraints for the habitability of deep water layers and introduced a new habitability classification (see the figure below) relevant for water-rich planets (from Mars-size to super-Earth-size planets). A new ocean model was developed that is coupled to a thermal evolution model of the mantle and core. This interior structure model takes into account depth-dependent thermodynamic properties and the possible formation of high-pressure ice. The results show that heat flowing out of the silicate mantle can melt an ice layer from below (in some cases episodically), depending mainly on the thickness of the ocean-ice shell, the mass of the planet, the surface temperature and the interior parameters like radioactive mantle heat sources (yellow in the figure below). The high pressure at the bottom of deep water-ice layers could also impede volcanism at the water-mantle boundary for both stagnant lid and plate tectonics silicate shells. It is concluded that water-rich planets with a deep ocean, a large planet mass, a high average density or a low surface temperature are likely less habitable than planets with an Earth-like ocean. The study (Noack et al., 2016, Icarus) was highlighted by Nature Physics and New Scientist, and has been the most downloaded paper of Icarus in 2016.



Left: habitability classes (H1 – habitable, H2 – restricted habitable, H3 – likely uninhabitable). Right: Monte-Carlo simulations where the habitability classes occur.

Atmospheric Entry and Descent of the ESA Schiaparelli lander

We finalized data processing tools to extract atmospheric conditions on Mars from atmospheric Entry, Descent, and Landing (EDL) vehicle flight data. One of these tools, which uses heat shield pressure data to derive atmospheric density, pressure, and temperature, was demonstrated with flight data from the 2012 Mars Science Laboratory (MSL) entry vehicle. The main focus of this work in 2016 was on the ExoMars mission that arrived at Mars in October 2016.

The ESA/Roscosmos ExoMars 2016 mission consists of an orbiter (Trace Gas Orbiter / TGO) and a landing platform. The 2016 lander is named EDM for Entry, Descent, and Landing (EDL) Demonstrator Module. The EDM vehicle recorded flight data along its trajectory, including accelerometer and gyroscope inertial measurements, and heat shield pressure data. EDM also transmitted a UHF radio signal that was received by TGO and a ground based radio antenna in Puna, India. From these observations, in situ atmospheric



ExoMars 2016 EDM: heat shield (left) and back shell (right) from Airbus Defense & Space (image credit: ESA).

conditions along the flight trajectory can be derived: profiles of temperature, density, and pressure. Benefits of such atmospheric profiles are their large altitude range and high spatial resolution, able to resolve atmospheric fluctuations difficult to observe remotely. Over the past few years, ROB has developed post-flight analysis tools for this purpose. Unfortunately, EDM did not perform a successful landing and failed shortly after parachute deployment. No more radio contact or flight data are available after this point, but the successful trajectory covers altitudes from about 120 km down to 10 km. Additional complications include one failed heat shield pressure sensors (out of four), and the loss of radio signal due to plasma blackout between 74 km and 27 km. With the available flight observations, the reconstruction of the atmospheric conditions must rely more on radio Doppler observations and trajectory simulation than would have been the case for a completely successful EDL. Preparatory Kalman filter tools for this purpose have been developed at ROB.

The radio links were analyzed and preliminary reconstructions of the trajectory were performed. We computed, amongst other things, the reconstruction of the trajectory using the tools previously

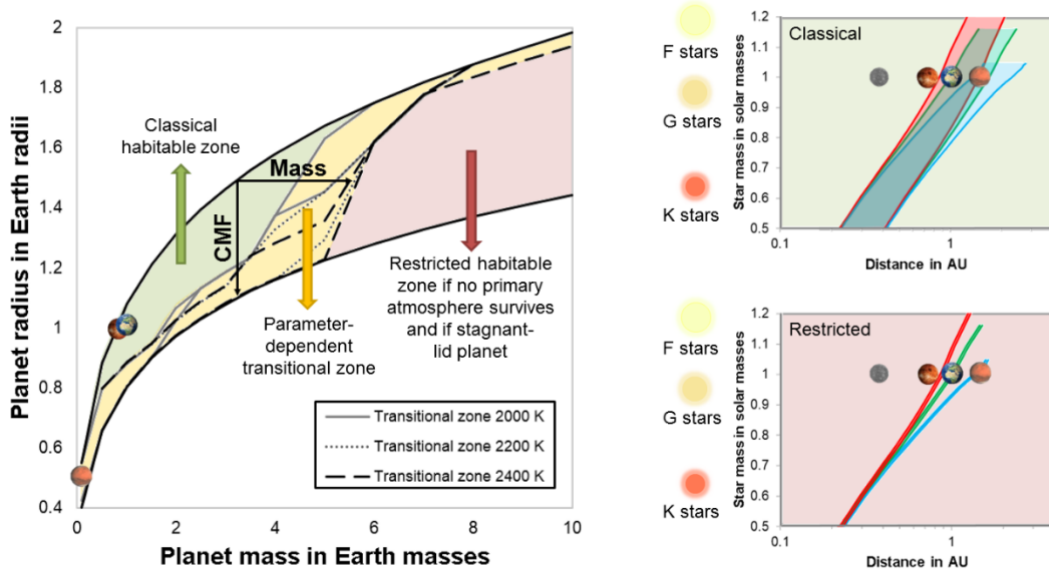
developed, as well as the angles between the lander-to-receiver line-of-sight and various significant vectors (inertial velocity, symmetry axis of the lander). These investigations are meant to help better understand the unexpected behavior of the Schiaparelli lander.

Geophysical limitations for the habitability of terrestrial planets

Rocky exoplanets are typically classified as potentially habitable planets, if liquid water exists at their surface. The latter depends on several factors like the abundance of water but also on the amount of available solar energy and greenhouse gases in the atmosphere for a sufficiently long time for life to evolve. The range of distances to the star, where surface water might exist, is called the habitable zone. We studied the effect of the planet interior of stagnant-lid planets on the formation of a secondary atmosphere through outgassing that would be needed to preserve surface water.

The results show that volcanic activity and associated outgassing in one-plate planets is strongly reduced after the magma ocean outgassing phase if their mass and/or core-mass fraction exceeds a critical value. As a consequence, the effective outer boundary of the habitable zone is closer to the host star (red background color in the figure below) than suggested by the classical habitable zone definition (green background color in the figure below). This sets an important restriction to the possible surface habitability of massive rocky exoplanets, if they did not keep a substantial amount of their primary atmosphere and that they are not in the plate tectonics regime.

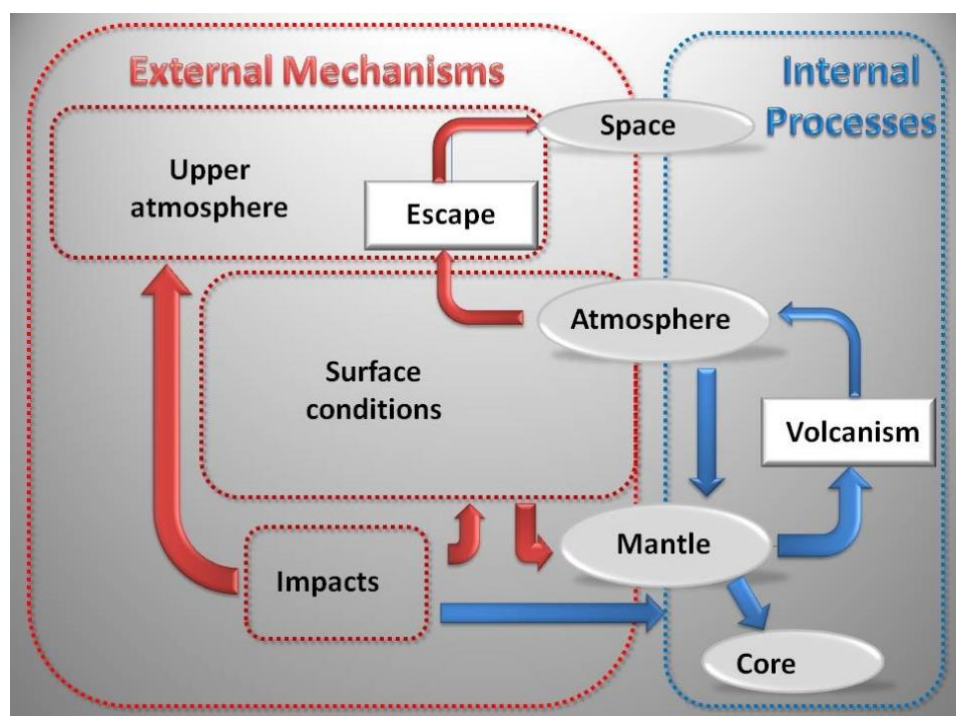
Habitable zone limitation by insufficient outgassing



Left: Sketch of a mass-radius diagram indicating the mass-radius range, where the classical HZ definition can be applied (green area), the range where the HZ may be restricted due to limited outgassing (red area) and the transitional regime in-between (yellow area). Black arrows indicate the influence of mass and core-mass fraction (CMF) on the transition from classical to restricted HZ definition. **Right:** Habitable zone without constraints (top) and without greenhouse gases (bottom) at different stellar ages 0 Gyr (red lines), 4.5 Gyr (green lines) and 10 Gyr (blue lines) using the moist and maximum green-house effect limits by Kopparapu et al. (2013, *The Astrophys. J. Letters*). The green and red background colors correspond to the colored areas in the left plot.

Evolution of the atmosphere and interior of Venus due to large impacts

We numerically investigated the effects of a single large impact, during either the Late Veneer or the Late Heavy Bombardment, on the evolution of the mantle and atmosphere of Venus. Single vertical impacts are simulated as instantaneous events affecting both the atmosphere and mantle of the planet by (i) eroding the atmosphere, causing atmospheric escape and (ii) depositing energy in the crust and mantle of the planet. The main impactor parameters include timing, size/mass, velocity and efficiency of energy deposition. We observe that impact erosion of the atmosphere is a minor effect compared to melting and degassing triggered by energy deposition in the mantle and crust. We are able to produce viable pathways that are consistent with the present-day Venus, especially for large Late Veneer Impacts. Small collisions (<100 km radius) have only local and transient effects. Medium-sized impactors (100–400 km) do not have much more consequence unless the energy deposition is enhanced, for example by a fast collision. In that case, they have comparable effects to the largest category of impacts (400–800 km): a strong thermal anomaly affecting both crust and mantle and triggering melting and a change in mantle dynamics patterns. Such an impact is a global event and can be responsible for volcanic events focused at the impact location and near the antipode. Depending on the timing of the impact, it can also have major consequences for the long-term evolution of the planet and its surface conditions by either (i) efficiently depleting the upper mantle of the planet, leading to the early loss of its water or (ii) imposing a volatile-rich and hot atmosphere for billions of years.



Mechanisms and feedbacks between layers in a terrestrial planet: current state of the model.

Seismology and Gravimetry

The main mission of the Operational Directorate Seismology and Gravimetry is studying seismic activity, its causes and its consequences in Western Europe. In support of this scientific research and to provide the authorities, the media and the public with relevant information about the seismic activity in real time in our region, this operational direction develops and maintains a network of seismic monitoring in Belgium

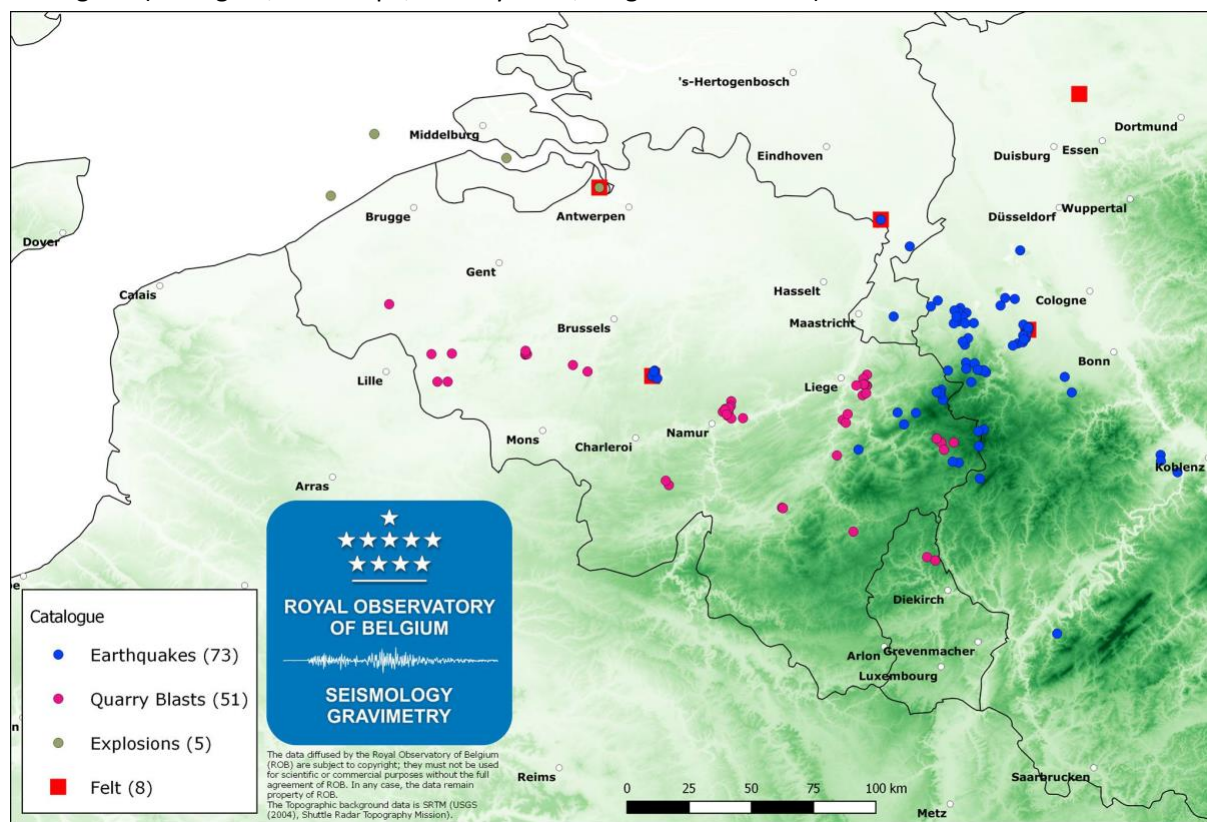
Seismic activity

In 2016, 73 earthquakes occurred in a zone between 0° and 10°E longitude and 47° and 53°N latitude. During the same period, the Royal Observatory of Belgium (ROB) measured 15 induced events, 51 quarry blasts and 5 controlled explosions. The catalogue is complete for natural earthquakes ($ML \geq 1.0$) and contains a selection of quarry blasts and earthquakes induced by human activities, e.g. linked to (rock) mass removal in open pit mines. In 2016, there were at least 4 measurable explosions at sea or close to the Belgian shore. Explosions are performed by the Belgian Army to destroy WW1 and WW2 bombs. The fifth explosion measured was linked to the destruction works of the docks along the Schelde in Antwerpen. This explosion, 5 seismic events and 2 induced events were felt by the local population in 2016.

The five felt earthquakes occurred in Court-Saint-Etienne on 3 February (magnitude $ML=1.2$), in Stramproy on 11 August (NL, $ML=1.6$), in Nörvenich on 4 November (DE, $ML=2.8$), in Dole on 3 December (FR, $ML=4.2$) and in St-Goar on 22 December (DE, $ML=2.7$). The Court-Saint-Etienne event was felt only very locally (2 km radius). The felt induced events occurred in Germany: south of Bremen on 22 April (DE, $ML=2.9$) and Königshardt on 28 May ($ML=2.8$). These events were felt by the local population who spontaneously answered the questionnaire on the ROB-BNS (University of Cologne) common macroseismic inquiry website.

The explosion in Antwerpen was felt – or heard – locally and 54 inquiries were submitted. The geolocation of the intensity data shows that the explosion was mostly felt in the south of Antwerpen, east of the Schelde. This location is close-by the explosion site and also downwind, which influences the propagation of sound waves in the atmosphere. The explosion was strong enough to be measurable up to Membach, the easternmost ROB permanent seismic station.

For comparison, last year in 2015, 52 earthquakes occurred in and around Belgium. The largest was located in Ramsgate on 22 May 2015 (United-Kingdom, magnitude $ML=4.1$) and two events were felt in Belgium (Ramsgate, and in Spa, 13 May 2015, magnitude $ML=2.9$).



Negative magnitude???

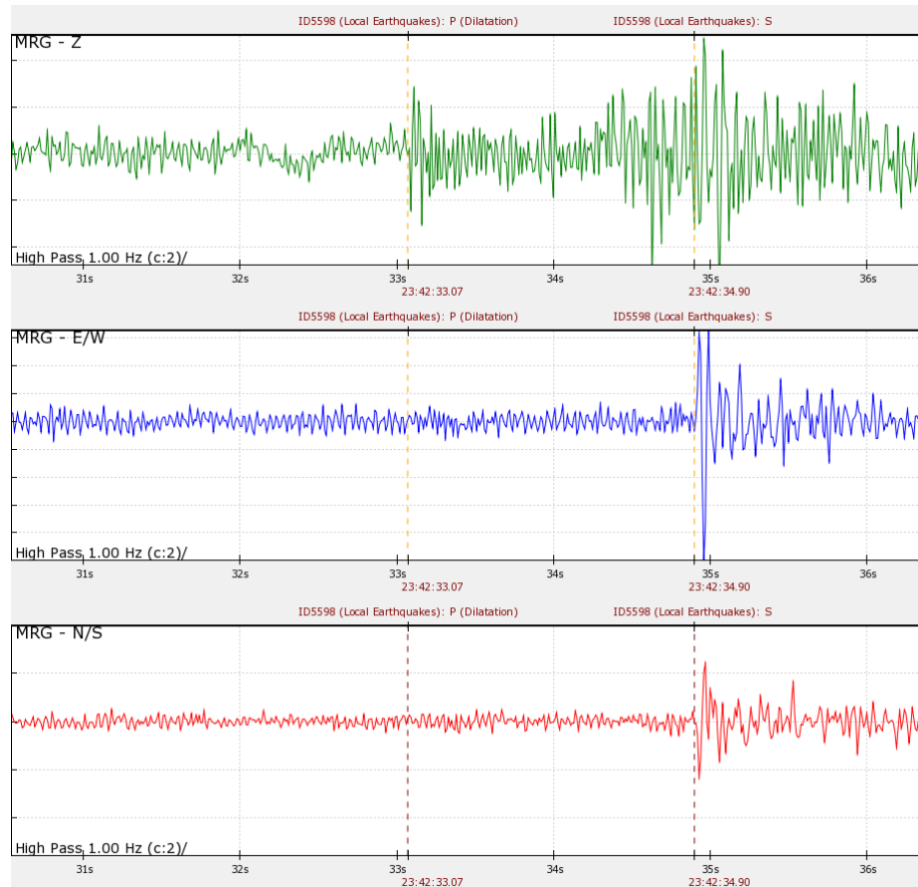
On December 4, 2016, A magnitude -0.1 earthquake occurred in Eupen (<http://www.seismologie.be/en/seismology/earthquakes-in-belgium/wk1x3dv16>). Why can a magnitude be negative?

This is because a magnitude 0 earthquake corresponds at depth to a very small displacement on a very small fault surface. Hence seismic waves that have small amplitudes are only recorded at short distance from the hypocenter and are not felt by humans.

Magnitude calculations are based on a logarithmic scale, so a ten-fold drop in amplitude decreases the magnitude by 1.

For example, a magnitude 1 earthquake corresponds to a vertical displacement of the ground of about 25 nanometers (or billionths of a meter) 10 km away from the earthquake source. In that case, the signal would be:

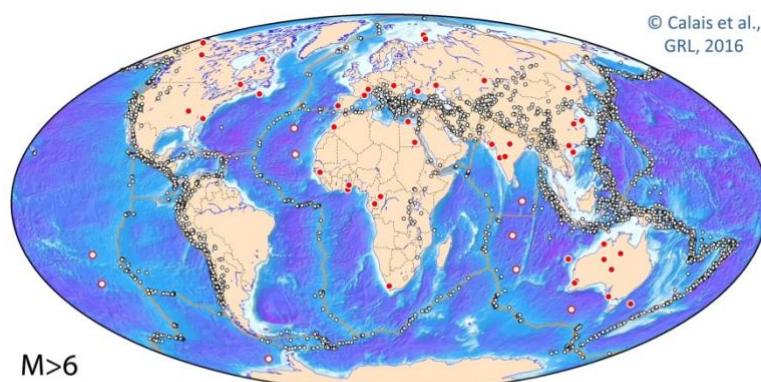
- 10 times larger (250 nanometers) for a magnitude of 2.0;
- 10 times less (2.5 nanometers) for a magnitude of 0.0;
- 100 times less (0.25 nanometers) for a magnitude -1.0.



December 4, 2016, magnitude -0.1 earthquake in Eupen, recording at the Mont Rigi station, 15 km far from the hypocentre.

A New Paradigm for Large Earthquakes in Stable Continental Plate Interiors

Large earthquakes within stable continental regions (SCR) show that significant amounts of elastic strain can be released on geological structures far from plate boundary faults, where the vast majority of the Earth's seismic activity takes place. SCR earthquakes show spatial and temporal patterns that differ from those at plate boundaries and occur in regions where tectonic loading rates are negligible. However, in the absence of a more appropriate model, they are traditionally viewed as analogous to their plate boundary counterparts, occurring when the accrual of tectonic stress localized at long-lived active faults reaches failure threshold. Here we argue that SCR earthquakes are better explained by transient perturbations of local stress or fault strength that release elastic energy from a prestressed lithosphere. As a result, SCR earthquakes can occur in regions with no previous seismicity and no surface evidence for strain accumulation. They need not repeat, since the tectonic loading rate is close to zero. Therefore, concepts of recurrence time or fault slip rate do not apply. As a consequence, seismic hazard in SCRs is likely more spatially distributed than indicated by paleoearthquakes, current seismicity, or geodetic strain rates.



M>6

Les grands cercles montrent les séismes intraplaques de magnitude M>6: rouges en régions continentales stables, blancs pour les régions océaniques stables

De grote cirkels tonen M>6 intraplaat aardbevingen: rood voor stabiele continentale regio's, wit voor stabiele oceanische regio's

Large circles show M>6 intraplate earthquakes: red for stable continental regions, white for stable oceanic regions

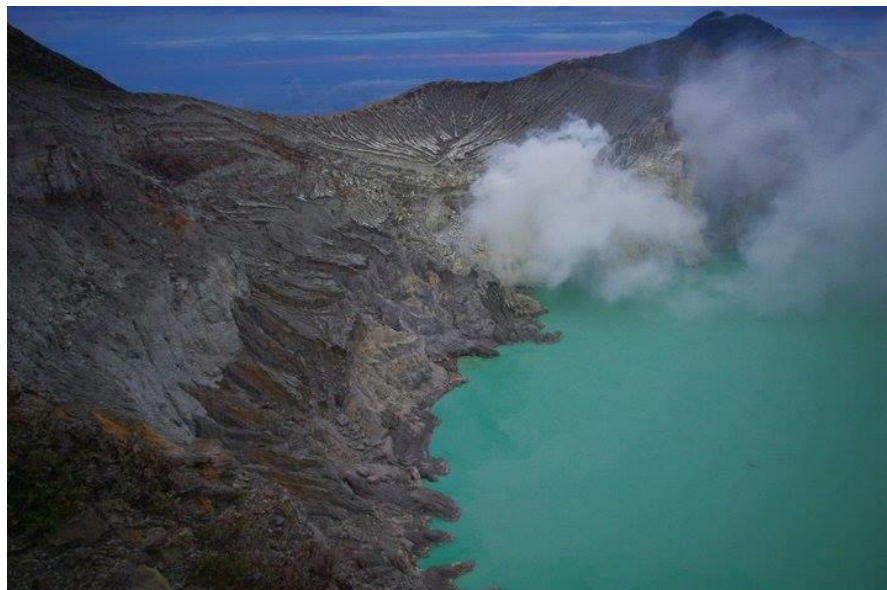
Localities where information is reported for the 3 December 1828 earthquake (published in J. Seismology)

Stratification at the Earth's largest hyperacidic lake and its consequences

Volcanic lakes provide windows into the interior of volcanoes as they integrate the heat flux discharged by a magma body and condense volcanic gases. Volcanic lake temperatures and geochemical compositions therefore typically serve as warnings prior to eruptions and support decision-making of volcano agencies.

Until now, hot hyper-acidic lakes were considered too convective to allow any heterogeneity within their waters. Kawah Ijen volcano, featuring the largest hyperacidic lake on Earth (volume of 27 million m³), is in fact homogeneous than previously thought. Hourly temperature measurements reveal the development of a stagnant layer of cold waters (<30 °C), overlying warmer and denser water (generally above 30 °C and density 1.083 kg/m³). Examination of 20 yrs of historical records and temporary measurements show a systematic thermal stratification during rainy seasons.

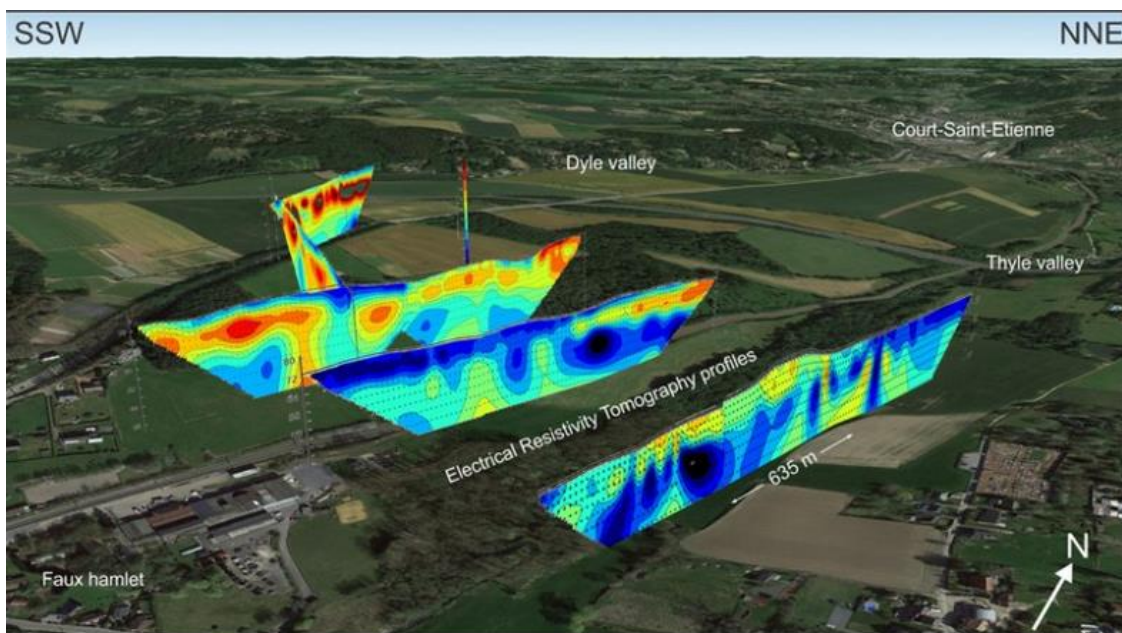
Importantly, every year at the end of the rainy season, this stratification is ruptured causing a sudden release of dissolved gases below the cold water layer. This rupture appears to generate a lake overturn, i.e. limnic eruption highlighting a new hazard for these extreme reservoirs. Even a minor non-volcanic event, such as a heavy rainfall or an earthquake, may act as a trigger. Spectacular degassing occurs when the dissolved gases, progressively stored during the rainy season, are suddenly released. These findings challenge the homogenization assumption at acidic lakes and stress the need to develop appropriate monitoring setups.



The aciditic lake in the Kawah Ijen volcano

Visualizing Cross-Sectional Data in a Real-World Context

If you could fly around your research results in three dimensions, wouldn't you like to do it? Visualizing research results properly during scientific presentations already does half the job of informing the public on the geographic framework of your research. Many scientists use [Google Earth™](#) mapping service because it's a great interactive mapping tool for assigning geographic coordinates to individual data points, localizing a research area, and draping maps of results over Earth's surface for displaying the results in three dimensions. Yet scientists often do not fully explore the Google Earth platform. K. Van Noten shows that combining the capabilities of an open-source drawing tool, i.e. Sketchup Make, with Google Earth allows researchers to visualize real-world cross-sectional data in three dimensions. The paper also includes an easy video tutorial to guide the user through the plotting process. This tool may give research results a better spatial visibility and allows more-dynamic scientific presentations.

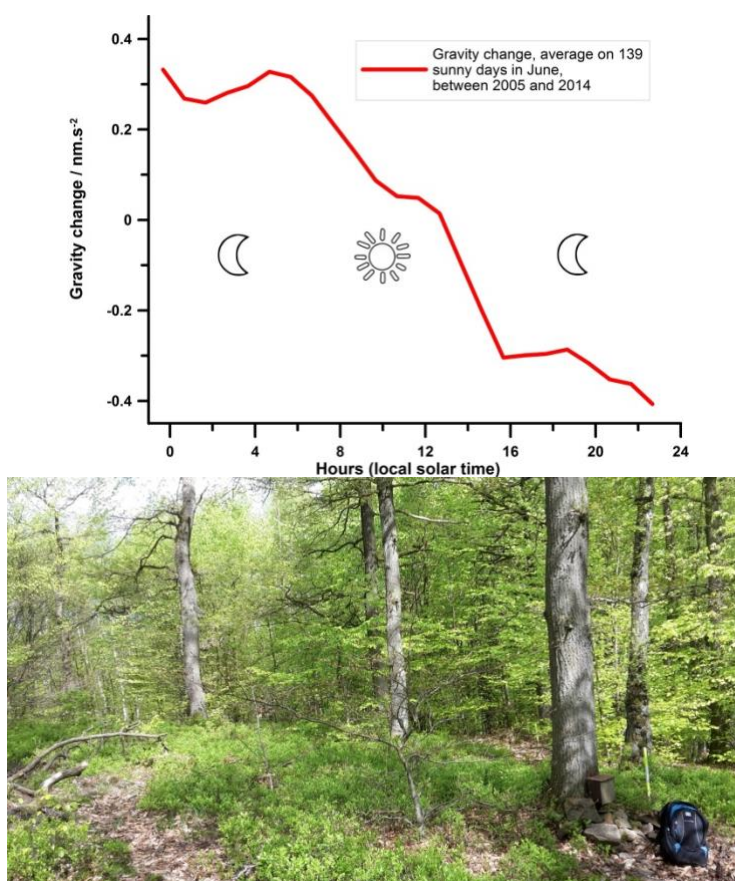


Parallel and crossing two-dimensional electrical resistivity tomography profiles obtained in search of potential surface expressions of the 2008–2010 seismic swarm in the Brabant Massif, Belgium.

Transpiring forest influences gravity

Evapotranspiration (ET) controls the flux between the land surface and the atmosphere. Assessing the ET ecosystems remains a key challenge in hydrology. We have found that the ET water mass loss can be directly inferred from continuous gravity measurements: as water evaporates and transpires from terrestrial ecosystems, the mass distribution of water decreases, changing the gravity field. Using continuous superconducting gravity measurements, we were able to identify daily gravity changes at the level of, or smaller than, $10^{-9} \text{ nm s}^{-2}$ (or 10^{-10} g) per day. This corresponds to 1.7 mm of water over an area of 50 ha. The strength of this method is its ability to enable a direct, traceable and continuous monitoring of actual ET for years at the mesoscale with a high accuracy.

Van Camp et al recently proposed a novel way to measure mesoscale evapotranspiration using continuous gravity measurements. As water evaporates and transpires from terrestrial ecosystems, the mass distribution of water decreases; this can be detected using contemporary, precise gravity monitoring instruments.



Gravity water content, or soil moisture (blue, in percent) and inverted gravity signal (red, in nm s^{-2} ; the actual gravity signal increases because the gravimeter is underground, below the surface soil moisture). Time is in hours (local solar time). Stacked values for 139 dry days; stacking is performed in the months of June from 2005 to 2014. Between 4:40 and 17:40 the gravity water content (or soil moisture) diminishes by -0.60 ± 0.02 percentage point and gravity increases by $0.7 \pm 0.1 \text{ nm/s}^2$, which is equivalent to $1.7 \pm 0.3 \text{ mm}$ of water. The photography shows the forest above the Membach station where the authors performed their study.

Our expertise in *Nature Physics*

How and why does gravity 'g' vary? Why do we measure it? How do we measure gravity accurately? See our paper in *Nature Physics*, which highlights our expertise in gravimetry.

measure for measure

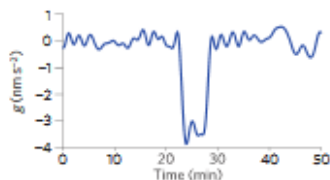
The slightness of gravimetry

Michel Van Camp and Olivier de Viron are attracted to the fluctuations in the Earth's gravitational pull.

When asked to give his age, the French humourist Alphonse Allais famously replied "I cannot, it changes all the time". This is all the more true for g , the gravitational acceleration felt near the Earth's surface, which varies in both time and space (between 9.78 and 9.83 m s^{-2}). These variations are a result of the gravitational attraction by the mass inside and around the Earth, centrifugal effects due to the Earth's rotation, the distance to the centre of the Earth, geographical latitude, the mass distribution in the Earth's interior, and the relative positions of the Earth, the Moon, the Sun and the planets. Precise determination of g is essential in several scientific domains. As geophysical processes are associated with deformations of the solid Earth and mass distribution changes in its climate system, monitoring local variations in gravity provides information on tectonic deformations, past and present ice-mass changes, tides, the dynamics of the oceans and the hydrosphere and the structure of the Earth¹.

Gravity surveys are also useful in geology and mineral exploration, and are indispensable for the determination of the geoid — the reference equipotential surface of the Earth's gravity field — and hence of altitude. In volcanology, gravity measurements complement deformation monitoring to discriminate between intrusions of lava, water or gas. In metrology, g is key in the new realization of the kilogram with the Watt balance experiment weighing electrical and mechanical powers². Consequently, g plays a major role in state-of-the-art measurements of Planck's constant. Finally, gravimeters have also been useful in investigations of free oscillations of the Earth (global vibration modes excited by major earthquakes) through the monitoring of inertial acceleration³.

Measuring local gravity is conceptually simple: one drops an object and measures the free-fall time over a given distance. However, before the 1960s, the best way of measuring g (with an accuracy of one part in 10^5) was by means of Kater's reversible pendulum. First introduced in 1817, this instrument (essentially a compound two-pivot-point



pendulum) enables a determination of g by measuring the pendulum's period of oscillation¹. Realizing a free-fall experiment for determining g with sufficient precision — as physics students may experience — was practically impossible because it requires very accurate measurements of both distance and time. In 1971, ballistic absolute gravimeters based on optical interferometry became the new standard¹; today, these enable an accuracy for g of 10^{-8} m s^{-2} or, as gravimetrists would say, $1 \mu\text{Gal}$. (The gal, named after Galilei, is the cgs unit of acceleration.) The working principle lies in repeatedly measuring the time and distance along a 20–30 cm path travelled by a freely falling mass in a vacuum chamber. In the 1990s, cold-atom gravimeters were developed⁴; one of their advantages is that they allow for continuous measurements because they have no moving parts and, consequently, do not experience wear. Atom gravimeters are now being miniaturized to facilitate the portability of precise absolute gravimeters, useful for field studies.

Since the 1970s, the motion of satellites has been used to compute global models of the mean Earth's gravitational field⁵. In 2002, the Gravity Recovery and Climate Experiment (GRACE) twin satellites started providing information on the temporal variation of gravity, with a precision equivalent to a few kilograms per square metre on spatial scales of ~400 km at a sampling rate of once per month. The temporally constant part of the gravity field is now known at a level of 1 part in 10^6 with a spatial resolution that can reach 200 m in the best-covered areas by combining data from satellite and ground measurements.

In relative gravimeters, which only measure changes in g , a mass is prevented from falling by holding it and g is determined

by measuring how much force is required to do so. Spring relative gravimeters are an example; they are portable devices that report gravity changes with respect to a reference. In superconducting gravimeters, a hundred times more precise and much more stable than spring instruments, a superconducting sphere is made to levitate in a magnetic field⁶, resulting in a highly sensitive instrument with a drift of a few 10^{-9}g per year — spring instruments typically have a drift of 10^{-2} – 10^{-7}g per day. Superconducting gravimeters are also capable of measuring variations in g with a precision that is a hundred times better than that of absolute gravimeters for periods shorter than a day. In contrast to spring gravimeters, the most common mode of operation of superconducting gravimeters is continuous at a fixed location. The levels of precision achievable today — a few 10^{-11}g — are such that the effect of rain showers or the motion of a person operating the instrument are detectable (as seen in the plot after about 22 minutes when the operator sits above the gravimeter for 5 minutes).

When Newton realized that a falling apple obeys the same law as the Moon, could he have imagined that atoms play the same game⁴, now verified with an accuracy of 10^{-9}g ? □

MICHEL VAN CAMP is at the Seismology-Gravimetry Service, Royal Observatory of Belgium, Avenue Circulaire 3, 1180 Uccle, Belgium.
e-mail: michel.vancamp@oma.be

OLIVIER DE VIRON is at Littoral, Environnement et Sociétés, UMR7266, Université de La Rochelle and CNRS, 2 rue Olympe de Gouges, 17000 La Rochelle, France.
e-mail: olivier.de_viron@univ-lr.fr

References

1. Michaele, T. in *Geodäsie 2nd edn* (ed. Worthing, T. A.) Ch. 4, 41–64 (*Treatise on Geophysics 2*, Elsevier, 2012).
2. Stock, M. *Meteoritics* 50, 21 (2015).
3. Agnew, D. et al. *EGS* 67, 203–211 (1986).
4. Peltier, A. et al. *Nature* 400, 849–852 (1999).
5. Berardis, G., Dittishawala, M. R., Rosenfeld, R. & von Steiger, R. (eds) *Earth Gravity Field from Space—from Sensors to Earth Sciences* (Springer, 2003).
6. Goodkind, J. M. *Rev. Sci. Instrum.* 70, 4131–4152 (1999).



Astronomy and Astrophysics

The astronomers of the Operational Directorate Astronomy and Astrophysics do research in astronomy and they also observe solar system objects. Stellar evolution, mass loss of stars, variable and multiple stars as well as rapidly rotating stars are studied. Astrometry of minor planets is carried out and planetary satellites are observed. The researchers are active in the preparation and/or reduction and interpretation of data coming from dedicated observational campaigns, large scale surveys and space telescopes. The service maintains databases and provides software for scientists. General information on astronomical and related phenomena are distributed to public and press. Digitisation and archiving of photographic plates is also a task of this group.

The project Gaia

First results for variable stars of the Cepheid and RR Lyrae type

The first data release of Gaia (GDR1) occurred on Sep. 14, 2016 under huge interest from the scientific community, as well as from the press and the public. Several papers describing the Gaia mission and the GDR1 were prepared. The **Gaia Coordination Unit 7** (CU7) developed the Specific Objects Study (SOS) pipeline to validate and fully characterise Cepheids and RR Lyrae stars observed by the spacecraft, and published the first results on the Gaia Cepheid and RR Lyrae variable stars (Fig. 1).

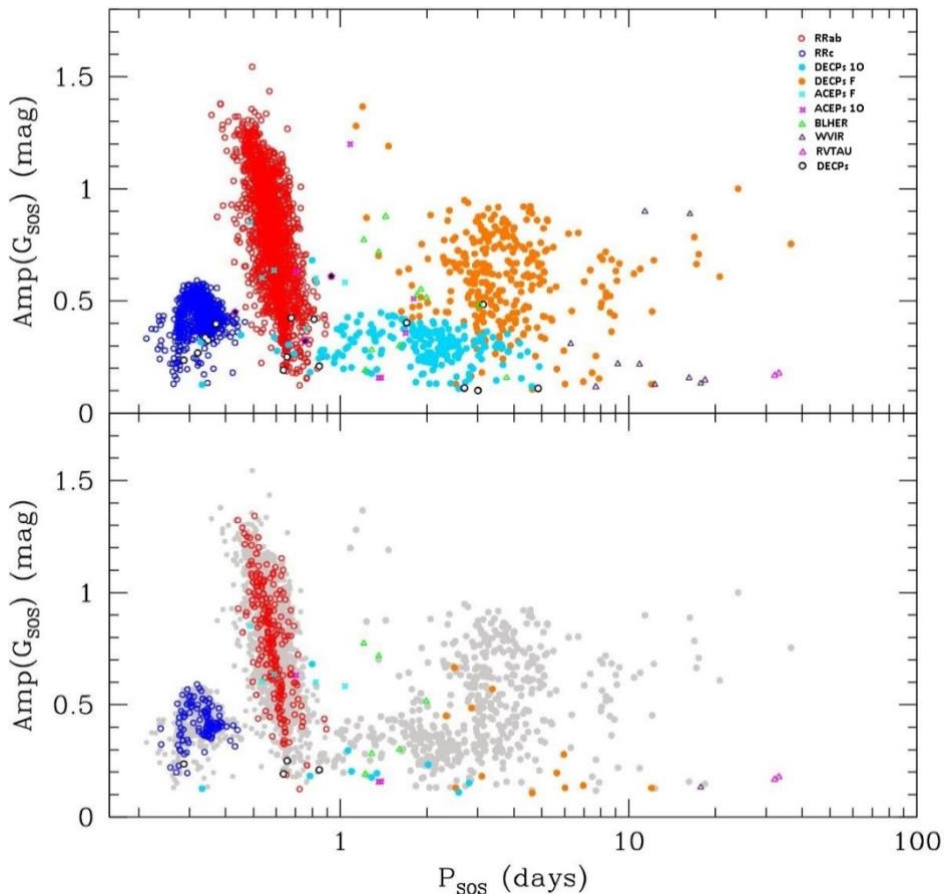


Fig. 1. G-band amplitude diagram versus period for the Cepheids and RR Lyrae stars published in *Gaia* DR1.
The *upper panel* shows all 3194 sources, while in the *lower panel* new discoveries by *Gaia* are plotted in colour and known variables in grey.

The mission of CU7 is to systematically detect variability, classify the variable objects, derive characteristic parameters for specific variability classes, and provide global descriptions of the variable phenomena. These tasks were divided into five large work packages (WPs): 1) Special Variability Studies, 2) Variability Characterisation, 3) Variability Classification, 4) Specific Object Studies, and 5) Global Variability Studies, but new activities were added when necessary, an example is the Variability detection (WP0). The whole sequence of processing is called VariPipe. The tasks of the ROB scientists concerned the supervision of the general package Characterization and the realization of the sub-package Period Search.

Besides the development, testing and validation of the VariPipe software, the activities of CU7 were mostly aimed at the data release of a specific set of Cepheid and RR Lyrae variables identified from

the processing of the 28-day Ecliptic Pole Scanning Law data during the satellite commissioning phase.

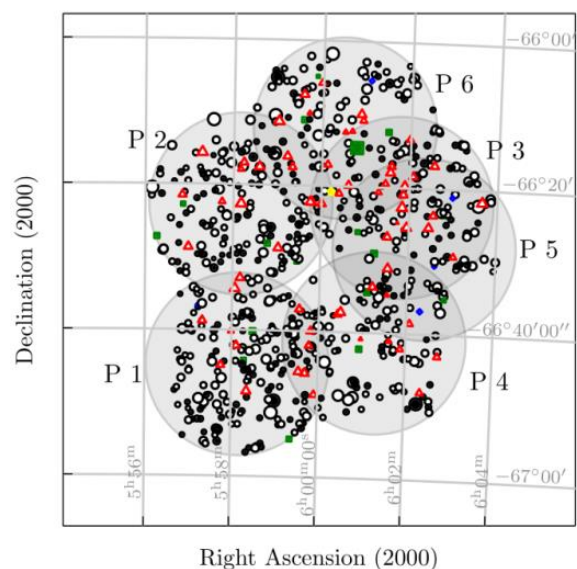
The full chain of the CU7 pipeline was run on these time-series photometry starting from the general Variability Detection, general Characterisation (including Period Search), proceeding through the global Classification and ending with the detailed checks and typecasting by the Special Object Study group for Cepheids and RR Lyrae stars. For the final analysis, the data were extended with over a year of Nominal Scanning by the Gaia satellite.

A total sample of 3,194 variable stars, 599 Cepheids and 2,595 RR Lyrae stars, of which 386 (43 Cepheids and 343 RR Lyrae stars) were new discoveries made by Gaia, was published. All 3,194 stars are distributed over an area extending 38 degrees on either side from a point offset from the centre of the Large Magellanic Cloud (LMC) by about 3 degrees to the North and 4 degrees to the East. The vast majority is located within the LMC. A few bright RR Lyrae stars that trace the outer halo of the Milky Way in front of the LMC were included as well.

A test field for Gaia: a radial velocity catalogue of stars in the South Ecliptic Pole

Gaia, ESA's latest astrometric space mission launched on Dec. 19, 2013, currently measures more than one billion stars with the goal to create a highly accurate 3D map of our Galaxy and its surroundings. The mission also provides spectrally-dispersed photometry (with an average of 70 measurements per target). In addition, the brighter stars are observed by means of the radial velocity spectrometer (RVS) (with an average of 40 measurements per target).

The spectrometer covers the spectral region of the near-IR Ca II triplet and higher members of the Paschen series (845 - 872 nm). Gaia will classify the stars down to the G-magnitude of 20.7 mag and derive the radial velocity of the stars brighter than 16.2 mag. ROB astronomers are taking part in the development of the pipeline which automatically analyses the data. They also contribute to the result validation before publication of the various Gaia Data Releases. The first Gaia Data Release occurred on Sep. 14, 2016.



The six FLAMES fields in the direction of the SEP and the targets observed during two years . The filled symbols indicate stars of the Large Magellanic Cloud (LMC).

targets in a single shot. The figure on the left shows the FLAMES fields as well as the 747 stars with magnitudes ranging from 12 to 17 mag, which were monitored for more than two years. A total of 3741 spectra was analyzed. All targets were characterized in terms of effective temperature, surface gravity and chemical composition. Radial velocities were also measured.

We identified 203 stars in the LMC (filled symbols), one galaxy (yellow pentagon), as well as six new chemically peculiar S-type stars (blue diamonds). A statistical analysis enabled us to define a sample

of 145 stars of constant radial velocity, which represents a high-quality reference for the RVS. We also reported 78 new variable stars. Our RV catalogue was already used to validate the first Gaia radial velocities during the commissioning in 2014 and has been accepted for publication. With Gaia's routine mission on-going, it is now being used to monitor and assess the RVS performances in the faint star regime as a full part of the nominal RVS ground-based processing pipeline.

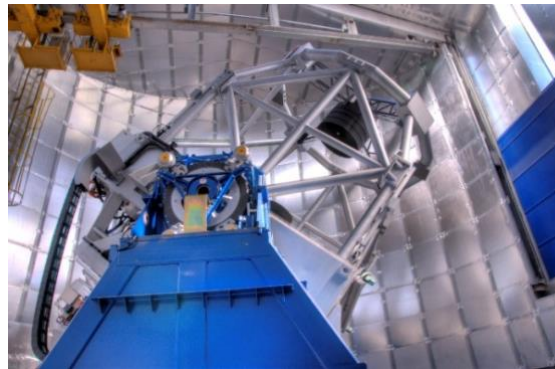
The BINA project

A bilateral network between the Belgian and Indian astronomical communities has been set up in 2016 under the auspices of the agencies BELSPO and DST (the Department of Science & Technology of India). The **Belgo-Indian Network for Astronomy and Astrophysics (BINA)** is a collaboration between Belgian and Indian institutes with the main aim to optimize the scientific output of the Indo-Belgian telescopes, namely the 3.6-m Devasthal Optical Telescope (DOT) and the 4.0-m International Liquid Mirror Telescope (ILMT). Both facilities are located at the Devasthal Observatory near Nainital, India. The BINA network organized its first event, a scientific workshop held in Nainital, India, from Nov. 15 – 18, 2016. This workshop was attended by 107 participants, 11 of which came from Belgian institutes.

The international workshop entitled “Instrumentation and Science with the 3.6-m DOT and the 4-m ILMT telescopes” was held in Nainital, a small village in the foothills of the Himalaya Mountains. It was organized by the Aryabhatta Research Institute of Observational Science (ARIES) under the lead of Dr. S. Joshi. The Belgian PI, Dr. P. De Cat, co-organized this workshop. During four days, exchanges were done by the participants who came from eight countries. Many interested young students also attended the workshop. Contacts were manifold and diverse. A description of the currently available and foreseen instruments was given, and a variety of potential scientific programmes was discussed. P. De Cat presented the astronomical topics of interest on behalf of the ROB team (De Cat et al. 2017). This experience furthermore allowed some enjoyable moments of human contacts and discussions outside of the scientific scope. On the last day, an excursion was organized to the Devasthal Observatory situated some 3 hours from Nainital, during which we enjoyed the view unto the impressive Himalayan mountains, as well as a guided tour of the Devasthal Optical Telescope.



The participants of the 1st BINA workshop held at Nainital, Uttarakhand, India.



The Devasthal Optical Telescope (DOT) has been designed and assembled by the Belgian company AMOS. Astronomers from Belgian institutes will get guaranteed time for their observations. © P. Lampens

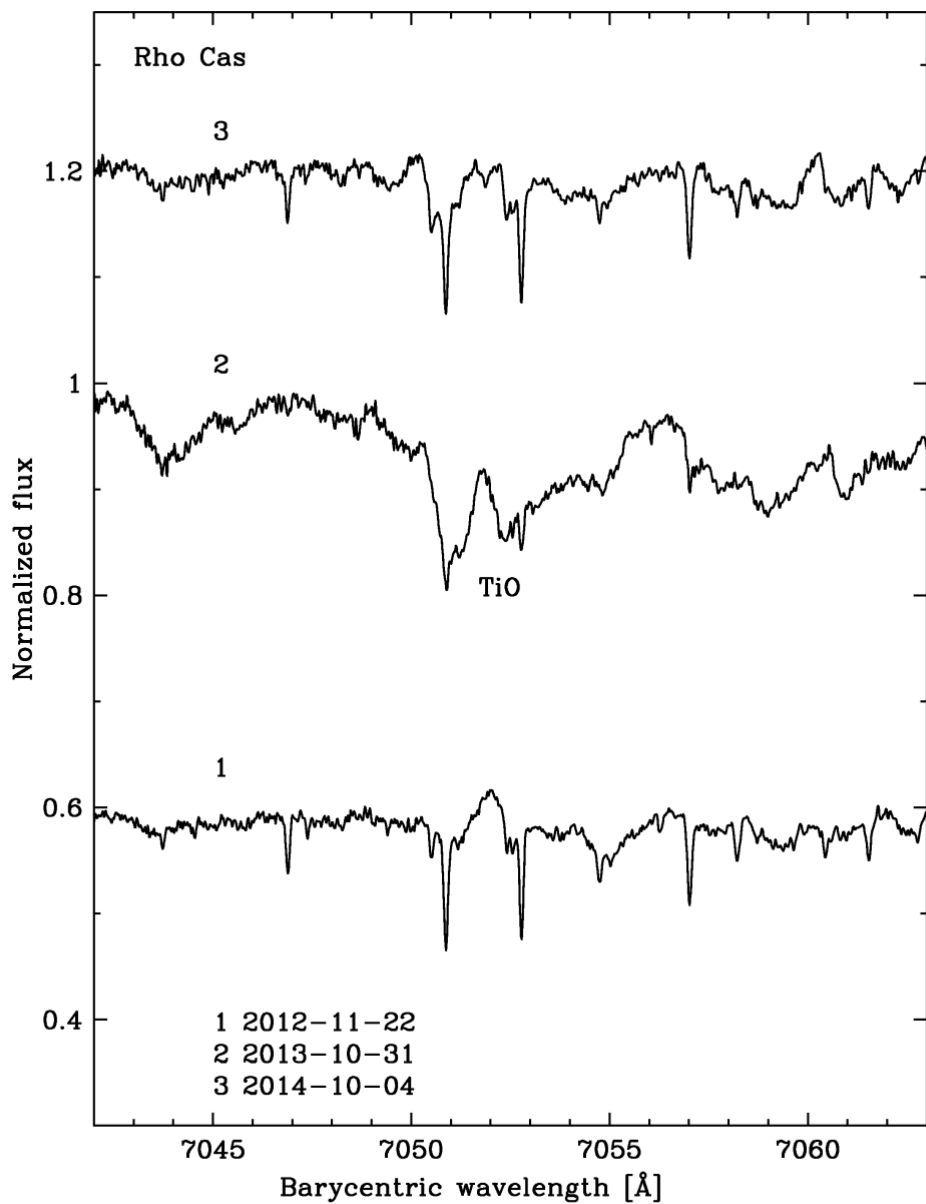
Luminous Blue Variables: animaging perspective on their binarity and near environment & Long-termspectroscopic monitoring of the Yellow Hypergiant Rho Cas.

The study of hot and cool hypergiant stars is important for stellar astrophysics because these very massive stars are the progenitors of core collapse supernovae. They exist near the Eddington luminosity limit and exhibit a wide range of uncommon stellar properties. Their atmospheres are unstable which causes quasi-periodic pulsation variability, strongly developed large-scale velocity fields, excessive mass-loss, and extended circumstellar envelopes. The Luminous Blue Variables (LBVs) are rare massive hot hypergiants. They are characterized by strong photometric and spectroscopic variability related to transient eruptions. The mechanism at the origin of these eruptions is not well known. In addition, their formation is still problematic and the presence of a companion could help to explain how they form.

An international team of researchers including the ROB published a study of seven LBVs (about 20% of the known Galactic population), some Wolf-Rayet stars, and massive binaries. It probes the environments surrounding these massive stars with near-, mid-, and farinfrared images, investigating potential nebula/shells and the companion stars. The study investigates large spatial scales using seeing-limited and near diffraction-limited adaptive optics images to obtain a differential diagnostic about the presence of circumstellar matter and to determine their extent. From the images the team searched for the presence of binary companions on a wide orbit. Once a companion was detected, its gravitational binding to the central star was tested. The tests include the chance projection probability, the proper motion estimates with multi-epoch observations, flux ratio, and star separations. The new results show that two out of seven LBVs may have a wide orbit companion. Most of the LBVs display a large circumstellar envelope or several shells. In particular, HD 168625, known for its rings, possesses several shells with possibly a large cold shell at the edge of which the rings are formed. For the first time this investigation directly imaged the companion of LBV stars.

Over the last 7 years astronomers at the ROB performed long-term high-resolution spectroscopic monitoring of hot and cool hypergiants with HERMES on the Mercator Telescope at La Palma. An important property of hypergiants is recurring outbursts that signal the final stages in the fast evolution of the most massive stars. These outburst events reveal very large changes of Teff and commensurate strong spectral variability. For example, in 1999-2000 the yellow hypergiant (YHG) Rho Cas decreased Teff from above 7000 K to below 4000 K during an outburst event that lasted ~2 years. Following the rapid V brightness decrease of 1.3 mag, it revealed TiO absorption bands in the near-IR spectrum which disappeared after returning to average V brightness level. During the outburst, the mass-loss rate increased from about $10^{-6} M_{\odot} \text{ yr}^{-1}$ to $5 \times 10^{-2} M_{\odot} \text{ yr}^{-1}$. The hypergiant expelled ~3% of the solar mass, equivalent to ten thousand times the mass of the Earth. The stellar radius increased by a factor two resulting in a tremendous cooling of the atmosphere by 3000-4000 K. Similar large outburst events have been observed in Rho Cas in 1946 and possibly 1893. The large eruptions are therefore thought to occur about every half century and they represent the main mass-loss mechanism of YHGs.

The large mass-loss rates cause their fast evolution on a blue loop in the Hertzsprung-Russell diagram. A smaller outburst event occurred in Rho Cas in 2013 during which we also observe the temporal TiO bands with HERMES. A similar weak outburst event was observed in 1986 in Rho Cas.



Three spectra of Rho Cas of Nov 2012 (1), Oct 2013 (2), and Oct 2014 (3) observed with Mercator-HERMES.

Spectrum (2) reveals a broad flux depression around the wavelength of 7050 Å due absorption by TiO molecules formed during a fast cooling of the hypergiant's atmosphere. The TiO absorption bands appeared during only a few months in an outburst event of Rho Cas with a visual brightness minimum in Oct 2013. The near-IR TiO bands are absent in spectra (1) and (3) outside of this brightness minimum.

Solar Physics and Space Weather

The Operational Directorate Solar Physics and Space Weather studies the outer layers and the atmosphere of the Sun, with a particular focus on solar activity and the influence it exerts on the Earth and its space environment (space weather).

Highlights in solar radio astronomy at ROB

Solar radio emissions accompanying eruptive events (flares, filament eruptions, Coronal Mass Ejections) can occur at any wavelength of the radio spectrum. The VHF and UHF band (30 – 3000 MHz) is of uttermost importance as it corresponds to heights covering the whole corona, from the transition region with the chromosphere to the boundaries of the interplanetary space. Particles accelerated during flares or by shock waves produce radio signatures observable over this whole frequency range, providing insights in the eruptive processes taking place.

Since 2008, the Observatory operates in Humain, near Marche-en-Famenne, a small solar spectrograph called Callisto, covering the frequency band 45 – 447 MHz. Callisto is an analogic receiver based on a commercial TV tuner driven by a dedicated electronics and designed by C. Monstein from ETH Zürich. It is connected to a broad band antenna mounted on the side of a 6-m Sun-tracking parabola. The Callisto receiver in Humain is part of a worldwide network of identical instruments that provide near real-time radio observations of the Sun.

In 2015 and 2016, the radio group of the solar physics department set up two new receivers that are aimed at expanding the frequency range and at improving the frequency resolution of Callisto (200 frequencies spread over the whole band). One of the receiver, HSRS, is connected to a broad band antenna (300 – 5000 MHz) located at the focus of the 6-m dish. It was set up in August 2015 and has since observed more than 60 noticeable radio events, despite the low level of solar activity. The second receiver, ARCAS, installed in October 2016, shares the same antenna as Callisto.

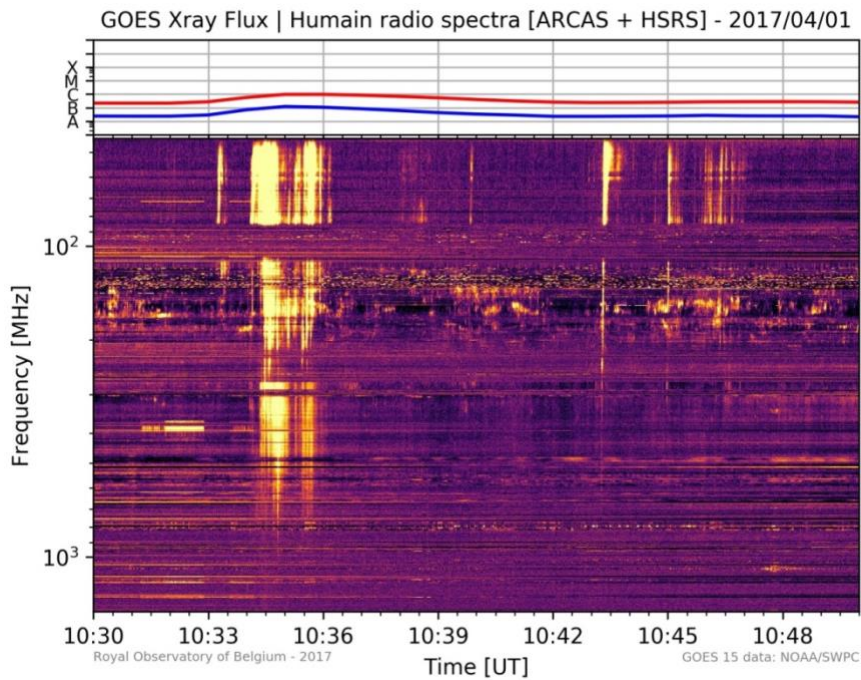
HSRS and ARCAS are identical digital receivers based on Software Defined Radio devices. They differ only by a single removable electronic card that defines the frequency band. Both receivers were programmed using an open source library to implement a wide band spectrometer. The instantaneous bandwidth is about 20 MHz, a limitation that results from the amount of data that can transit through the Ethernet port connecting each receiver to its PC. To scan a certain band, one has to tune the receiver at a certain frequency, calculate the spectrum over 20 MHz (through a FFT) and tune again the receiver to the next frequency, ~ 20 MHz apart. The overall performances of the instrument now operational in Humain are summarized in the following table:

	<i>Callisto</i>	<i>ARCAS</i>	<i>HSRS</i>
<i>Frequency band</i>	45 – 447 MHz	45 – 450 MHz	275 – 1495 MHz
<i>Frequency resolution</i>	63 kHz	98 kHz	98 KHz
<i>Time resolution</i>	250 ms	~ 84 ms	~ 250 ms
<i>Number of freq.</i>	200	~ 4200	~ 12500

Technical performances of the solar radio spectrographs in Humain. The frequency resolution of Callisto varies in practice and is bigger than the one mentioned here

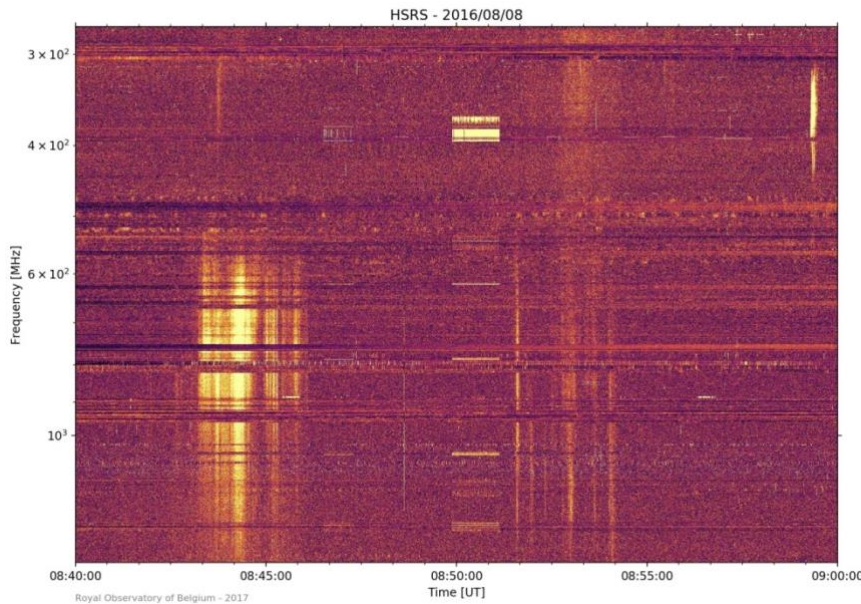
The finer frequency resolution of the new receivers allows us to observe in bands that were mostly inaccessible with Callisto (like the band 110 – 150 MHz). For example, relatively narrow band emissions such as noise storms associated with strong sunspots can now fully be observed with ARCAS. The combination of ARCAS and HSRS gives to the scientists of the department an unprecedented view on radio emissions linked to eruptive processes. An example is given in the Figure below, where a group of intense type III bursts, superposed on a noise storm, is observed in association with a B9.8 flare on April 1st 2017¹⁴.

¹⁴ The low level of solar activity since the setup of ARCAS in Oct. 2016 forces us to illustrate this instrument with an event that took place in the spring of 2017



A group of type III bursts linked to a B9.8 flare. The "interruption" around 100 MHz is due to a filter that attenuates the FM band. Between 100 and 200 MHz, a noise storm can be seen as narrow band intermittent emissions

The HSRS spectrograph covers a frequency range that is monitored only by a few instruments in Western Europe. Above ~ 500 MHz, in the decimetric frequency range, radio bursts closely related to particle acceleration taking place near flare sites can be observed, such as decimetric pulsations (see figure belowsError! Reference source not found.).



Pulsations observed above 600 MHz with HSRS on August 8th, 2016

Numerical and Observational Study of Stealth CMEs

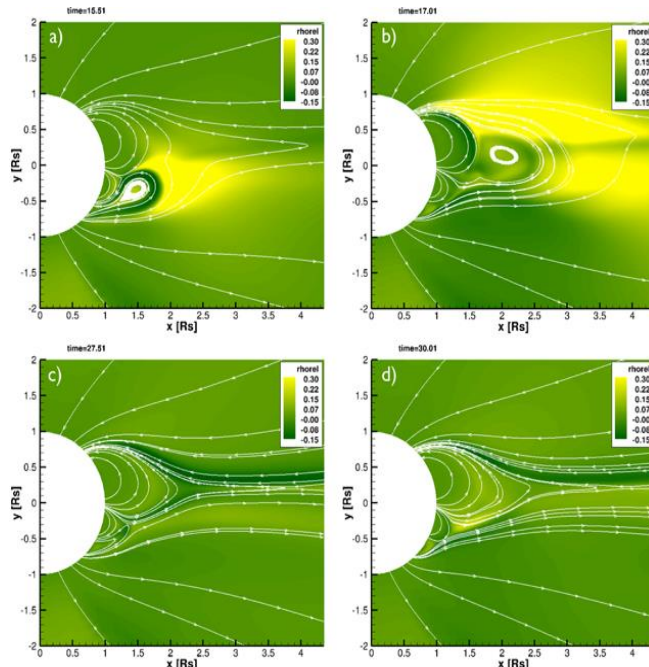
The prediction of space weather is a core service provided by the Solar Influences Data analysis Center (SIDC) at the Royal Observatory of Belgium (ROB). Despite the availability of various datasets providing a continuous view of the Sun and its activity, occasionally space weather events occur that are stealthy enough to surprise even the experienced forecasters.

Examples are front-sided coronal mass ejections (CMEs) without a clear source region and their associated geomagnetic storms. For these events, there are little warning signs to alert the forecaster of their occurrence and hence the resulting storm will likely not be predicted.

In order to improve the forecasting for this type of geomagnetic storms, we need a better understanding of the initiation of such stealth events.

In this PhD project, which started at ROB on 16 October 2016, the focus is on stealth CMEs and the way they differ from more typical solar eruptions. Stealth CMEs are unusual CMEs that are clearly observed in multi-viewpoint coronagraph observations as front-sided events, but lack signatures of eruption in the low corona and on the solar disk.

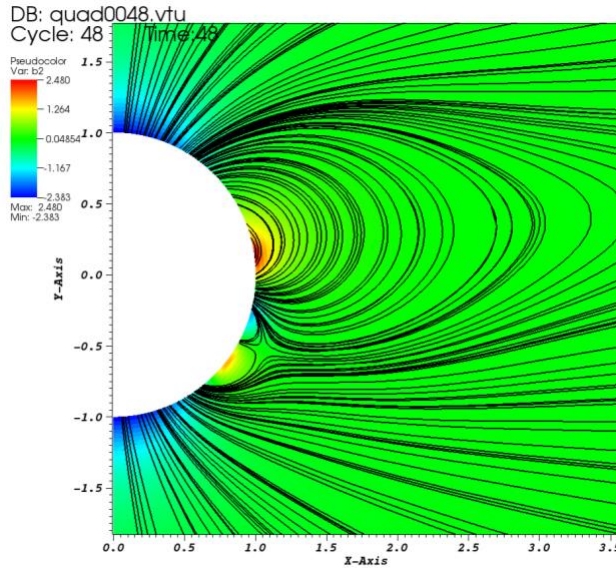
The objective for this study is to combine observational and numerical studies of stealth eruptions in order to determine how these events are triggered and driven and in what sense they differ from more typical solar eruptions. We aim to improve the forecasting of the geomagnetic impact of stealth eruptions by searching for similarities between the observed events and by comparing the observations to the results of the numerical modelling. Because these stealth eruptions may cause hazardous space weather conditions without being detected, improvements in our understanding of their origins will advance our ability to predict the onset of such space weather events.



Snapshots of the time evolution of the relative density and of the selected field lines during the formation of the structure associated with the first CME (a), its movement towards the equator (b), the rise of the southern arcade (c) and the associated second CME (d) (Bemporad et al. 2012).

Dana Talpeanu, PhD student supervised by Elke D'Huys at ROB, started simulating stealth CMEs with the code AMRVAC developed at KU Leuven by trying at first to reproduce the previous work of

Francesco Zuccarello and Alessandro Bemporad (Zuccarello et al. (2012)¹⁵ and Bemporad et al. (2012)¹⁶). They numerically modelled a sympathetic event, very similar to a stealth CME (see figure above), using an earlier version of the code. The figure below represents one of the current simulations of θ component of the magnetic field (color scale) and magnetic field lines (black lines). As it can be seen, the overall configuration resembles the one from Bemporad et al. (2012), but it is not perfectly matching. This is a work in progress and once the structures coincide, Dana Talpeanu will start applying the shearing motions in order to obtain CMEs in a similar way as Francesco Zuccarello and Alessandro Bemporad did.



The simulated background magnetic configuration using MPI-AMRVAC; θ component of the magnetic field (color scale) and magnetic field lines (black lines).

Afterwards, this study will be extended by using events from the list of 40 events identified by Elke D'Huys during her PhD thesis (D'Huys et al. (2014)¹⁷) and make a parameter study on them, which could reveal the range of global magnetic field strength that allows stealth events and may identify other crucial parameters as well.

In a second phase of the project, the plan is to study the geo-effective stealth CMEs. The starting point will be a list of CMEs that produced geomagnetic storms and that are suspected to be stealth events.

¹⁵ Zuccarello, F.P., Bemporad, A., Jacobs, C., Mierla, M., Poedts, S., Zuccarello, F., *The role of streamers in the deflection of coronal mass ejections: comparison between STEREO three-dimensional reconstructions and numerical simulations*, The Astrophysical Journal, 744, pp. 66, 2012.

¹⁶ Bemporad, A., Zuccarello, F.P., Jacobs, C., Mierla, M., Poedts, S., *Study of multiple coronal mass ejections at solar minimum conditions*, Solar Physics, 281, pp. 223-236, 2012.

¹⁷ D'Huys, E., Seaton, D.B., Poedts, S., Berghmans, D., *Observational characteristics of coronal mass ejections without low-coronal signatures*, The Astrophysical Journal, 795, pp. 49, 2014.

CCSOM – Constraining CMEs and Shocks by Observations and Modelling throughout the inner heliosphere

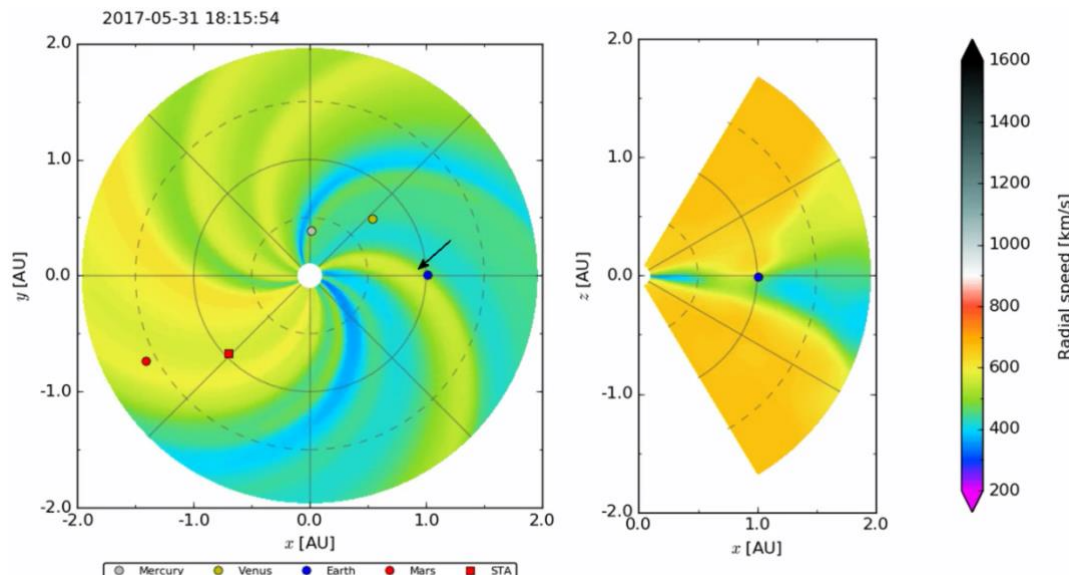
As a response to the BRAIN networking call, the project proposal with the acronym CCSOM (Constraining CMEs and Shocks by Observations and Modelling throughout the inner heliosphere) was submitted and successfully accepted in the second half of year 2016.

CCSOM is led by Royal observatory of Belgium (ROB) with J. Magdalénic as a project coordinator. The project is based on the close collaboration of ROB, Katholieke Universiteit Leuven (KU Leuven), University of Helsinki and Graz University.

The project aims at making a breakthrough in studies of coronal mass ejections (CMEs) and CME-driven shock wave propagation in the inner heliosphere by combining observations with numerical simulations that will be well beyond the current state of the art.

In the framework of CCSOM, the observations will be compared with modeling results of EUHFORIA (EUropean Heliospheric FOREcasting Information Asset), recently developed model at the KU Leuven and University of Helsinki (lead by: S.Poedts and J.Pomoell, respectively). EUHFORIA is a physics-based prediction model of the solar wind and CMEs in the inner heliosphere (presently similar to state-of-the-art model ENLIL).

This project will ultimately deliver, together with a number of scientific publications, a fully operational and scientifically validated heliospheric code for modeling the solar wind and CME propagation. During and at the end of the project the model will be set up and running principally at ROB for the use in space weather operations of the Regional Warning Center Belgium.



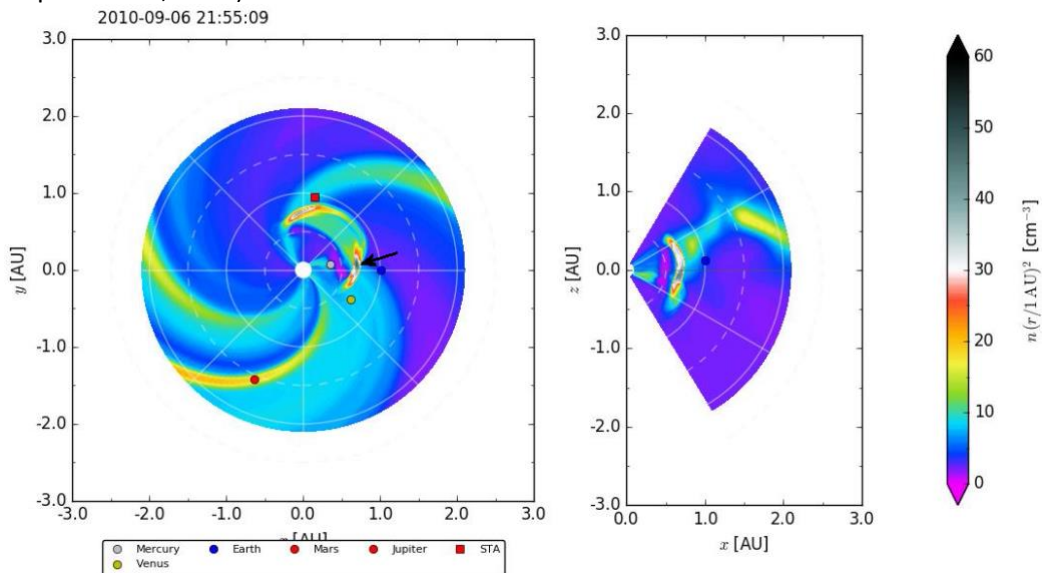
The solar wind modeling with EUHFORIA predicting arrival of the fast flow associated with the coronal hole which crossed central solar meridian late on May 27, 2017.

The color indicates the solar wind radial speed in the ecliptic plane as well as a meridional plane containing Earth. The fast solar wind of about 650 km/s was expected to arrive at the Earth on May 31 at about 18:00 UT. The black arrow points the fast solar wind flow which reached the Earth.

First tests of EUHFORIA were performed during last several months. Presently, EUHFORIA is modeling the solar wind propagation (see figure above) and the first statistical studies of solar wind modeling with EUHFORIA, in the framework of CCSOM, are in progress (Graz University).

Further on, initial tests of EUHFORIA modeling the CME propagation are being performed by M. Mierla from ROB and C. Scolini, PhD student under supervision of L. Rodriguez and S. Poedts.

The figure below shows the results of modeling CME propagation (event was first observed on the Sun on September 4, 2010) with EUHFORIA.



First results of EUHFORIA modeling the propagation of the CME (presently starting height of modeling is 0.1 AU, similar to ENLIL) observed on the Sun on September 4, 2010.

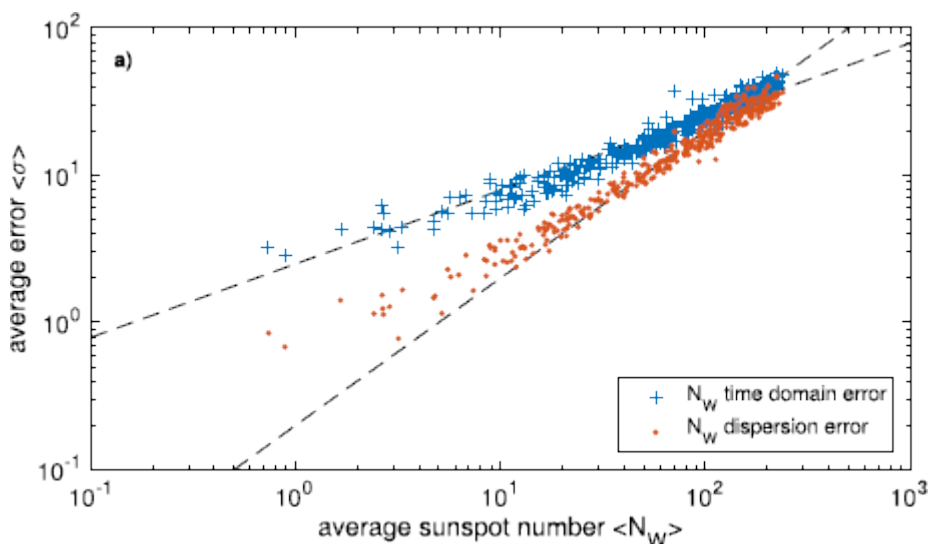
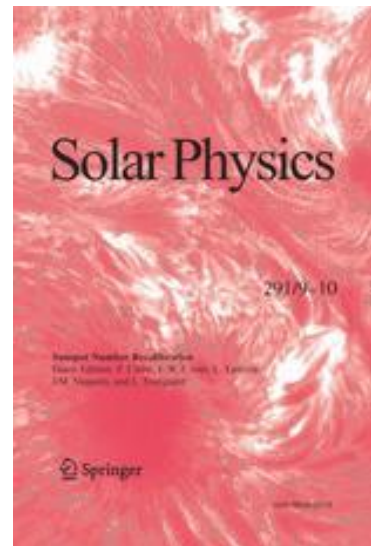
The color indicates the plasma density change in the ecliptic plane as well as a meridional plane containing Earth. The black arrow points the CME front approaching to the Earth (blue circle).

Topical issue of Solar Physics "Sunspot Number Recalibration"

2016 was marked by a new milestone in the ongoing recalibration and redefinition of the International Sunspot Numbers series initiated in 2015 by the World Data Center (WDC) SILSO run by the OD Solar Physics at the ROB. In just a few months, the 2015 release of the first revised version of the reference sunspot number series triggered a revival of international research in the field of the long-term solar activity studies.

In response to this global interest, two researchers from the ROB (Frédéric Clette, Laure Lefèvre) together with colleagues from the National Solar Observatory (USA), Stanford University (USA) and the University of Extremadura (Spain) proposed a special topical issue dedicated to the revised sunspot number to the editors of Solar Physics (Springer), the main journal dedicated to solar research. The proposed topic was approved and the proposers acted as guest editors for this special volume, which proved to be highly successful. Indeed, the final printed volume gathered 34 articles, to which a few more late articles were added in on-line form. (Vol. 291, N° 9-10, 659 pages, <http://link.springer.com/journal/11207/291/9/page/1>, ISSN: 0038-0938 (Print) 1573-093X (Online)).

Moreover, the SILSO researchers contributed three main articles as first authors, and were associated with three other articles jointly with different foreign collaborators. Those articles described all main corrections introduced in the current official version of the sunspot number distributed by the WDC-SILSO, while one article led by T. Dudok de Wit investigated for the first time the statistical properties of the random errors present in the raw sunspot data forming the base of this reference sunspot index. This state-of-the-art study reveals a dual nature, mixing two distinct contributions, one associated with the random solar variations themselves and one truly associated with errors in visual sunspot counts.



Variation of the time domain error (blue) and dispersion error (red) as a function of the average sunspot number. The clear double distribution show the relative contribution of two distinct components of the random errors in sunspot counts: random component of solar variability (Poisson statistics) and counting errors made by the observers (Gaussian statistics).

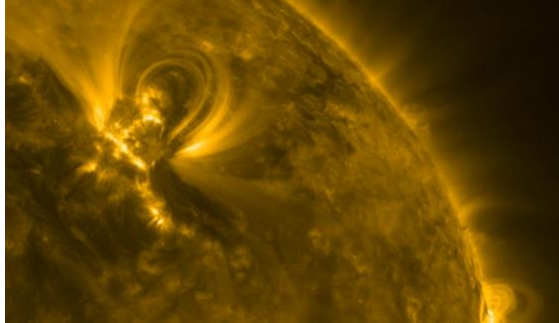
This topical issue covered various implications of the ongoing SILSO revision work. Several papers presented newly recovered sunspot data and updated historical databases. Other papers presented new additional or alternate corrections to the sunspot number series, demonstrating that further improvements are needed and will benefit from the recovery of lost or neglected data combined with state-of-the-art statistical processing methods. As a validation of recent changes, several articles investigated the correlation between the updated sunspot number series and other direct or indirect solar activity indices, like total magnetic field measurements or cosmogenic isotopes from polar ice cores. Most results confirm that following the revision, there is a better agreement between the new sunspot series and the parallel indices and those past unexplained discrepancies are reduced or eliminated.

Finally, a few articles are considering implications of the revision by repeating some past analyses that rely on the sunspot number as a key input parameter. Indeed, a wide range of studies in various disciplines rely on the multi-secular sunspot number series. Overall, this volume thus concentrates a first wave of studies in a single broad panorama. Already abundantly cited after just a few months, it should provide over coming years a key reference for all solar physicists contributing to the growing research on the long-term reconstruction and prediction of solar activity and its impact on the Earth.

MHD modeling of torsional waves in the solar corona

Solar corona, an outer layer of the solar atmosphere, is filled with rarified and magnetized plasmas. Due to symmetry, coronal plasma is structured into cylindrical magnetic tubes. Thus, magnetic loops and open field lines are basic bricks of the solar corona.

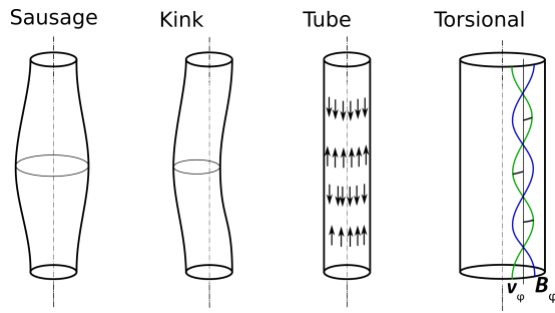
Magnetic tubes support various types of oscillations. Existence of these oscillations is important in particular for the fundamental problem of solar corona heating: oscillations are considered among two main candidates to transport energy from the lower layers of the solar atmosphere into the corona, where the energy is released. By means of numerical analysis we studied how torsional oscillations can dissipate, i.e. release their energy in the solar corona.



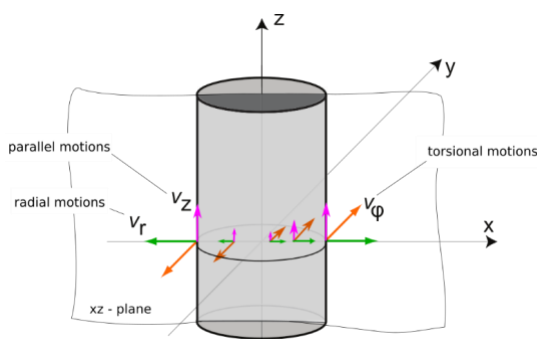
Solar corona observed in extreme ultraviolet wavelength $\lambda=17.1$ nm by AIA/SDO telescope (left) and a sketch with open and closed magnetic field lines (right).

There are four basic types of oscillations in magnetic flux tubes: sausage, kink, tube, and torsional.

The first three types of oscillations are called compressive, since during oscillation period plasma density is perturbed. These types of oscillations are extensively studied since pioneering work of Edwin & Roberts in 1983. Compressive oscillations are prone to decay and reflection in the transition region of the solar atmosphere (the region where plasma density drastically decreases by several orders of magnitude to 10^9 cm^{-3} , and plasma temperature increases from several thousands, to approximately one million of Kelvins), so the amount of energy they can release in the corona is not enough to solve the fundamental problem of coronal heating. Torsional oscillations differ from the previous three types: they are incompressible and are less susceptible to dissipations in the transition region, so there is higher possibility they carry necessary amount of energy to the corona. But indeed, it is important to figure out the mechanisms how torsional oscillations dissipate their energy in the corona.



Types of oscillations in magnetic flux tubes



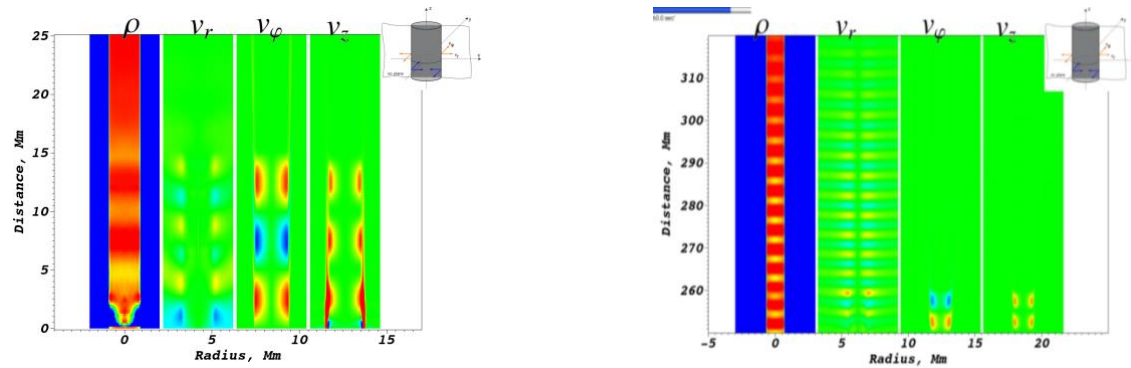
Magnetic flux tube with original torsional motions and induced radial motions and parallel motions.

We numerically analyzed the dynamics of propagating torsional waves and payed particular attention to nonlinear effects. These effects are usually not considered at all when one analyzes the oscillations analytically. Not surprisingly, because the effects are small and tend to disappear when the initial oscillation is weak. But they are always present in real solar plasma and make their small but constant contribution.

We found many effects that may result in energy dissipation. For example, torsional motions induce parallel and radial motions. Parallel motions are pulsating (periodically change from zero to particular value), but are always directed toward the same direction. Radial motions are oscillating inward and outward, i.e. constituent one of the oscillations mentioned above – sausage oscillations (they are compressible and also prone to decay). The energy necessary for the development of induced parallel and radial motions is obtained from the energy of initial wave! Torsional motions also result in other effects, such as wave steepening and nonlinear phase mixing. Snapshots with results of numerical simulations are presented in the figure below.

We found another effect that has not been foreseen by analytical theories: the observed nonlinear effects are more pronounced near the tube boundary and are absent near the tube axis. This fact proves that our understanding of the phenomena need be improved.

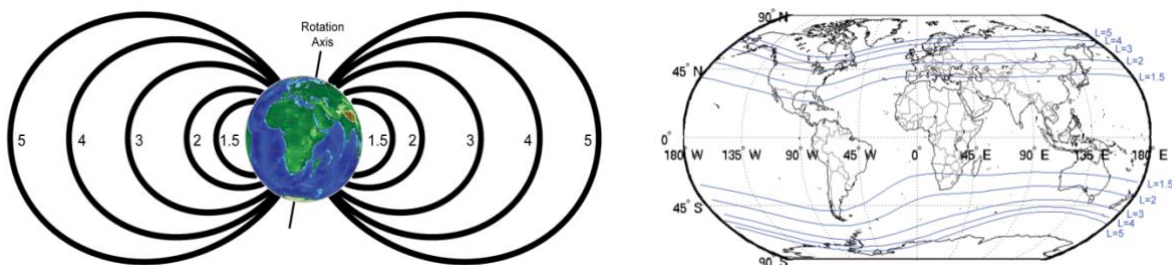
All the observed nonlinear effects can serve as a mechanism for the dissipation of energy of torsional oscillations in the solar corona.



Central cross-section of a magnetic flux tube with plasma density ρ , radial velocity v_r , azimuthal velocity v_ϕ , and parallel velocity v_z . Left panel: early phase of the wave propagation. Right panel: late phase of the wave propagation, induced sausage wave travels ahead of mother torsional wave.

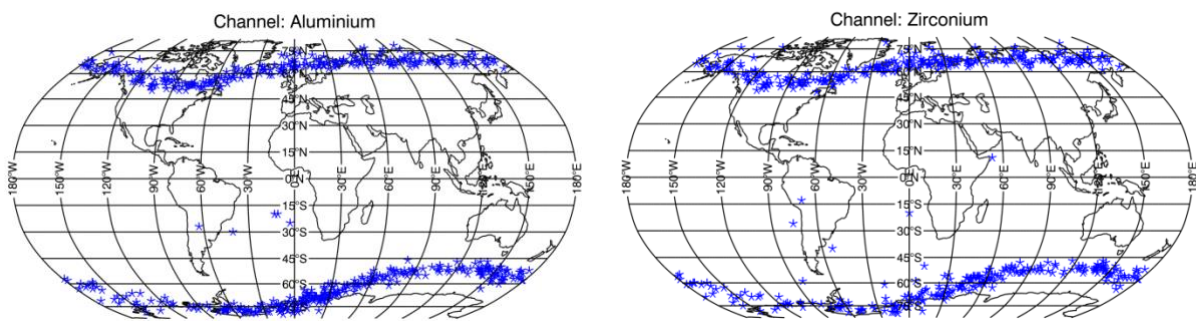
The detection of ultra-relativistic electrons by the LYRA on-board PROBA2

PROBA2 is a small European Space Agency's (ESA) satellite with a scientific mission to explore the solar "surface" (also called corona) and the Sun's effect on the near-earth environment. LYRA (Large Yield RAdiometer, formerly LYman alpha RAdiometer) is one of the two main instruments on-board the satellite, designed to observe ultraviolet to soft X-ray emission from the solar corona with extremely high cadence. It measures light from four different ranges of wavelengths chosen for their relevance to solar physics, aeronomy and space weather in three redundant units (i.e. each unit contains all four bands).



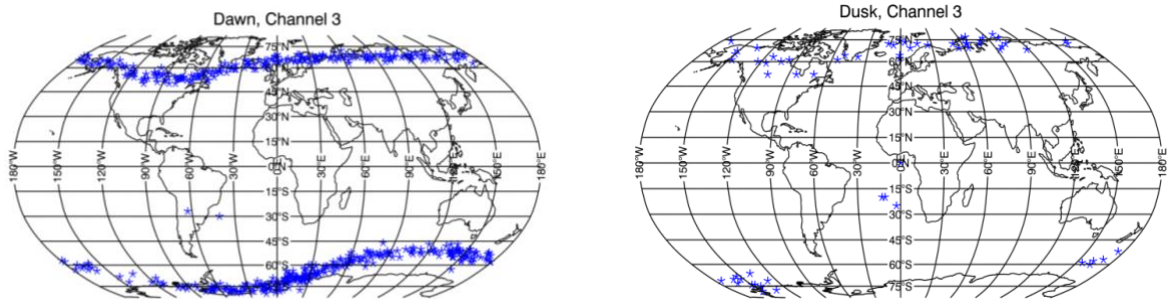
A conceptual drawing of Earth's magnetic field (left) and the map of the magnetic field lines on the surface of Earth (right). Both images depict the Earth's magnetic field when undisturbed by space weather. The left image is an approximate representation while the right image is calculated by a semi-observation model fitting. The magnetic field lines of the left image that close 1.5, 2, 3, 4, and 5 Earth radii away of Earth's center are labelled as L=1.5, 2, 3, 4, and 5 on the right image.

Although LYRA is designed to detect light, it also succeeded to detect ultra-relativistic electrons (i.e. electrons with energies above 1 MeV) that penetrate the Earth's ionosphere and reach the altitude of PROBA2 (~700 km). Those electrons are known to originate from the solar wind and get trapped by Earth's magnetic field at an altitude of thousands of kilometers. LYRA's detections demonstrate that, under certain conditions, these particles can become "trapped" by Earth's magnetic field and fall to the altitude of PROBA2 and possibly below.



Maps of the location of the detections made on the Aluminium (left) and Zirconium (right) channels of LYRA. Also known as channels 3 and 4 respectively, those channels are named after the ions of the solar corona they are designed to observe best. The concurrence of the detections is strong evidence of the detection of highly relativistic electrons.

Perhaps the most intriguing characteristic of the electron detections is the effect that the local time has on the likelihood of detecting the phenomenon. To ensure continuous viewing of the Sun, PROBA2 flies from pole-to-pole and from dawn-to-dusk (i.e. on the “side” of the Earth, as it faces the Sun). It was therefore possible to split each orbit to two parts and study the effect the sunlight has to the phenomenon. The compelling result is that there are eight times more events during the dawn than the dusk part of the orbit!



Maps of the detections made on channel 3 (Aluminium) when the satellite flies over the dawn (left) and dusk (right) sides of the Earth. Although the geographical distribution of the detections remains the same, it is eight times more likely for a detection to take place at the dawn part of the orbit than the dusk.

Various mechanisms have been proposed by a team of scientists, led by the PROBA2 science team, for the explanation of the physical process that leads to the LYRA detections. Nevertheless, those explanations are qualitative, while a full quantitative model is so far elusive and it may take years until we have a more detailed view of this captivating phenomenon.

Information service

The activities related to the information service consist of several tasks: answering questions and inquiries from public and press, assisting in all kind of outreach activities, giving general information on ROB and on astronomy and astronomy related subjects, advising the planetarium, organize the visits to the ROB, including the organization and coordination of open doors days and related activities, all kind of assistance for exhibitions and public relations activities (press communications, press conferences etc.) and preparing of texts for printing or for the web site. (<http://www.astro.oma.be/en/news/>)

Information to public, media and authorities

In 2015 the scientific information service of the ROB had to answer to about 814 questions from the public sent to the ROB by email (about 423, not included the ones related to visits or visit requests), telephone (more than 322) or by letter or fax (69). As usual most were about sunset and sunrise, twilights, equinoxes and solstice, horizontal coordinates of sun and moon, the amount of shadow, sun dials, moon rise and set, moon phases, eclipses in 2016 and other years, all sort of calendar topics (Easter dates, beginning and end of Ramadan, time keeping, time zones, ...) tides, star maps and visibility of constellations over the world, comets now and in history, Mars, Venus and other planets in the sky, fireballs, meteors, UFOs, satellite re-entries, candidate meteorites, information about historical scientific instruments, the profession of astronomer, external influences (sun, planets, universe,...) on climate change, structure of the universe, on satellites and space missions, photographs and images of the Observatory, history of the observatory, amateur astronomy associations and public observatories, planets and the moon, atmospheric halos, goniometry and positional astronomy, names of asteroids, giving and/or registering of stars names, adopting or buying stars, black holes, etc. 15 researches are done in the archives to reply to the questions.



Questions about the sun and its influence on earth (space weather etc.); about seismology, gravimetry and GPS, about asteroids and impact of asteroids on earth were forwarded to other sections of the observatory. Questions about weather and climate were sent to the Meteorological Institute and those about space travel and aeronomy to the Belgian Institute for Aeronomy.

Information to the media (TV, radio and written press) was given by the service

on numerous occasions. Other members of the ROB appeared in news items on other topics (Solar activity, space weather, seismic activity, Mars, comets and mission Rosetta, exoplanets ...).

As each year groups and individual visitors had to be guided in the Observatory this year. The individual visitors were mainly journalists and other media related persons or amateur astronomers with a specific demand and/or students. Groups were, in general, received on the first Tuesday of the month. In order to give some idea on the work load: there were in 2016 29 groups visiting and more than 360 emails (in/out) related to visits or inquiries. We welcomed, amongst other groups, the experts of the scientific review of ROB, members of the RotaNut Workshop, members of Pro Lege, the association of former Parliament and Senate members, participants of the Early Career Day and members of the Demetra workshop.

J. Cuypers presented the 'History and activities of the ROB' as an introductory talk to the visiting groups and he guided these in the museum and the dome(s). He helped with the organisation of some other visits when he was not participating (e.g. Asgard event on 28/04).

Website

There was no consistent information on the number of visitors to our webpages directly available for 2016. Starting January 2017 the results of the new tool for web site analytics and statistics became also available for the web pages of the information services. First data (only on 2 weeks) indicate about 600 to 1100 unique visits per day, but this will be more detailed in 2017.

The content of web pages with the answers to frequently asked questions was regularly up-dated. For 2016, the pages on daylight saving time and on the Islamic calendar (Ramadan) had at least one update or revision. New data about the position of the sun during the year were added.

The Dutch versions of the pages on the celestial phenomena of the month (information given by R. Dejaiffe, put on the web by H. Langenaken) were revised on a regular basis.

J. Cuypers, with from September on the help of Lê Binh San Pham initiated or assisted in putting new items, as e.g. press releases or announcements on the 'News' pages of the ROB. In 2016 there were 18 topics published (always in 3 languages: NL/FR/EN).

Social networks @ ROB



From 14 December 2016, the Royal Observatory of Belgium has its own Facebook page (<https://www.facebook.com/ORBKSB/>) and Twitter account (https://twitter.com/ORB_KSB). In these accounts are published links of the web news and press releases related to ROB and also other news and items related to ROB colleagues (interviews, articles, astronomical pictures...) and ROB research (astronomy, astrophysics, solar physics, planetology etc.). After one week, the Facebook page gained 85 likes and the Twitter page 14 followers. Those numbers continue to increase, and so the engagement of the followers.

Night of the Shooting Stars



A shooting star photographed during the Night of the Shooting Star 2016 at the Royal Observatory of Belgium.
(Photo: H. Coeckelberghs)

In the evening and night of 12 August 2016 the Observatory welcomed the public for an observation evening of the sky and the shooting ('falling') stars. The Planetarium was the main organizer of this event, with ROB and BISA assisting. Amateur astronomers, individuals and organizations put telescopes at the disposal of the visitors to observe the sky. BISA showed how to detect meteors with radio signals. The Schmidt telescope was also open for public visits.

The number of visitors was limited to 500 by pre-registration. However, not all showed up because of the bad weather. Two people

from the security were charged of guarding the entry building.

J. Cuypers represented the Observatory at the coordination meetings and was contact person for the event. J. Cuypers coordinated part of the organization at ROB and helped with the general organization. He informed the media on the event. During the event he gave explanations in the Schmidt dome.

Exhibitions

As each year, the Royal Palace in Brussels opened its doors to the public in summer: in 2016 from 22 July to 4 September. The public got the opportunity to discover the exhibition *Cartographiae* showing maps and cartography throughout the centuries. The ROB, mainly P. Lampens, provided items and information related to the project "Carte du Ciel" (see <http://www.astro.oma.be/en/scientific-research/astronomy-astrophysics/carte-du-ciel/>) and showed also an Ertel theodolite. J. Cuypers forwarded and corrected texts for the on-line catalogue and attended the press conference on July 19 in the Royal Palace.



Above: Two objects exposed during the exhibition *Cartographiae* at the Royal Palace. On the left: the "Carte du Ciel" book. On the right: copper engraving of the twice magnified glass plate image N° 214 (zone 35° N°159) of the "Carte du Ciel". Below: astrographic equatorial telescope which has contributed since 1908 to the mapping of the Uccle zone for the "Carte du Ciel" project (Photo: P. Van Cauteren).

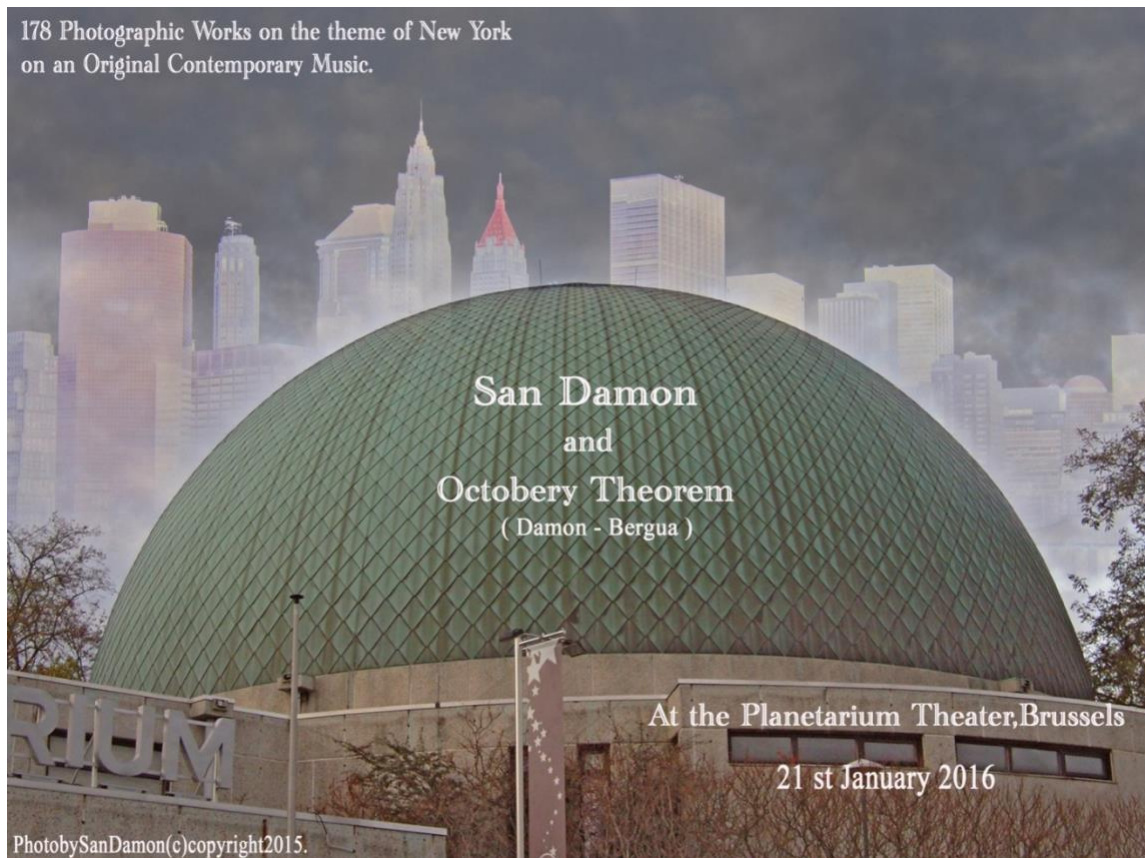
The information service also contributed to other exhibitions, with material, text or other inputs, such as the Cabinet de Curiosités, Entre Art et Nature, which took place between 06 and 20 March 2016 at Château-Ferme de Macon.

The Planetarium



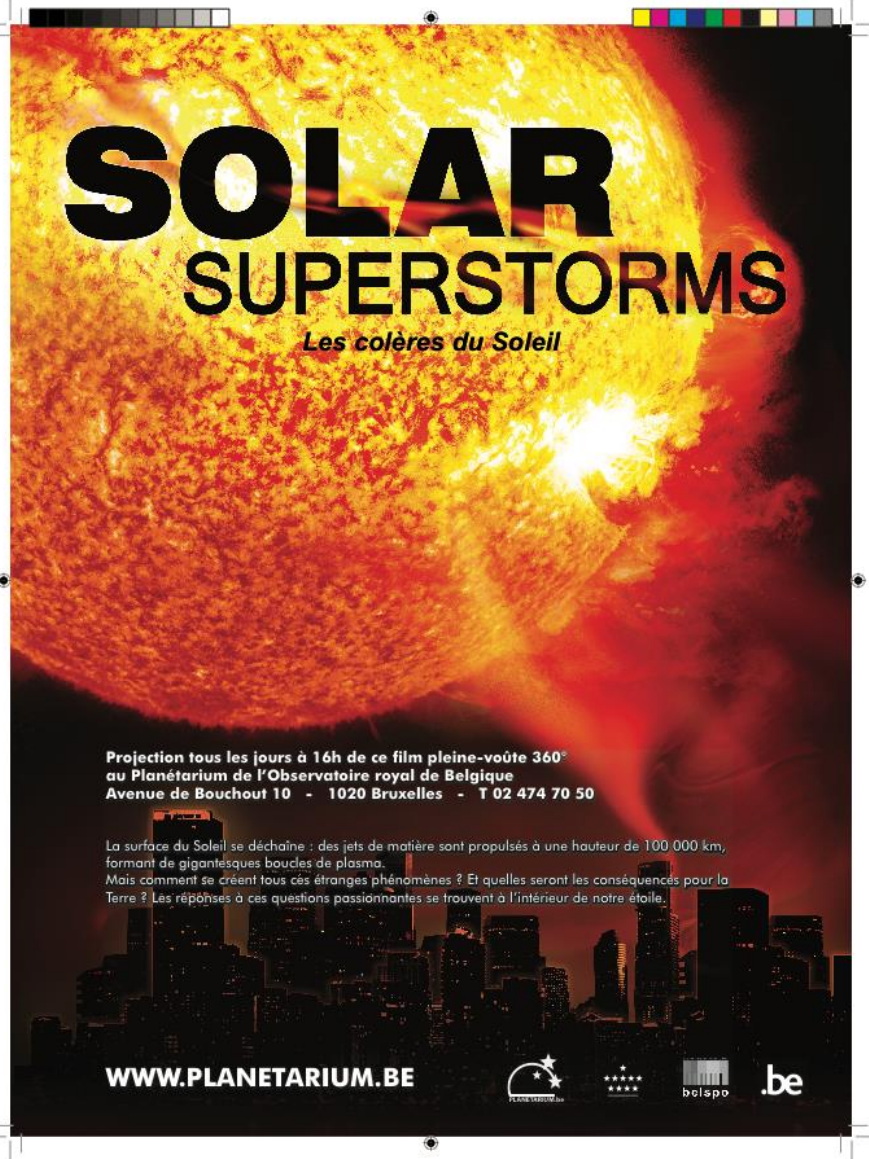
Oniroscopy and New York at the Planetarium

On January 21, the full dome exhibition San Damon and Octobery theorem took place at the Planetarium. Its purpose was to reconcile the planetarium science with artistic insights. Artist San Damon's photographic works on the theme of New York were projected on the Planetarium dome accompanied with contemporary classic jazz music (« symphorhapsody » build in 15 movements composed by San Damon and Denis Bergua). San Damon was the creator of the oniroscopy (oniros-dream, scopos-movement). He was notably known for setting contemporary art in magenta tonalities over the four kilometers of Franklin Roosevelt Avenue in Brussels, between January and March 2015.



New show: “Solar superstorm / Les colères du Soleil”

On April 26, a new show of the Planetarium was presented in avant-premiere: « Solar superstorms / Les colères du Soleil ». It is an impressive film about solar activity and its impact on Earth. It was favorably received by the public thanks to its remarkable visual qualities. To complete the essentially American view of this film produced by Spitz Creative Media, a supplementary sequence was especially internally created for this occasion so that the implication of the Observatory in solar physics research can be shown. This sequence of several minutes is broadcasted at the end of the film, at each projection.



The star projector Zeiss amongst the 100 masterpieces of Brussels

The star projector Zeiss has been selected amongst the 100 masterpieces of Brussels in the framework of the action "Master 100" of the Brussels Museums Council. On this occasion, four special evenings were organized in May and June in the form of live session animated by educators of the Planetarium.

Special activities

As each year, the Planetarium (and its ESERO office) organized several special activities at the Planetarium and at different places. Amongst these activities are the Concert of OSA Mayor, Mercury transit, the "Zonnekijkdag", Poetry under the stars, the "Nuit de l'Obscurité", the "Wetenschapsweek", and the Night of the Shooting stars in collaboration with the Observatory.

Annex 1: Publications

Publications with peer review

- [1] Aerts W., Bruyninx C., Defraigne P., Vandenbosch G. and Zeimetz P.
Influence of RF absorbing material on the calculated GNSS station position
GPS Solutions, GPS Solut 20: 1., 1-7, DOI: 10.1007/s10291-014-0428-y, 2016.
- [2] Baire Q. , Bruyninx C. , Legrand J. , Pottiaux E. , Aerts W. , Defraigne P. , Bergeot N. and Chevalier J.M
Erratum to: Influence of different GPS receiver antenna calibration models on geodetic positioning,
GPS Solutions, 20 (1), pp 135-135, 2016.
- [3] Baland, R.-M., Yseboodt, M. and Van Hoolst, T.
The obliquity of Enceladus.
Icarus, 268, pp. 12-31, DOI: 10.1016/j.icarus.2015.11.039., 2016.
- [4] Besliu-Ionescu, D., Mierla, M. and Maris-Muntean, G.
Analysis of the Energy Transferred from the Solar Wind into the Magnetosphere during the April 11, 2001 Geomagnetic Storm
Sun and Geosphere, 11 issue 2, pp 97 -104, ISSN 2367-8852, 2016.
- [5] Beuthe M.
Crustal control of dissipative ocean tides in Enceladus and other icy moons.
Icarus, 280, pp. 278-299, DOI: 10.1016/j.icarus.2016.08.009., 2016.
- [6] Beuthe M., Rivoldini A. and Trinh A.
Enceladus's and Dione's floating ice shells supported by minimum stress isostasy.
Geophysical Research Letters 43, 10088-10096, DOI: 10.1002/2016GL070650, 2016.
- [7] Blomme, R., Cuypers, J., Frémat, Y., Pauwels, T., De Cat, P., Lobel, A., Van Hemelryck, E., Jonckheere, A., Martayan, C. and the Gaia Collaboration
The Gaia Mission/ Gaia, Collaboration
Astronomy and Astrophysics, 595, pp A1, DOI: 10.1051/0004-6361/201629272, 2016.
- [8] Blomme, R., Cuypers, J., Frémat, Y., Pauwels, T., De Cat, P., Lobel, A., Van Hemelryck, E., Jonckheere, A., Martayan, C. and the Gaia Collaboration
Gaia Data Release 1 - Summary of the astrometric, photometric, and survey properties / Gaia, Collaboration
Astronomy and Astrophysics, 595, pp. A2, 2016.
- [9] Brenguier, F., Rivet, D., Obermann, A., Nakata, N., Boué, P., Lecocq, T., Campillo, M. and Shapiro, N.
4-D noise-based seismology at volcanoes: Ongoing efforts and perspectives.
Journal of Volcanology and Geothermal Research vol. 321 pp. 182-195, DOI: 10.1016/j.jvolgeores.2016.04.036, 2016.
- [10] Brenguier, F., Kowalski, P., Ackerley, N., Nakata, N., Boué, P., Campillo, M., Larose, E., Rambaud, S., Pequegnat, C., Lecocq, T., Roux, P., Ferrazzini, V., Villeneuve, N., Shapiro, N. and Chaput, J.
Toward 4D Noise-Based Seismic Probing of Volcanoes: Perspectives from a Large-N Experiment on Piton de la Fournaise Volcano
Seismological Research Letters vol. 87 pp. 15-25, 2016.
- [11] Čadek O., Tobie G., Van Hoolst T., Massé M., Choblet G., Lefèvre A., Mitri G., Baland R.M., Běhouková M., Bourgeois O. and Trinh A.
Enceladus's internal ocean and ice shell constrained from Cassini gravity, shape, and libration data.
Geophysical Research Letters, 43(11), pp. 5653-5660, DOI: 10.1002/2016GL068634, 2016.

- [12] Calais, E., Camelbeeck, T., Stein, S., Liu, M. and Craig, T.
A New Paradigm for Large Earthquakes in Stable Continental Plate Interiors
 Geophysical Research Letters vol. 43, DOI: 10.1002/2016GL070815, 2016.
- [13] Canning, R. E. A., Ferland, G. J., Fabian, A. C., Johnstone, R. M., van Hoof, P. A. M., Porter, R. L., Werner, N. and Williams, R. J. R.
Collisional excitation of [C II], [O I] and CO in massive galaxies
 Monthly Notices of the Royal Astronomical Society, 455, pp. 3042-3057, DOI: 10.1093/mnras/stv2390, 2016.
- [14] Caporali A., Bruyninx C., Fernandes R., Ganas A., Kenyeres A., Lidberg M., Stangl G., Holger S. and Zurutuza J.
Stress drop at the Kephalonia Transform Zone estimated from the 2014 seismic sequence
 Tectonophysics, Vol. 666, pp. 164–172, doi: 10.1016/j.tecto.2015.11.004, 2016.
- [15] Caudron, C., Mauri, G., Williams-Jones, G., Lecocq, T., Syahbana, D., Plaen, R., Peiffer, L., Bernard, A. and Saracco, G.
New insights into the Kawah Ijen hydrothermal system from geophysical data
 Geological Society, London vol. Special Publications, 437, 57-72, DOI: 10.1144/SP437.4, 2016.
- [16] Chatzinikos M. and Dermanis A.
A coordinate-invariant model for deforming geodetic networks: understanding rank deficiencies, non-estimability of parameters, and the effect of the choice of minimal constraints
 Journal of Geodesy (30 November 2016), online version, doi: 10.1007/s00190-016-0970-1, 2016.
- [17] Clementini, G., Ripepi, V., Leccia, S., Mowlavi, N., Lecoeur-Taibi, I., Marconi, M., Szabados, L., Eyer, L., Guy, L. P., Rimoldini, L., Jevardat de Fombelle, G., Holl, B., Busso, G., Charnas, J., Cuypers, J., De Angeli, F., De Ridder, J., Debosscher, J., Evans, D. W., Klagyivik, P., Musella, I., Nienartowicz, K., Ordóñez, D., Regibo, S., Riello, M., Sarro, L. M. and Süveges, M.
Gaia Data Release 1. The Cepheid and RR Lyrae star pipeline and its application to the south ecliptic pole region
 Astronomy & Astrophysics, 595, pp. A133, DOI: 10.1051/0004-6361/201629583, 2016.
- [18] Clette, F., Cliver, E. W., Lefèvre, L., Svalgaard, L., Vaquero, J. M. and Leibacher, J. W.
Preface to Topical Issue: Recalibration of the Sunspot Number
 Solar Physics, 291 issue 9-10, pp. 2479-2486, DOI: 10.1007/s11207-016-1017-8, 2016.
- [19] Clette, F., Lefèvre, L., Cagnotti, M., Cortesi, S. and Bulling, A.
The Revised Brussels-Locarno Sunspot Number (1981 - 2015)
 Solar Physics, 291 issue 9-10, pp. 2733-2761, DOI: 10.1007/s11207-016-0875-4, 2016.
- [20] Clette, F. and Lefèvre, L.
The New Sunspot Number: Assembling All Corrections
 Solar Physics, 291 issue 9-10, pp. 2629-2651, DOI: 10.1007/s11207-016-1014-y, 2016.
- [21] Cockell C.S., Bush T., Bryce C., Direito S., Fox-Powell M., Harrison J.P., Lammer H., Landenmark H., Martin-Torres J., Nicholson N., Noack L., O'Malley-James J., Payler S.J., Rushby A., Samuels T., Schwendner P. and Zorzano M.P.
Habitability: A Review.
 Astrobiology, 16(1), pp. 89-117, DOI: 10.1089/ast.2015.1295, 2016.
- [22] Coyette A., Van Hoolst T., Baland R.M. and Tokano T.
Modeling the polar motion of Titan.
 Icarus 265, pp. 1-28, DOI: 10.1016/j.icarus.2015.10.015., 2016.
- [23] Defraigne P. and Sleewaegen J.-M.

Code-Phase Clock Bias and frequency offset in PPP clock solutions
IEEE transactions on ultrasonics, ferroelectrics, and frequency control, vol. 63 (7), pp. 986-992, 2016.

- [24] Dehant V., Asael D., Baland R.M., Baludikay B.K., Beghin J., Beuthe M., Breuer D., Chernonozhkin S., Claeys Ph., Cornet Y., Cornet L., Coyette A., Delvigne C., Deprost M.H., De WIInter N., Duchemin C., Debaille V., El Atrassi F., François C., De Keyser J., Gillmann C., Glosener E., Goderis S., Hidaka Y., Höning D., Huber M., Hublet G., Javaux E., Karatekin Ö., Kodolanyi J., Lobo LR., Maes L., Maggiolo R., Mattielli N., Maurice M., McKibbin S., Morschhauser A., Neumann W., Noack L., Pham L.B.S., Pittarello L., Plesa A.C., Rivoldini A., Robert S., Rosenblatt P., Spohn T., Storme J-Y., Tosi N., Trinh A., Valdes M., Vandaele A.C., Vanhaecke F., Van Hoolst T., Van Roosbroek N., Wilquet V. and Yseboodt M.
PLANET TOPERS: Planets, Tracing the Transfer, Origin, Preservation, and Evolution of their ReservoirS.
Origins of Life and Evolution of Biospheres, 46(4), pp. 369-384, DOI: 10.1007/s11084-016-9488-z., 2016.
- [25] D'Huys, E., Berghmans, D., Seaton, D.B. and Poedts, S.
The effect of limited sample sizes on the accuracy of the estimated scaling parameter for power-law-distributed solar data
Solar Phys 291:1561–1576 DOI 10.1007/s11207-016-0910-5, 2016.
- [26] D'Huys, E., Seaton, D.B., De Groof, A., Berghmans, D. and Poedts, S.
Solar signatures and eruption mechanism of the 2010 August 14 CME
Journal of Space Weather and Space Climate , Volume 7, id.A7, 16 pp, DOI: 10.1051/swsc/2017006, 2016.
- [27] De Plaen, R., Lecocq, T., Caudron, C., Ferrazzini, V. and Francis, O.
Single station monitoring of volcanoes using seismic ambient noise
Geophysical Research Letters vol. 43. DOI: 10.1002/2016GL070078, 2016.
- [28] Dissauer, K., Temmer, M., Veronig, A. M., Vanninathan, K. and Magdalenic, J
Projection Effects in Coronal Dimmings and Associated EUV Wave Event
The Astrophysical Journal, 830 issue 2, article id. 92, 11 pp. DOI: 10.3847/0004-637X/830/2/92, 2016.
- [29] Domagal-Goldman S.D., Wright K.E., Adamala K., Antonio M., de la Rubia L.A., Bond, L., Dartnell, A. Goldman, I. Lima, K. Lynch, M.-E. Naud, K. Singer, X. Abrevaya, R. Anderson J., Arney G., Atri D., Azua-Bustos A., Bowman J., Brazelton W., Brennecke G., Carns R., Chopra A., Colangelo-Lillis J., Crockett C., DeMarines J., Frank E., Frantz C., de la Fuente, D. Galante, J., Glass, D. Gleeson, C. Glein, C. Goldblatt, R. Horak, L. Horodyskyj E., Kacar B., Kereszturi A., Knowles E., Mayeur P., McGlynn S., Miguel Y., Montgomery M., Neish C., Noack L., Rugheimer S., Stueken E., Tamez-Hidalgo P. and Walker S.I.
Astrobiology Primer 2.0.
Astrobiology, 16(8), pp. 561-653, DOI:10.1089/ast.2015.1460, 2016.
- [30] Dudok de Wit, T., Lefèvre, L. and Clette, F.
Uncertainties in the Sunspot Numbers: Estimation and Implications
Solar Physics, 291 issue 9-10, pp. 2709-2731 10.1007/s11207-016-0970-6, 2016.
- [31] Duev D.A., Pogrebenko S.V., Cimò G., Molera Calvés G., Bocanegra Bahamón T.M., Gurvits L.I., Kettenis M.M., Kania J., Tudose V., Rosenblatt P., Marty J.-C., Lainey V., de Vicente P., Quick J., Nickola M., Neidhardt A., Kronschnabl G., Ploetz C., Haas R., Lindqvist M., Orlati A., Ipatov A.V., Kharinov M.A., Mikhailov A.G., Lovell J.E.J., McCallum J.N., Stevens J., Gulyaev S.A., Natush T., Weston S., Wang W.H., Xia B., Yang W.J., Hao L.-F., Kallunki J. and Witasse O

Planetary Radio Interferometry and Doppler Experiment (PRIDE) technique: A test case of the Mars Express Phobos fly-by.

Astronomy & Astrophysics, 593, id. A34, 10 pp, DOI: 10.1051/0004-6361/201628869, 2016.

- [32] Gillmann C., Golabek G.J. and Tackley P.J.
Effect of a single large impact on the coupled atmosphere-interior evolution of Venus.
Icarus, 268, pp. 295-312, DOI: 10.1016/j.icarus.2015.12.024, 2016.
- [33] Gonzalez, A., Delouille, V. and Jacques, L.
Non-parametric PSF estimation from celestial transit solar images using blind deconvolution
Journal of Space Weather and Space Climate, 6, pp. A1, DOI: 10.1051/swsc/2015040, 2016
- [34] Gray, R. O., Corbally, C. J., De Cat, P., Fu, J. N., Ren, A. B., Shi, J. R., Luo, A. L., Zhang, H. T., Wu, Y., Cao, Z., Li, G., Zhang, Y., Hou, Y. and Wang, Y.
LAMOST Observations in the Kepler Field: Spectral Classification with the MKCLASS Code
The Astronomical Journal, 151, pp. 13, DOI: 10.3847/0004-6256/151/1/13, 2016.
- [35] Grossir G., Van Hove B., Paris S., Rambaud P. and Chazot O.
Free-stream static pressure measurements in the Longshot hypersonic wind tunnel and sensitivity analysis
Experiments in Fluids, 57(5), article Id. #64, 13 p, DOI: 10.1007/s00348-016-2137-5, 2016.
- [36] Guerova G., Jones J., Douša J., Dick G., de Haan S., Pottiaux E., Bock O., Pacione R., Elgered G., Vedel H. and Bender M.
Review of the state of the art and future prospects of the ground-based GNSS meteorology in Europe
Atmospheric Measurement Technique (AMT), 9, pp. 5385-5406, DOI: 10.5194/amt-9-5385-2016, 2016.
- [37] Guzmán, F., Badnell, N. R., Williams, R. J. R., van Hoof, P. A. M., Chatzikos, M. and Ferland, G. J.
H, He-like recombination spectra - I. I-changing collisions for hydrogen
Monthly Notices of the Royal Astronomical Society, 459, pp. 3498-3504, DOI: 10.1093/mnras/stw893, 2016.
- [38] Hayes, L.A., Gallagher, P.T., Dennis, B.R., Ireland, J., Inglis, A.R. and Ryan, D.F.
Quasi-periodic Pulsations during the Impulsive and Decay phases of an X-class Flare
The Astrophysical Journal Letters, 827 issue L30, DOI: 10.3847/2041-8205/827/2/L30, 2016.
- [39] Hoff M., Harlander U. and Triana S.A.
Study of turbulence and interacting inertial modes in a differentially rotating spherical shell experiment
Physical Review Fluids 1, 043701, 2016.
- [40] Huang W. and Defraigne P.
CGGTT Results with BeiDou Using the R2CGGTTs
IEEE transactions on ultrasonics, ferroelectrics, and frequency control, vol. 63 (7), pp. 1005-1012, 2016.
- [41] Kahraman Aliçavus, F. Niemczura, E. De Cat, P. Soydugan, E., Kolaczkowski, Z., Ostrowski, J., Telting, J. H., Uytterhoeven, K., Poretti, E., Rainer, M., Suárez, J. C., Mantegazza, L., Kilmartin, P. and Pollard, K. R.
Spectroscopic survey of γ Doradus stars - I. Comprehensive atmospheric parameters and abundance analysis of γ Doradus stars
Monthly Notices of the Royal Astronomical Society, 458, pp. 2307-2322 DOI: 10.1093/mnras/stw393, 2016.
- [42] Karoff, C., Knudsen, M. F., De Cat, P., Bonanno, A., Fogtmann-Schulz, A., Fu, J., Frasca, A., Inceoglu, F., Olsen, J., Zhang, Y., Hou, Y., Wang, Y., Shi, J. and Zhang, W.

Observational evidence for enhanced magnetic activity of superflare stars
Nature Communications, 7, pp. 11058, DOI: 10.1038/ncomms11058, 2016.

- [43] Keresztfuri A. and Noack L.
Review on the role of planetary factors on habitability
Origins of Life and Evolution of Biospheres, 46(4), pp. 473-486, DOI: 10.1007/s11084-016-9514-1, 2016
- [44] Krupar, V., Eastwood, J., Kruparova, O., Santolik, O., Soucek, J., Magdalenic, J., Vourlidas, A., Maksimovic, M., Bonnin, X., Bothmer, V., Mrotzek, N., Pluta, A., Barnes, D., Davies, J., Carlos, J., Oliveros, M. and Bale, S.
An Analysis of Interplanetary Solar Radio Emissions Associated with a Coronal Mass Ejection
The Astrophysical Journal Letters, 823 issue 1, article id. L5, 7 pp., DOI: 10.3847/2041-8205/823/1/L5, 2016.
- [45] Laha, S., Keenan, F. P., Ferland, G. J., Ramsbottom, C. A., Aggarwal, K. M., Ayres, T. R., Chatzikos, M., van Hoof, P. A. M. and Williams, R. J. R.
Ultraviolet emission lines of Si II in cool star and solar spectra
Notices of the Royal Astronomical Society, 455, pp. 3405-3412 DOI: 10.1093/mnras/stv2566, 2016.
- [46] Lainey V., Jacobson R.A., Tajeddine R., Cooper N.J., Murray C., Robert V., Tobie G., Guillot T., Mathis S., Remus F., Desmars J., Arlot J.-E., De Cuyper J.-P., Dehant V., Pascu D., Thuillot W., Le Poncin-Lafitte Ch. and Zahn J.-P.
New constraints on Saturn's interior from Cassini astrometric data.
Icarus, 281, pp. 286-296, DOI: 10.1016/j.icarus.2016.07.014, 2016.
- [47] Lefèvre, L., Aparicio, A. J. P., Gallego, M. C. and Vaquero, J. M.
An Early Sunspot Catalog by Miguel Aguilar for the Period 1914 - 1920
Solar Physics, 291 issue 9-10, pp. 2609-2628 DOI: 10.1007/s11207-016-0905-2, 2016.
- [48] Lefèvre, L., Vennerstrøm, S., Dumbović, M., Vršnak, B., Sudar, D., Arlt, R., Clette, F. and Crosby, N.
Detailed Analysis of Solar Data Related to Historical Extreme Geomagnetic Storms: 1868 – 2010
Solar Physics, 291 issue 5, pp. 1483-1531, DOI: 10.1007/s11207-016-0892-3, 2016.
- [49] Le Gall A., Malaska M. J., Lorenz R. D., Janssen M. A., Tokano T., Hayes A. G., Mastrogiovanni M., Lunine J. I., Veyssiére G., Encrenaz P. and Karatekin Ö.
Composition, seasonal change, and bathymetry of Ligeia Mare, Titan, derived from its microwave thermal emission
Journal of Geophysical Research: Planets, 121(2), pp. 233-251, DOI: 10.1002/2015JE004920, 2016.
- [50] Le Gall A., Malaska M. J., Lorenz R. D., Janssen M. A., Tokano T., Hayes A. G., Mastrogiovanni M., Lunine J. I., Veyssiére G., Encrenaz P. and Karatekin Ö.
Composition, seasonal change, and bathymetry of Ligeia Mare, Titan, derived from its microwave thermal emission.
Journal of Geophysical Research: Planets, 121(2), pp. 233-251, DOI: 10.1002/2015JE004920, 2016.
- [51] Lemaire, J. and Stegen, K.
Improved Determination of the Location of the Temperature Maximum in the Corona
Solar Physics, 291 issue 12, pp. 3659-3683 (2016) 10.1007/s11207-016-1001-3
- [52] Le Maistre S.

InSight coordinates determination from direct-to-Earth radio-tracking and Mars topography model.

Planetary and Space Science, 121, pp. 1-9, DOI: 10.1016/j.pss.2015.11.003, 2016.

- [53] Le Maistre S., Folkner W. M., Jacobson R.A. and Serra D.
Jupiter spin-pole precession rate and moment of inertia from Juno radio-science observations.
Planetary and Space Science, 126, pp. 78-92, DOI: 10.1016/j.pss.2016.03.006, 2016, May 2016.
- [54] Lombaert, R., Decin, L., Royer, P., de Koter, A., Cox, N. L. J., González-Alfonso, E., Neufeld, D., De Ridder, J., Agúndez, M., Blommaert, J. A. D. L., Khouri, T., Groenewegen, M. A. T., Kerschbaum, F., Cernicharo, J., Vandenbussche, B. and Waelkens, C.
Constraints on the H₂O formation mechanism in the wind of carbon-rich AGB stars
Astronomy and Astrophysics, 588, pp. A124, DOI: 10.1051/0004-6361/201527049, 2016
- [55] Lombardi, D., Benoit, L., Camelbeeck, T., Martin, O., Meynard, C. and Thom, C.
Bimodal pattern of seismicity detected at the ocean margin of an Antarctic ice shelf
Geophysical Journal International vol. 206 pp. 1375-1381, DOI: 10.1093/gji/ggw214, 2016.
- [56] Martayan, C., Lobel, A., Baade, D., Mehner, A., Rivinius, T., Boffin, H. M. J., Girard, J., Mawet, D., Montagnier, G., Blomme, R., Kervella, P., Sana, H., Štefl, S., Zorec, J., Lacour, S., Le Bouquin, J.-B., Martins, F., Mérand, A., Patru, F., Selman, F. and Frémat, Y.
Luminous blue variables: An imaging perspective on their binarity and near environment
Astronomy and Astrophysics, 587, pp. A115, DOI: 10.1051/0004-6361/201526578, 2016.
- [57] Masias-Meza, J., Dasso, S., Demoulin, P., Rodriguez, L. and Janvier, M.
Superposed epoch study of ICME sub-structures near Earth and their effects on Galactic cosmic rays
Astronomy & Astrophysics, Volume 592, id.A118, 13 pp, DOI: 10.1051/0004-6361/201628571, 2016.
- [58] Mason, B. D., Balega, Y., Docobo, J., Arenou, F., Scardia, M., Tamazian, V., Ten Brummelaar, T., Lampens, P., Reipurth, B. and Tokovinin, A.
Division G Commission 26: Double Multiple Stars
Transactions of the International Astronomical Union, Series A, 29, pp. 388-412, DOI: 10.1017/S1743921316000879, 2016.
- [59] Meurers, B., Van Camp, M., Francis, O., Palinkas, V.
Temporal variation of tidal parameters in superconducting gravimeter time series
Geophysical Journal International (2016).
- [60] Michel P., Cheng A., Küppers M., Pravec P., Blum J., Delbo M., Green S.F., Rosenblatt P., Tsiganis K., Vincent J.B., Biele J., Ciarletti V., Hérique A., Ulamec S., Carnelli I., Galvez A., Benner L., Naidu S.P., Barnouin O.S., Richardson D.C., Rivkin A., Scheirich P., Moskovitz N., Thirouin A., Schwartz S.R., Campo Bagatin A., Yu Y.
Science case for the Asteroid Impact Mission (AIM): a component of the Asteroid Impact & Deflection Assessment (AIDA) mission.
Advances in Space Research, 57(12), pp. 2529-2547, DOI: 10.1016/j.asr.2016.03.031, 2016.
- [61] Moon, K., Li, J., Delouille, V., De Visscher, R., Watson, F. and Hero III, A.O.
Image patch analysis of sunspots and active regions. I. Intrinsic dimension and correlation analysis
Journal of Space Weather and Space Climate, 6, pp. A2, DOI: 10.1051/swsc/2015044, 2016.
- [62] Moon, K., Delouille, V., Li, J., De Visscher, R., Watson, F. and Hero III, A.O.
Image patch analysis of sunspots and active regions. II. Clustering via dictionary learning
Journal of Space Weather and Space Climate, 6, pp. A3, DOI: 10.1051/swsc/2015043, 2016.

- [63] Moretti, M. I., Clementini, G., Ripepi, V., Marconi, M., Rubele, S., Cioni, M.-R. L., Muraveva, T., Groenewegen, M. A. T., Cross, N. J. G., Ivanov, V. D., Piatti, A. E. and de Grijs, R.
The VMC survey - XX. Identification of new Cepheids in the Small Magellanic Cloud
Monthly Notices of the Royal Astronomical Society, 459, pp. 1687-1697, DOI: 10.1093/mnras/stw716, 2016.
- [64] Noack L., Hoening D., Rivoldini A., Heistracher C., Zimov N., Journaux B., Lammer H., Van Hoolst T. and Bredehoeft J.H.
Water-rich planets: how habitable is a water layer deeper than on Earth?
Icarus, 277, 215-236, DOI: 10.1016/j.icarus.2016.05.009, 2016.
- [65] Noack L., Rivoldini A., and Van Hoolst T.
Modeling the Evolution of Terrestrial and Water-rich Planets and Moons.,
International Journal On Advances in Systems and Measurements, 9(1/2), pp. 66-76, 2016.
- [66] Panning M.P., Lognonné P., Banerdt W.B., Garcia R., Golombek M., Kedar S., Knapmeyer-Endrun B., Mocquet A., Teanby N.A., Tromp J., Weber R., Beucler E., Blanchette-Guertin J.-F., Bozdağ E., Drilleau M., Gudkova T., Khan A., Lekić V., Murdoch N., Plesa A.-C., Rivoldini A., Schmerr N., Ruan Y., Verhoeven O., Gao C., Christensen U., Clinton J., Dehant V., Giardini D., Mimoun D., Pike W.T., Smrekar S., Wieczorek M., Knapmeyer M. and Wookey J.
Planned Products of the Mars Structure Service for the InSight Mission to Mars.
Space Sci. Rev., DOI: 10.1007/s11214-016-0317-5, 2016.
- [67] Pant, V., Willems, S., Rodriguez, L., Mierla, M., Banerjee, D. and Davies, J.
Automated Detection Of Coronal Mass Ejections In STEREO Heliospheric Imager Data
The Astrophysical Journal, Volume 833, Issue 1, article id. 80, 15 pp, DOI: 10.3847/1538-4357/833/1/80, 2016.
- [68] Patsourakos, S., Georgoulis, M.K., Vourlidas, A., Nindos, A., Sarris, E., Anastasiadis, A., Daglis, I., Iliopoulos, I., Kouloumvakos, A., Moratis, K., Pavlos, G., Tziotziou, K., Podladchikova, O., Malandraki, O., Turner, D., Xenakis, M., Sarris, T., Tsinganos, K. and Vlahos, L.
THE MAJOR GEOEFFECTIVE SOLAR ERUPTIONS OF 7 MARCH 2012: COMPREHENSIVE SUN-TO-EARTH ANALYSIS
The Astrophysical Journal, 817 issue 14, pp. 1-22, 2016.
- [69] Pätzold M., Häusler B., Tyler G.L., Andert T., Asmar S.W., Bird M.K., Dehant V., Hinson D.P., Rosenblatt P., Simpson R.A., Tellmann S., Withers P., Beuthe M., A.I. Efimov, Hahn M., Kahan D., Le Maistre S., Oschlinski J., Peter K. and Remus S.
Mars Express 10 years at Mars: Observations by the Mars Express Radio Science Experiment (MaRS).
Planetary and Space Science, 127, pp. 44-90, DOI: 10.1016/j.pss.2016.02.013, 2016.
- [70] Pavluk, Y., Podladchikova, O. and Podladchikov, V.N.
Stereoscopic Analysis of A Coronal Wave
System Research Information Technologies, 97, pp. 73-77, 2016.
- [71] Petit G. and Defraigne P.
The performance of GPS time and frequency transfer: Comment on ‘A detailed comparison of two continuous GPS carrier-phase time transfer techniques’
Metrologia, 53 (3), pp. 1003-1008, 2016.
- [72] Pham L. B. S. and Karatekin Ö.
Scenarios of atmospheric mass evolution on Mars influenced by asteroid and comet impacts since the late Noachian.
Planetary and Space Science, 125, pp. 1-11, DOI: 10.1016/j.pss.2015.09.022, 2016.

- [73] Plotnikov, I., Rouillard, A.P., Davies, J., Bothmer, V., Eastwood, J. P., Gallagher, P.T., Harrison, R.A., Kilpua, E., Möstl, C. and Rodriguez, L.
Long-Term Tracking of Corotating Density Structures using Heliospheric Imaging
Solar Physics, Volume 291, Issue 6, pp.1853-1875, DOI: 10.1007/s11207-016-0935-9, 2016.
- [74] Rau, G., Paladini, C., Hron, J., Aringer, B., Groenewegen, M. A. T. and Nowotny, W.
Modelling a set of C-rich AGB stars: the cases of RU Vir and R Lep
Memorie della Società Astronomica Italiana, 87, pp. 260, 2016.
- [75] Rauw, G., Blomme, R., Nazé, Y., Spano, M., Mahy, L., Gosset, E., Volpi, D., van Winckel, H., Raskin, G. and Waelkens, C.
Testing the theory of colliding winds: the periastron passage of 9 Sagittarii. I. X-ray and optical spectroscopy
Astronomy and Astrophysics, 589, pp. A121, DOI: 10.1051/0004-6361/201526871, 2016.
- [76] Rekier J., Füzfa A., and Cordero-Carrión I.,
Nonlinear cosmological spherical collapse of quintessence.
Phys. Rev. D 93, 043533 (2016) – Published 17 February 2016
- [77] Ren, Anbing, Fu, Jianning, De Cat, Peter, Wu, Yue, Yang, X., Shi, J., Luo, A., Zhang, H., Dong, S., Zhang, R., Zhang, Y., Hou, Y., Wang, Y., Cao, Z. and Du, B.
LAMOST Observations in the Kepler Field. Analysis of the Stellar Parameters Measured with LASP Based on Low-resolution Spectra
The Astrophysical Journal Supplement Series, 225 issue 2, pp. A28 (1-17), DOI: 10.3847/0067-0049/225/2/28, 2016.
- [78] Ripepi, V., Marconi, M., Moretti, M. I., Clementini, G., Cioni, M.-R. L., de Grijs, R., Emerson, J. P., Groenewegen, M. A. T., Ivanov, V. D. and Piatti, A. E.
The VMC Survey. XIX. Classical Cepheids in the Small Magellanic Cloud
The Astrophysical Journal Supplement Series, 224, pp. 21, DOI: 10.3847/0067-0049/224/2/21, 2016.
- [79] Robert V., Pascu D., Lainey V., Arlot J.-E., De Cuyper J.-P., Dehant V. and Thuillot W.
New astrometric measurement and reduction of USNO photographic observations of the main Saturnian satellites: 1974–1998.
Astr. Astrophys. 596, A37, DOI: 10.1051/0004-6361/201629807, 2016.
- [80] Rosenblatt P., Charnoz S., Dunseath K.M., Terao-Dunseath M., Trinh A., Hyodo R., Genda H. and Toupin S.
Accretion of Phobos and Deimos in an extended debris disc stirred by transient moons.
Nature Geoscience, 9(8), pp. 581-583, DOI: 10.1038/ngeo2742, 2016.
- [81] Ryan, D., Dominique, M., Seaton, D., Stegen, K. and White, A.
Effects of flare definitions on the statistics of derived flare distributions
Astronomy & Astrophysics, 592, id A133, DOI: 10.1051/0004-6361/201628130, 2016.
- [82] Shevchuk, N. V., Melnik, V. N., Poedts, S., Dorovskyy, V.V., Magdalénic, J., Konovalenko, A.A., Brazhenko, A.I., Briand, C., Frantsuzenko, A.V., Rucker, H.O. and Zarka, P.
The Storm of Decameter Spikes During the Event of 14 June 2012
Solar Physics, 291, pp. 211-228, 2016.
- [83] Slemzin, V.A., Ulyanov, A., Gaikovich, K., Kuzin, S.V., Perstov, A., Berghmans, D., Dominique, M.
Validation of the Earth atmosphere models using the solar EUV solar occultation data from the CORONAS and PROBA 2 instruments
Journal of Space Weather and Space Climate, Volume 6, id.A7, 6 issue 27, DOI: 10.1051/swsc/2015045, 2016.

- [84] Tanga, P., Mignard, F., Dell'Oro, A., Muinonen, K., Pauwels, T., Thuillot, W., Berthier, J., Cellino, A., Hestroffer, D., Petit, J.-M., Carry, B., David, P., Delbo` M., Fedorets, G., Galluccio, L., Granvik, M., Ordenovic, C. and Pentikäinen, H.
The daily processing of asteroid observations by Gaia
Planetary and Space Science, 123, pp. 87-94, DOI: 10.1016/j.pss.2015.11.009, 2016.
- [85] Vamvatira-Nakou, C., Hutsemékers, D., Royer, P., Waelkens, C., Groenewegen, M. A. T. and Barlow, M. J.
Herschel observations of the nebula M1-67 around the Wolf-Rayet star WR 124
Astronomy and Astrophysics, 588, pp. A92, DOI: 10.1051/0004-6361/201527667, 2016.
- [86] Van Camp, M. and de Viron, O.
The slightness of gravimetry
Nature Physics vol. 12 pp. 816. DOI: 10.1038/nphys3847, 2016.
- [87] Van Camp, M., de Viron, O. and Avouac, J.
Separating climate-induced mass transfers and instrumental effects from tectonic signal in repeated absolute gravity measurements
Geophysical Research Letter, Volume 43, Issue 9, DOI: 10.1002/2016GL068648, 2016.
- [88] Van Camp, M., de Viron, O., Pajot-Métivier, G., Casenave, F., Watlet, A., Dassargues, A. and Vanclooster, M.
Direct measurement of evapotranspiration from a forest using a superconducting gravimeter
Geophysical Research Letters vol. 43, DOI: 10.1002/2016GL070534, 2016.
- [89] Van Camp, M., Meurers, B., de Viron, O. and Forbirger, T.
Optimized strategy for the calibration of superconducting gravimeters at the one per mille level
Journal of Geodesy vol. 90 pp. 91-99, DOI: 10.1007/s00190-015-0856-7, 2016.
- [90] Van Hoolst T., Baland R.M., and Trinh A.
The diurnal libration and interior structure of Enceladus.,
Icarus, 277, 311-318, DOI: 10.1016/j.icarus.2016.05.025, 2016.
- [91] Van Noten, K.
Visualizing Cross-Sectional Data in a Real-World Context
EOS, Transactions AGU vol. 97 pp. 16-19, DOI: 10.1029/2016EO044499, 2016.
- [92] Vaquero, J. M., Svalgaard, L., Carrasco, V. M. S., Clette, F., Lefèvre, L., Gallego, M. C., Arlt, R., Aparicio, A. J. P., Richard, J.-G. and Howe, R.
A Revised Collection of Sunspot Group Numbers
Solar Physics, 291 issue 9-10, pp. 3061-3074, DOI: 10.1007/ et al s11207-016-0982-2, 2016.
- [93] Vennerstrom, S., Lefevre, L., Dumbović, M., Crosby, N., Malandraki, O., Patsou, I., Clette, F., Veronig, A., Vršnak, B., Leer, K. and Moretto, T.
Extreme Geomagnetic Storms - 1868 - 2010
Solar Physics, 291 issue 5, pp. 1447-1481, DOI:10.1007/s11207-016-0897-y, 2016.
- [94] Ventura, P., García-Hernández, D. A., Groenewegen, M. and van Loon, J. T.
AGB stars: a key ingredient in the understanding and interpretation of stellar populations: European Week of Astronomy and Space Science
Memorie della Società Astronomica Italiana, 87, pp. 225, 2016.
- [95] Vincent D., Karatekin Ö., Vallaeys V., Hayes A.G., Mastrogiovanni M., Notarnicola C., Dehant V. and Deleersnijder E,
Numerical study of tides in Ontario Lacus, a hydrocarbon lake on the surface of the Saturnian moon Titan.
Ocean Dynamics, DOI: 10.1007/s10236-016-0926-2, 2016.

- [96] Wauters, L., Dominique, M., Dammasch, I. E.
LYRA Mid-Term Periodicities
Solar Physics, 291, pp. 2135–2144, DOI: 10.1007/s11207-016-0960-8, 2016.
- [97] Zhu P., Wild M., van Ruymbeke M., Thuillier G., Meftah M. and Karatekin Ö,
Inter annual variation of global net radiation flux as measured from space,
J. Geophys. Res., 121(12), pp. 6877-6891, DOI: 10.1002/2015JD024112, 2016.

Publications without peer review

- [98] Altobelli N., Tosi F., Van Hoolst T., Krupp N., and Masters A.
JUICE Payload Operations Scenario for Europa Flybys.
ESA report, 19 Jan 2016.
- [99] Baland R.M., Yseboodt M., Rivoldini A. and Van Hoolst T.
The influence of an inner core, tides, and precession of the pericenter on the orientation of the rotation axis of Mercury.
Extended Abstract, AAS/DPS meeting #48/ EPSC 11, Pasadena, Ca, USA, October 16-21, 2016.
- [100] Barnouin O., Bellerose J., Carnelli I., Carroll K., Ciarletti V., Cheng A.F., Galvez A., Green S.F., Grieger B., Hirabayashi M., Herique A., Kueppers M., Minton D.A., Mellab K., Michel P., Rivkin A.S., Rosenblatt P., Tortora P., Ulamec S., Vincent J.B. and Zannoni M.
The Asteroid Impact and Deflection Assessment (AIDA) mission: Science proximity Operations.
Extended Abstract 2567558, DPS/EPSC meeting, Pasadena, CA, USA, 16-21 October, 2016.
- [101] Blanc M., Prieto-Ballesteros O. and the JEM core team (including T. Van Hoolst)
JEM, Joint Europa Mission, a multi-scale study of Europa to characterize its habitability and search for extant life.
Proposal in response to the call for a medium-size mission opportunity in ESA's Science Programme [M5], 2016.
- [102] Bruyninx C., Araszkiewicz A., Brockmann E., Kenyeres A., Pacione R., Söhne W., Stangl G., Szafranek K., Völksen C.
EPN Regional Network Associate Analysis Center Technical Report 2015
In International GNSS Service Technical Report 2015, Eds Y. Jean, R. Dach, Astr.Inst. Univ. Bern, doi: 10.7892/boris.80307, 2016.
- [103] Calders, S., Verbeeck, C., Lamy, H., Martinez Picar, A.
The Radio Meteor Zoo: a citizen science project
Proceedings of the International Meteor Conference 2016 (eds. A. Roggemans, P. Roggemans), pp. 46-49, 2016.
- [104] Cliver, Edward W., Clette, F., Lefèvre, L. and Svalgaard, L.
Comparison of New and Old Sunspot Number Time Series
American Astronomical Society, SPD meeting #47, pp. 11.01, 2016.
- [105] Dehant V. and Gross R.
Precession, Nutation, and Rotation: Understanding the Earth Core and Nutation.
EOS Earth and Space Sciences News, American Geophysical Union, Wiley, EOS December 2016, DOI: 10.1029/EOS2016S005368, 2016.
- [106] Deproost M.-H., Rivoldini A. and Van Hoolst T.
Mercury's internal structure and core thermal evolution.
Extended Abstract, American Astronomical Society, AAS/DPS meeting #48/ EPSC 11, Pasadena, Ca, USA, Poster 117.04, October 16-21, 2016.
- [107] Dumoulin C., Tobie G., Verhoeven O., Rosenblatt P. and Rambaux N.
Tidal constraints on the interior of Venus.
Abstract 2568358, DPS/EPSC meeting, Pasadena, CA, USA, Oct. 16-21 October, 2016.
- [108] Gillmann C.
MAVEN, à quoi ça sert ?
Bulletin 67 de l'Association Planète Mars (Mars Society France), April 2016. Review of scientific results by the MAVEN probe, 2016.
- [109] Gillmann C., Golabek G. and Tackley, P.

Large impacts on Venus: Effects on long term evolution.

Proc. International Venus conference, Oxford, 4-8 april 2016.

- [110] Grasset O., Witasse O., Barabash S., Brandt P., Bruzzone L., Bunce E., Cecconi B., Cavalie T., Cimo G., Coustenis A., Cremonese G., Dougherty M., Fletcher L., Gladstone R., Grasset O., Gurvits L., Hartogh P., Hoffmann H., Hussmann H., Iess L., Jaumann R., Kasaba Y., Kaspi Y., Krupp N., Langevin Y., Mueller-Wodarg I., Palumbo P., Piccioni G., Plaut J.J., Poulet F., Roatsch T., Rutherford K., Rothkaehl H., Santolik O., Stevenson D.J., Van Hoolst T., Wahlund J.-E., Witasse O., Wurz P., Altobelli N., Accomazzo A., Boutonnet A., Erd C. and Vallat C.
The rotation of Titan and Ganymede.
AAS/DPS meeting #48/ EPSC 11, Pasadena, Ca, USA, October 16-21, 2016.
- [111] Halain, J.-P., Rochus, P., Renotte, E., Hermans, A., Jacques, A., Mazzoli, A., Auchere, F., Berghmans, D., Harra, L., Schuhle, U., Schmutz, W., Aznar Cuadrado, R., Dumesnil, C., Gyo, M., Kennedy, T., Verbeeck, C. and Smith, P.
The qualification campaign of the EUI instrument of Solar Orbiter
Proc. SPIE, 9905 issue Space Telescopes and Instrumentation 2016: Ultraviolet to Gamma Ray, 99052X, DOI: 10.1117/12.2232372, July 18, 2016.
- [112] Jones G., and the AKON core team (including T. Van Hoolst)
Akon Europa Penetrator Mission.
Proposal in response to the call for a medium-size mission opportunity in ESA's Science Programme [M5], 2016.
- [113] Lainey V., Thuillot W., Pasewaldt A., Robert V., Rosenblatt P., Vermeersen B., Arlot J.E., Bauer S., Dehant V., Gurvits L.I., Marty J.-C., Hussmann H., Oberst J. and the ESPaCE team
The ESPaCE consortium as a European producer of spacecraft and natural moon ephemerides.
Proc. 6th International Conference on Astrodynamics Tools and Techniques (ICATT), ESOC, 3 pages, March 14-17, 2016.
- [114] Lainey V., Cooper N., Murray C., Noyelles B., Pasewaldt A., Robert V., Rosenblatt P., Andert T., Paetzold M. and Thuillot W.
Physical librations and possible homogeneity of natural moons from astrometry.
Abstract 2567222, DPS/EPSC meeting, Pasadena, CA, USA, 16-21 October, 2016.
- [115] Martínez Picar, A., Marqué, C., Verbeeck, C., Calders, S., Ranvier, S., Gamby, E., Anciaux, M., Tetard, C. and Lamy, H.
Numerical simulation of the BRAMS interferometer in Humain
Proceedings of the International Meteor Conference Egmond, the Netherlands, 2–5 June 2016, pp. 175-178, 2016.
- [116] Mason, B. D., Balega, Y., Docobo, J., Arenou, F., Scardia, M., Tamazian, V., Ten Brummelaar, T., Lampens, P., Reipurth, B. and Tokovinin, A.
Division G Commission 26: Double Multiple Stars
Transactions of the International Astronomical Union, Series A, 29, pp. 388-412, DOI: 10.1017/S1743921316000879, 2016.
- [117] Péters M.J., Yseboodt M., Dehant V., Le Maistre S. and Marty J.-C.
The Martian rotation from Doppler measurements: Simulations of future radioscience experiments.
Extended Abstract, American Astronomical Society, AAS/DPS meeting #48/ EPSC 11, Pasadena, Ca, USA, Poster, October 16-21, 2016.
- [118] Rau, G., Paladini, C., Hron, J., Aringer, B., Groenewegen, M. A. T. and Nowotny, W.
Modelling a set of C-rich AGB stars: the cases of RU Vir and R Lep
Memorie della Società Astronomica Italiana, 87, pp. 260, 2016.

- [119] Richardson D.C., Barnouin O.S., Benner L.A., Bottke W., Bagatin A.C., Cheng A.F., Eggli S., Hamilton D.P., Hestroffer D.H., Hirabayashi M., Maurel C., McMahon J.W., Michel P., Murdoch N., Naidu S.P., Pravec P., Rivkin A.S., Rosenblatt P., Sarid G., Scheeres D.J., Scheirich P., Tsiganis K. and Zhang Y.
Dynamical and physical properties of 65803 Didymos, the proposed AIDA mission target.
Abstract 2566232, DPS/EPSC meeting, Pasadena, CA, USA, 16-21 October, 2016.
- [120] Rivoldini A., Van Hoolst T., Beuthe M. and Deprost M.-H.
Mercury's interior structure constrained by geodesy and present-day thermal state.
Extended Abstract, American Astronomical Society, AAS/DPS meeting #48 / EPSC 11, Pasadena, Ca, USA, Poster 117.04, October 16-21, 2016.
- [121] Rosenblatt P., Charnoz S., Dunseath K.M., Dunseath-Terao M., Trinh A., Hyodo R., Genda H. and Toupin S.
Formation of Phobos and Deimos in a giant collision scenario facilitated by a large transient moon.
Abstract 2568051, DPS/EPSC meeting, Pasadena, CA, USA, 16-21 October, 2016.
- [122] Sterken C., Dehant V. and Mathews P.M.
Book Review: Precession, Nutation, and Wobble of the Earth.
The Journal of Astronomical Data, Vol. 22, id. 2, 2016.
- [123] Suard N., Kanj A., Delporte J., Uhrich P., Tuckey P., Defraigne P., Sesia I., Signorile G. and Armagou Miret E.
The EGNOS time offset to UTC,
Proceedings of the Europ. Nav. Conf., Helsinki, June 2016.
- [124] Tavella P., Sesia I., Cerretto G., Signorile G., Calonico D., Costa R., Clivati C., Cantoni E., De Stefano C., Frittelli M., Formichella V., Cerabolini P., Rotiroti L., Biserni E., Leone V., Zarroli E., Sormani D., Defraigne P., Ozdemir N., Baire Q., Gandara M., Hamoniaux V., Varriale E., Morante Q., Widomski T., Kaczmarek J., Uzycki J., Borgulski K., Olbrys P., Kowalski J., Cernigliaro A., Fiasca F., Perucca A., Mantero S., Dhiri V., Veiga T., Suárez T., Diaz J., Mangiantini M., Wallin A.E., Galleani L. and Hindley D.
The European Project DEMETRA: Demonstrating Time Dissemination Services,
Proceedings of the Precise Time and Time Interval meeting, Monterey, January 2016.
- [125] Tavella P., Sesia I., Cerretto G., Signorile G., Calonico D., Costa R., Clivati C., Cantoni E., De Stefano C., Frittelli M., Formichella V., Cerabolini P., Rotiroti L., Biserni E., Leone V., Zarroli E., Sormani D., Defraigne P., Ozdemir N., Baire Q., Gandara M., Hamoniaux V., Varriale E., Morante Q., Widomski T., Kaczmarek J., Uzycki J., Borgulski K., Olbrys P., Kowalski J., Cernigliaro A., Fiasca F., Perucca A., Mantero S., Dhiri V., Veiga T., Suárez T., Diaz J., Mangiantini M., Wallin A.E. and Galleani L.
Experimental Time Dissemination Services Based on European GNSS Signals: the H2020 DEMETRA Project;
Proceedings of the Europ. Freq. and Time Forum, York, April 2016.
- [126] Tavella P., Sesia I., Cerretto G., Signorile G., Calonico D., Costa R., Clivati C., Cantoni E., De Stefano C., Frittelli M., Formichella V., Cerabolini P., Rotiroti L., Biserni E., Leone V., Zarroli E., Sormani D., Defraigne P., Ozdemir N., Baire Q., Gandara M., Hamoniaux V., Varriale E., Morante Q., Widomski T., Kaczmarek J., Uzycki J., Borgulski K., Olbrys P., Kowalski J., Cernigliaro A., Fiasca F., Perucca A., Mantero S., Dhiri V., Veiga T., Suárez T., Diaz J., Mangiantini M., Wallin A.E. and Galleani L.
Time Dissemination Services: The Experimental Results of the European H2020 DEMETRA Project,
Proceedings of the Int. Freq. Contr. Symp. 2016, May 2016, New Orleans.

- [127] Tavella P., Sesia I., Cerretto G., Signorile G., Calonico D., Costa, R., Clivati C., Cantoni E., De Stefano C., Frittelli M., Formichella V., Cerabolini P., Rotiroti L., Biserni E., Leone V., Zarroli E., Sormani D., Defraigne P., Ozdemir N., Baire Q., Gandara M., Hamoniaux V., Varriale E., Morante Q., Widomski T., Kaczmarek J., Uzycki J., Borgulski K., Olbrys P., Kowalski J., Cernigliaro A., Fiasca F., Perucca A., Mantero S., Dhiri V., Veiga T., Suárez T., Diaz J., Mangiantini M., Wallin A.E., Galleani L. and Hindley D.
The European Project DEMETRA, "Timing services based on European GNSS: First experimental results",
Proceedings of the IEEE workshop on Metrology in Aerospace, Firenze, June 2016.
- [128] Turbet M., Forget F., Gillmann C., Karatekin Ö., Svetsov V., Popova O. and Wallemacq Q.,
3D Global Climate Modelling of the environmental effect of meteoritic impacts on Early Mars.
Extended Abstract, American Astronomical Society, AAS/DPS meeting #48/ EPSC 11,
Pasadena, Ca, USA, Poster 117.04, October 16-21, 2016.
- [129] Vallat C., Van Hoolst T., Grasset O., Tosi F., Krupp N., Masters A., Cavalié T. and Fletcher L.
JUICE Payload operations GCO-500 'hard core' scenario.
ESA report, 19 Jan 2016.
- [130] Van Hoolst T., Coyette A., Baland R.M. and Trinh A.
The rotation of Titan and Ganymede.
Extended Abstract, AAS/DPS meeting #48/ EPSC 11, Pasadena, Ca, USA, October 16-21, 2016.
- [131] Van Hoolst T. and Grasset O.
WG1 science assessment of the core scenario of 2015.
ESA/JUICE report, 8 January 2016.
- [132] Van Noten, K. and Camelbeeck, T.,
Influence of site effects in central Belgium on earthquake strong ground motions
Final report of FNRS Project T.0116.14F, 2016.
- [133] Ventura, P., García-Hernández, D. A., Groenewegen, M. and van Loon, J. T.
AGB stars: a key ingredient in the understanding and interpretation of stellar populations: European Week of Astronomy and Space Science
Memorie della Società Astronomica Italiana, 87, pp. 225, 2016.
- [134] Verbeeck, C., Argo, M., Brown, P., Molau, S., Rendtel, J. and Martinez Picar, A.
Summary of the Open Session at the IMC 2016
Proceedings of the International Meteor Conference Egmond, the Netherlands, 2–5 June
2016, pp. 305-306, 2016.
- [135] Yseboodt M.
The LaRa Doppler observable, visibility conditions and the Martian orientation parameters signatures.
PRODEX technical note, LARA-TN-ROB-00024_v1.1_observable_Doppler.pdf, September 2016.
- [136] Yseboodt M., Dehant V., Péters M.-J. and Folkner W.M.
Signatures of the Martian rotation parameters in the Doppler and range observables.
Extended Abstract, American Astronomical Society, AAS/DPS meeting #48/ EPSC 11,
Pasadena, Ca, USA, Poster, October 16-21, 2016.

Other publications

- [137] F. Clette, E.W. Cliver, L. Lefèvre, J.M. Vaquero and L. Svalgaard
Sunspot Number Recalibration
Solar Physics, Vol. 291, N° 9-10, 659 pages? ISSN: 0038-0938 (Print) 1573-093X (Online)), 2016,
<http://link.springer.com/journal/11207/291/9/page/1>.
- [138] Pauwels, T., Bruyninx, C., Cuypers, J. and Roosbeek, F.
Annuaire de l'Observatoire royal de Belgique – Jaarboek van de Koninklijke Sterrenwacht van België 2016
Fedopress, ISSN 03734900, 2016
- [139] Van Noten, K.
GeoTalk: A smart way to map earthquake impact.
GeoLog | The official blog of the European Geosciences Union, 28 April 2016, 2016.

Annex 2:

Human Resources

Personeel / Personnel

Algemeen directeur: Van der Linden Ronald

Vastbenoemd personeel / Personnel statutaire

Wetenschappelijk personeel / Personnel scientifique

<u>Name/Nom</u>	<u>Functie/Fonction</u>
Alexandre Pierre	Premier assistant
Alvarez Rodrigo	Premier assistant
Berghmans David	Eerstaanwezend werkleider
Blomme Ronny	Werkleider
Bruyninx Carine	Eerstaanwezend werkleider
Camelbeeck Thierry	Chef de travaux principal
Clette Frédéric	Premier assistant
Collin Fabienne	Premier assistant
Cuypers Jan	Eerstaanwezend werkleider
De Cat Peter	Werkleider
Defraigne Pascale	Chef de travaux principal
Dehant Véronique	Maître de recherches
Frémat Yves	Premier assistant
Groenewegen Martin	Werkleider
Hochedez Jean-François	Chef de travaux
Lampens Patricia	Onderzoeksleider
Lecocq Thomas	Assistant
Legrand Juliette	Premier assistant
Pauwels Thierry	Eerstaanwezend werkleider
Roosbeek Fabian	Premier assistant
Van Camp Michel	Chef de travaux principal
Van De Steene Griet	Werkleider
Van Hoolst Tim	Eerstaanwezend werkleider
Vanneste Kris	Werkleider
Yseboodt Marie	Premier assistant

Technisch en administratief personeel / Personnel technique et administratif

	<u>Name/Nom</u>	<u>Functie/Fonction</u>
<u>A:</u>	Milis Andre	Adviseur A3
	De Knijf Marc	Attaché A3
	Dufond Jean-Luc	Attaché A2
	Rogge Vincent	Attaché A2
	Jans Thimoty	Attaché A1
	Kochuyt Anne-Lize	Attaché A1
	Rapagnani Giovanni	Attaché A1
	Rezabek Oleg	Attaché A1
	Wellens Véronique	Attaché A1
<u>B:</u>	Boulvin Olivier	Expert technique
	Bukasa Baudouin	Expert technique
	Castelein Stefaan	Technisch deskundige
	Claerhout Alexandre	Expert ICT
	Dumortier Louis	Expert ICT
	Duval David	Expert ICT
	Ergen Aydin	Expert technique

	Frederick Bert	Expert technique
	Hendrickx Marc	Expert technique
	Herremans David	Expert ICT
	Langenaken Hilde	Technisch deskundige
	Lemaitre Olivier	Expert technique
	Martin Henri	Expert technique
	Mesmaker Dominique	Expert technique
	Moyaert Ann	ICT deskundige
	Somerhausen André	Expert ICT
	Strubbe Marc	Technisch deskundige
	Van Camp Lydia	Technisch deskundige
	Van De Putte William	Technisch deskundige
	Van Der Gucht Ignace	Technisch deskundige
	Vandekerckhove Joan	Technisch deskundige
	Vandercoilden Leslie	Expert technique
	Van de Meersche Olivier	Expert financier
	Vermeiren Katinka	ICT deskundige
	Vermeylen Lore	Technisch deskundige
	Wintmolders Sabrina	Administratief deskundige
<u>C:</u>	Bizerimana Philippe	Assistant technique
	Brebant Christian	Assistant administratif
	Bruyninckx Martine	Administratief assistent
	Consiglio Sylvia	Administratief assistent
	Depasse Béatrice	Assistant administratif
	De Wachter Rudi	Technisch assistent
	Feldberg Liesbeth	Administratief assistent
	Segers Cindy	Administratief assistent
	Trocmet Cécile	Assistant administratif
	Vanden Elshout Ronny	Assistant technique
<u>D:</u>	Motte Philippe	Collaborateur technique
	Vanparijs Thomas	Technisch medewerker

Personeel met externe beurzen / Personnel sur bourses externes

<u>Name/Nom</u>	<u>Functie/Fonction</u>
Gloesener Elodie	Boursier FRIA (30/09/2016)

Contractueel personeel beheerd door de POD Wetenschapsbeleid / Personnel contractual géré par le SPP Politique Scientifique

	<u>Name/Nom</u>	<u>Functie/Fonction</u>
<u>SW11</u>	Katsiyannis Athanassios	Assistant
<u>B:</u>	Malisse Vincent	ICT-deskundige
	Vandersyppe Anne	Administratief expert
<u>C:</u>	De Dobbeleer Rudy	Technisch assistant
	Mouling Ilse	Administratief assistent
	Semeraro Vanessa	Administratief assistent
	<i>Sinchiri Kevin</i>	Administratief assistent
<u>D:</u>	Clauwaert Eveline	Technische medewerker
	Inkeleer Jérémie	Collaborateur technique
	<i>Motte Philippe</i>	Collaborateur technique
	Rodrigues Carolina	Collaborateur technique

Contractueel personeel / Personnel contractuel

Wetenschappelijk personeel / Personnel scientifique

<u>Naam/Nom</u>	<u>Functie/Fonction</u>
Andries Jesse	Werkleider
Attié Raphaël	Assistant
Baire Quentin	Assistant
Balland Rose-Marie	Assitant
Benmoussa Ali	Chef de travaux
Bergeot Nicolas	Chef de travaux
Bertrand Bruno	Assistant
Beuthe Mikael	Chef de travaux
Bonte Katrien	Assistent
Bourgoignie Bram	Assistent
Champagne Georges	Assistant
Chatzinilos Miltiadis	Assistant
Chevalier Jean-Marie	Assistant
Dammasch Ingolf	Assistant
Decraemer Bieke	Assistent-stagiaire
De Cuyper Jean-Pierre	Werkleider
Delouille Véronique	Chef de travaux
Deprost Marie-Hélène	Assistant-stagiaire
Devos Andy	Assistant
D'Huys Elke	Assistent
Dolla Laurent	Assistant
Dominique Marie	Assistant
Fábián András	Assistant
Gerbal Nicolas	Assistent-stagiaire
Gillmann Cédric	Assistant
Giordanengo Boris	Chef de travaux
Gissot Samuel	Chef de travaux
Gloesener Elodie	Assitant
Huang Wei	Assistant
Janssens Jan	Assistent
Joukov Andrei	Chef de travaux
Karatekin Ozgur	Chef de travaux
Knuts Elisabeth	Assistant
Kraaijkamp Emil	Assistent
Laguerre Raphael	Assistant
Lefevre Laure	Chef de travaux
Le Maistre Sébastien	Assistant
Lobel Alex	Werkleider
Magdalenic Jasmina	Chef de travaux
Martinez Picar Antonio	Assistent
Marqué Christophe	Chef de travaux
Mierla Marilena	Assistant
Mitrovic Michel	Assistant
Nicolaes Dries	Assitant-stagiaire
Nicula Bogdan	Chef de travaux
Noack Léna	Assistant
Özdemir Nilüfer Aslihan	Assistant
O'Hara Jennifer	Assitant-stagiaire

Parenti Suzanna	Chef de travaux
Péters Marie-Julie	Assistant-stagiaire
Pham Lê Binh San	Assitant
Podladchikova Olena	Chef de travaux
Pottiaux Eric	Chef de travaux
Pylyser Eric	Assistant
Rekier Jeremy	Assitant
Ryan Daniel	Assistant
Ritter Birgit	Assistant
Rivoldini Attilio	Assistant
Rodriguez Luciano	Chef de travaux
Rosenblatt Pascal	Chef de travaux
Saario Joonas	Assitant-stagiaire
Shestov Sergeï	Assistant
Stegen Koen	Assistent
Talpeanu Dana	Assistant-stagiaire
Triana Santiago	Assistant
Trinh Anthony	Assistent
Van Hoof Peter	Werkleider
Van Hove Bart	Assistent
Vanlommel Petra	Eerstaanwezend assistent
Van Noten Koen	Assistent
Van Ruymbeke Michel	Chef de travaux
Vansintjan Robbe	Assistent
Verbeeck Francis	Eerstaanwezend assistent
Verbeeck Koen	Assistent
Verdini Andrea	Assistant
Verstringe Freek	Assistent
Vleminckx Bart	Assistent
Wallemacq Quentin	Assistant
Wauters Laurence	Chef de travaux
West Matthew	Assistant
Zhu Ping	Assistant

Technisch en administratief personeel / personnel technique et administratif

	<u>Naam/Nom</u>	<u>Functie/Fonction</u>
<u>A:</u>	Van Elder Sophie	Attaché A1
	Cornet Denis	Attaché A1
	Mestdagh Pieter	Attaché A1
	De Decker Georges	Attaché A2
	Hanjoul Michel	Attaché A2
	Kussé Caroline	Attaché A2
	Willemse Sarah	Attaché A2
	Mampaey Benjamin	Attaché A2
	Van Hemelryck Eric	Attaché A2
<u>B:</u>	Bastin Véronique	Expert technique
	Coeckelberghs Hans	Technisch deskundige
	Delmeule Nicolas	Expert ICT
	Rigo Ghislain	Expert technique
	Vander Putten Wim	ICT-deskundige
<u>C:</u>	Hernando Ana Maria	Assistant administratif
	Michaux Kevin	Administratief assistant

Smet Gert	Technisch assistent
Smetryns Daan	Technisch assistent
Stokart Luc	Assistant techniquet
Vandeperre Arnold	Technisch assistent
Wijns Erik	Technisch medewerker
<u>D:</u>	
El Amrani Malika	Collaborateur technique
Herman Viviane	Collaborateur technique
Honet Vincent	Collaborateur technique
Ipuz Mendez Adriana	Collaborateur technique
Kurudere Hulya	Technisch medewerker
Piedfort Sandra	Technisch medewerker
Reghif Harraz Mohammed	Collaborateur technique
Ryssaert Laura	Collaborateur administratif
Vermeylen Jacqueline	Collaborateur technique
Verbraeken Ulrike	Technische medewerker

Gedetacheerd personeel / Personnel détaché

<u>Naam/Nom</u>	<u>Functie/Fonction</u>
Duynslaeger Thierry	Leraar

Staff statistics

In 2016, the Royal Observatory of Belgium (with the Planetarium) employed in total 179 agents, with 120 men and 59 women.

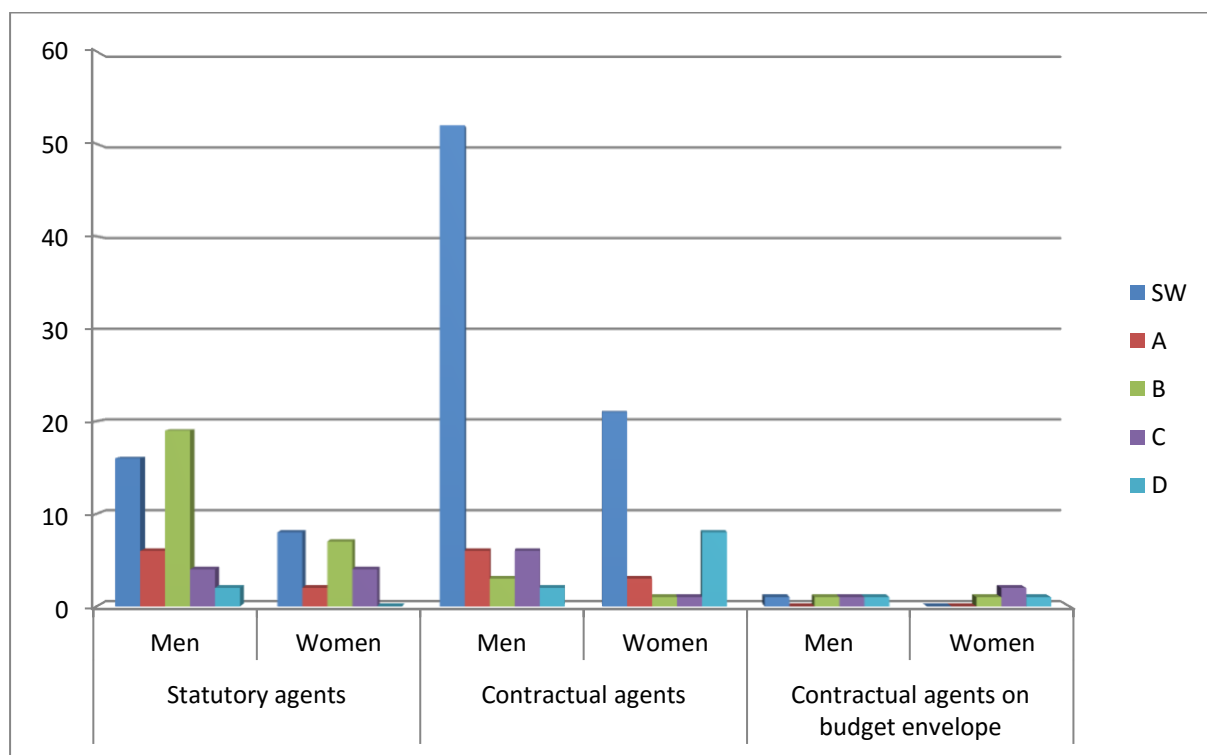
The majority of the employed agents are contractual agents (103 agents), whose 71% of them are scientists (SW) (52 men and 21 women). Apart from the contractual SW agents, there are 9 agents employed at the level A, 4 at the level B, 7 at the level C and 10 at the level D. Male contractual agents exceed in number female contractual agents at all levels except the level D (with 2 men and 8 women).

Among the statutory agents (68 agents), 24 of them are engaged at the level SW, 8 at the level A, 26 at the level B, 8 at the level C and 2 at the level D. There are more statutory agents at the level B than statutory agents at each of the other levels. More than two third of the statutory agents are male (47 male statutory agents against 21 female statutory agents).

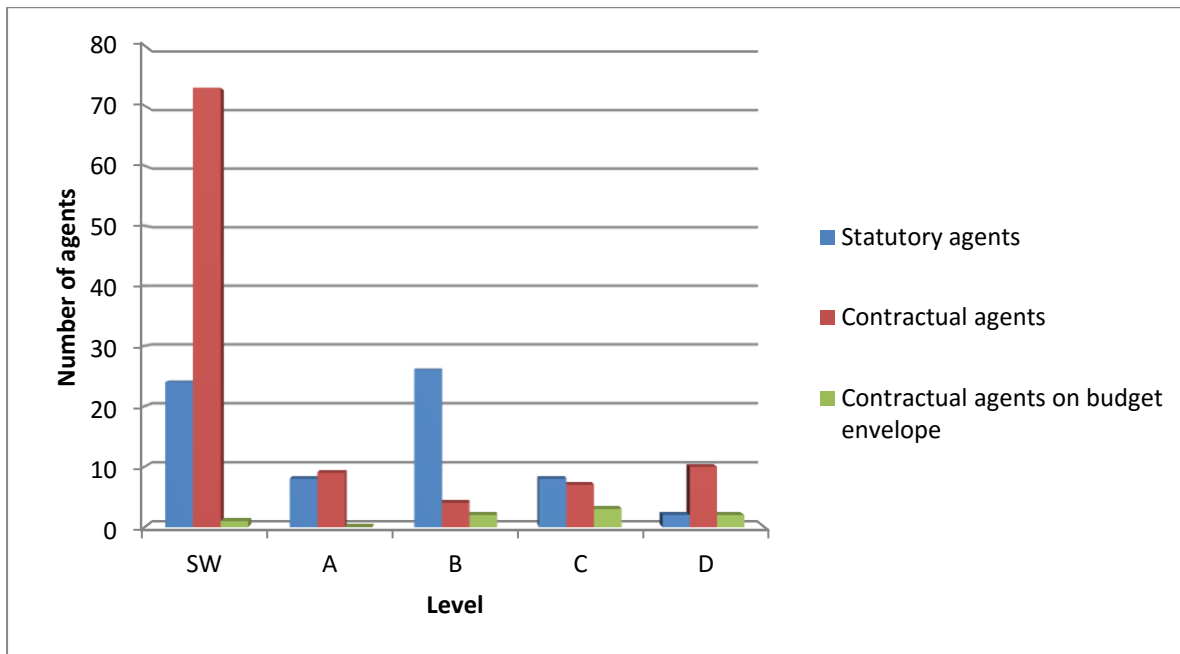
Finally, there are 8 contractual agents on budget envelope, with 4 men and 4 women.

		SW	A	B	C	D
Statutory agents	Men	16	6	19	4	2
	Women	8	2	7	4	0
Contractual agents	Men	52	6	3	6	2
	Women	21	3	1	1	8
Contractual agents on budget envelope	Men	1	0	1	1	1
	Women	0	0	1	2	1

Number of statutory, contractual and contractual on budget envelope agents by gender and by level (SW, A, B, C and D)



Number of statutory, contractual and contractual on budget envelope agents by level (SW, A, B, C and D)



Number of agents by gender and by levels (SW, A, B, C and D)

